DEHYDROGENATION OF PROPANE OVER GALLIUM LOADED HZSM-5 CATALYSTS

KORAWICH TRANGWACHIRACHAI

A THESIS SUBMITTED IN PARTIAL FULFILMENT OF THE REQUIREMENT FOR THE
DEGREE OF MASTER OF SCIENCE IN PETROCHEMICALS AND HYDROCARBONS
CHEMISTRY
DEPARTMENT OF CHEMISTRY
FACULTY OF SCIENCE
KING MONGKUT'S INSTITUTE OF TECHNOLOGY LADKRABANG
2018
KMITL-2018-SC-M-015-004

Thesis Title	Dehydrogenation of propane over Ga loaded HZSM-5 catalysts
Student Name	Korawich Trangwachirachai
Student ID	58605033
Degree	Master of Science (Petrochemicals and Hydrocarbons Chemistry)
Department	Chemistry
Year	2018
Thesis Advisor	Assoc. Prof. Dr. Tawan Sooknoi
Thesis Co-advisor	Dr. Natthida Numwong

Abstract

In this research, Ga-HZSM-5 catalysts were tested for the propane dehydrogenation. Ga-HZSM-5 catalysts with Si/Al ratio 28, 40, 140, 250, and 500 were prepared by wet-impregnation and characterized by X-ray diffraction technique (XRD), nitrogen adsorption technique (BET), temperature-programmed reduction (H_2-TPR), temperature-programmed desorption (IPA and NH_3-TPD), and *in-situ* X-ray absorption near edge spectrophotometry (XANES). The activity of catalysts was tested in a fixed-bed continuous flow reactor. The effect of reaction temperature (400-550 °C), feed dilution, contact time (1.81-5.43 $g.h.mol^{-1}$), a presence of H_2 in the feed, and Si/Al ratio on propane dehydrogenation were investigated. A high selectivity of propylene is observed when the propane feed is diluted and the Ga-HZSM-5 catalysts are reduced. With a low Si/Al (28 and 40), main active site is Ga^+. While $[Ga_2O_2]^{2+}$ is found as an active site for catalysts with high Si/Al ratio (more than 140). However, when the Ga-HZSM-5 catalysts were not reduced, $[GaO]^+$ is presented as active species. In this case, the side reaction, i.e. oligomerization and aromatization, take places resulting in the low propylene selectivity. The non-reduced catalyst is deactivated and the $[GaO]^+$ is reduced to the Ga^+ species during the reaction.

Keywords: Dehydrogenation, Gallium, HZSM-5, Propane, Propylene

Acknowledgement

The author desires to appreciatively thank my advisor, Assoc. Prof. Dr. Tawan Sooknoi, and my co-advisor, Dr. Nutthida Numwong, for suggestions, inspiration, carefulness, reassurance, experimental instrument, and knowledge in catalysis throughout this research

I would like to gratefully acknowledge chairperson and committee, Asst. Prof. Dr. Montree Thongkam, Dr. Amnat Permsubscul, and Assoc. Prof. Dr. Siriporn Jongpatiwut for judgment and valuable comments.

Moreover, I would like to acknowledge the financial support from the Faculty of Science, King Mongkut's Institute of Technology Ladkrabang for the equipment, chemicals, and facilities.

Sincerely thanks to Suranaree University of Technology, Scientific and Technological Research Equipment Centre, Department of Chemistry, Chulalongkorn University for the characterization of catalyst in this research.

Unforgettable, I would like to grateful to my friends in Catalytic Chemistry Research Unit (CCR group) for their help, advice, support, and encouragement.

Finally, I deeply appreciate and thank our parents and family for their love and support.

Mr. Korawich Trangwachirachai

CONTENTS

CONTENTS (Continued)

CONTENTS (Continued)

LIST OF TABLES

Table Page

LIST OF FIGURES

Figure Page

LIST OF FIGURES (Continued)

LIST OF SCHEMES

CHAPTER 1

INTRODUCTION

1.1 Motivation

Propylene is one of the most important starting materials in chemical industry, such as the production of polypropylene, propylene oxide, polyacrylonitrile, acrylic acid, and acrolein [1]. Propylene is usually obtained by steam cracking or fluid catalytic cracking process of naphtha. However, the global market demand, where the total propylene consumption was 83 million tons in 2013, is predicted to increase at 4.8% during 2013-2018 [2]. Thus, the production of propylene via the direct dehydrogenation of light alkanes, such as propane, without oxidizing agent is an alternative way to produce the propylene, with lower risk of the combustion. Today, propane can be largely obtained from shale gas and the natural gas production, and also from petroleum refining processes [3].

Recently, many research study the propane dehydrogenation at relatively high temperature (~600 °C) [1, 2, 4]. Metal loaded HZSM-5 such as chromium, platinum and indium are widely used as propane dehydrogenation catalyst [5-7]. However, the catalysts deactivation was found even use carbon dioxide as co-feed [5, 6]. Moreover, platinum and indium are expensive. Alternatively, gallium oxide loaded HZSM-48 was found to be more stable catalyst in the propane dehydrogenation [1]. Gallium loaded HZSM-5 was also found to be an active catalyst for dehydrogenation of ethane to ethylene without severe deactivation [7]. With the assist of H_2, the gallium hydride complex ($[GaH_2]^+$) was found to be an active species for dehydrogenation of ethane. Accordingly, it is interesting to use gallium loaded HZSM-5 as catalyst in propane dehydrogenation because of the high activity and stability of $[GaH_2]^+$ complex.

In this research, the gallium loaded HZSM-5 catalysts with different Si/Al ratio were chosen to study on the dehydrogenation of propane to produce propylene without oxidizing agent. The effect of reaction temperature was investigated in the range of 400-550 °C in fixed-bed continuous flow reactor. The catalyst acidity (Si/Al ratio = 28, 40, 140, 250, and 500), contact time, and catalysts pretreatment were also investigated.

1.2 Objectives

1.2.1 To produce the propylene via direct dehydrogenation of propane.

1.2.2 To understand the effect of reaction temperature, acidity, gallium species, and contact time that affect the propane conversion and propylene selectivity.

1.3 Scopes of the study

The scopes of this thesis are as follow:

1.3.1 Preparation of 3 wt.% gallium loaded HZSM-5 catalysts with various Si/Al ratio by wet-impregnation method.

1.3.2 Characterization of catalysts by X-ray diffraction spectroscopy (XRD), temperature-programmed reduction (H_2-TPR), temperature-programmed desorption (NH_3-TPD and IPA-TPD), X-ray absorption near edge spectroscopy (XANES), gas adsorption analysis (BET), and inductively couple plasma mass spectrometry (ICP-MS).

1.3.3 Testing on catalytic activity in a fixed-bed continuous flow reactor.

1.3.4 Study on the effect of temperature (400-550 °C), acidity (Si/Al ratio = 28, 40, 140, 250, and 500), and gallium species on propane dehydrogenation.

1.3.5 Products are analyzed and identified by online gas chromatography with flame ionization detector (GC-FID).

1.4 Expected Results

A high propane conversion and propylene selectivity catalysts without severe deactivation can be obtained.

CHAPTER 2

THEORY

2.1 Propane

2.1.1 General information [3]

Propane is a C_3 hydrocarbon with the molecular formula C_3H_8. It is an extremely flammable gas at standard temperature and pressure but can compress to a liquid form. It is colorless and odorless. The density of propane is 2.0098 kg/m^3. It is commonly used as a fuel for engines, oxy-gas torches, portable stoves, and residential central heating. Propane is one of liquefied petroleum gases (LPG) component.

2.1.2 Sources and productions [3]

Propane is produced as a by-product of two processes that are natural gas production and petroleum refining processes. The processing of natural gas involves removal of butane, propane, and large amounts of ethane from the raw gas, in order to prevent condensation of these volatiles in natural gas pipelines. Additionally, oil refineries produce some propane as a by-product of cracking petroleum into gasoline or heating oil.

2.1.3 Applications [8]

2.1.3.1 Residential

A full range of efficient propane appliances is available: from furnaces, space heaters, water heaters, and fireplaces to refrigerators, dryers, and indoor lighting. In outdoor applications, propane-powered equipment includes barbecues, pool heaters, generators, and portable heaters as well as lawn maintenance equipment.

2.1.3.2 Commercial, industrial, and institutional

Commercial-grade propane furnaces and water heaters are the solution to large-scale applications. From warehouses to manufacturing facilities to hospitals, propane is reliable and efficient. And propane water heaters work up to 2.5 times faster than their electric counterparts.

2.1.3.3 Construction

Whether in asphalt applications or to heat the construction site office, propane-powered construction heaters are available in a variety of sizes to meet any worksite need.

2.1.3.4 Agriculture

Environmentally friendly propane is used extensively in agricultural applications including crop drying, chemical-free pest and weed control, heating livestock facilities such as barns and brooding pens, and heating commercial greenhouses.

2.1.3.5 Food service

The instant, even and moist heat of propane is preferred by chefs and novice gourmets alike. A full range of efficient and reliable commercial appliances is available including ranges, fryers, and refrigerators.

2.1.3.6 Oil & gas

The portability of propane is a significant benefit to the oil and gas industry. Uses include portable power generators, remote camp heating, cooking and refrigeration and specialized well, and pipeline testing equipment.

2.1.3.7 Transportation

While personal vehicles can be converted for propane use, fleet vehicles are currently the most common application for propane as a transportation fuel. Propane is the most common alternative fuel used for vehicles in Canada and widely available at a broad network of retail outlets right across the country. Propane-powered fleet vehicles include taxis, delivery and service trucks, and school buses.

2.1.3.8 Fork lift trucks

Clean-burning propane is the perfect fuel for fork lift trucks for both external and internal applications. Propane fork lifts provide excellent fuel efficiency and reduced maintenance costs.

2.1.3.9 Petrochemical

Propane is one of many raw materials used by the petrochemical industry as a feedstock to make plastics products.

2.2 Propylene

2.2.1 General information [8]

Propylene or propene is an unsaturated C_3 hydrocarbon with the molecular formula C_3H_6. It is a flammable gas at room temperature and atmospheric pressure. The density of propylene is 1.81 kg/m^3 in the gas phase and 613.9 kg/m^3 in the liquid phase. It is colorless gas and has a faint petroleum-like odor.

2.2.2 Sources and productions [2, 8]

Propylene is usually obtained by steam cracking or fluid catalytic cracking process of naphtha and can be also obtained as a by-product of oil refining and natural gas production processes. Other that, propylene can be produced via olefin metathesis that is a reversible reaction between ethylene and butylene. Propylene can also be produced from dehydrogenation of propane.

2.2.3 Applications [9]

Propylene is second only to ethylene as an important raw material for the production of other organic chemicals and, like ethylene, it has virtually no use "as-is." In 2014, about 64% of total propylene produced for chemical uses worldwide went into the manufacture of polypropylene resins that is one of those most versatile polymers available with applications, both as a plastic and as a fiber, in virtually all of the plastics end-use markets [10]. About 7% of the world propylene is consumed in the production of propylene oxide that is a highly reactive chemical used as an intermediate for the production of numerous commercial materials. It reacts readily with compounds containing active hydrogen atoms such as alcohols, amines, and acids. Therefore, propylene oxide is used worldwide to produce such versatile products such as polyether polyols (polyglycol ethers), propylene glycol, and propylene glycol ether [11]. The third-largest end-use segment is acrylonitrile production, accounts for about 6% of total consumption. Acrylonitrile is used as a monomer for such products as polyacrylonitrile for acrylic fibers, in ABS (acrylonitrile-butadiene-styrene) and SAN (styrene-acrylonitrile) resin manufacture as a modifying monomer, and as a chemical intermediate in the manufacture of adiponitrile, acrylamide and a variety of other chemicals [12]. The remainder went into the manufacture of chemical intermediates such as acrylic acid, cumene, and oxo alcohols.

The major propylene markets are China, the United States, and Western Europe, which together accounted for about 55% of global consumption in 2014. As a result of new propylene and derivative capacity scheduled to be brought on stream during 2014-2019, the United States and especially the Chinese market will exhibit significant growth and account for about 76% of the total increase in propylene demand. Even though the Western European propylene market is projected to shrink slightly in the forecast period, it will likely remain the third-largest global producer and consumer of propylene. Figure 2.1 shows world consumption of propylene in 2014.

Propylene demand growth has been and continues to be driven primarily by developments in the polypropylene industry. The next-largest end uses of propylene are acrylonitrile, propylene oxide, and the combined oxo alcohol segment (2-ethyl hexanol and butanol), which make up 6-7% of global consumption each. This is not expected to change much in the forecast period to 2019.

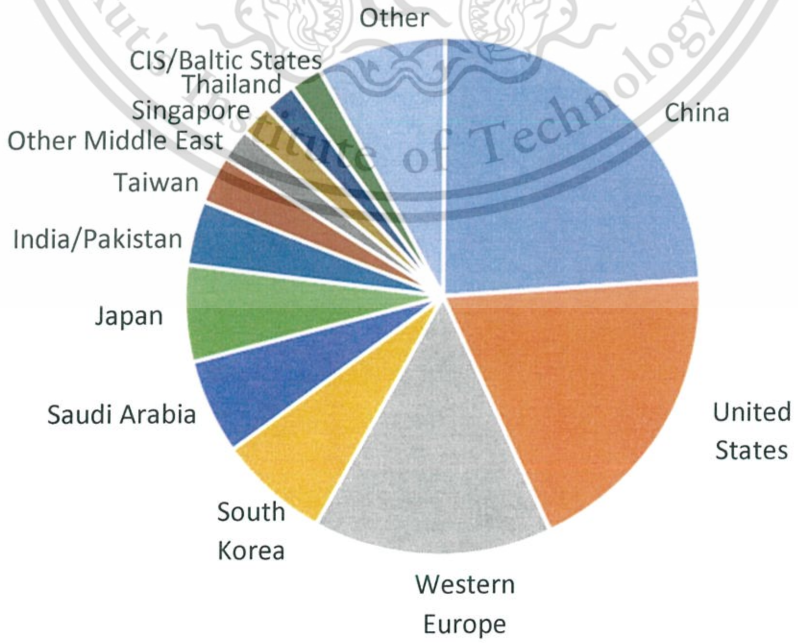

Figure 2.1 World consumption of propylene in 2014. [9]

The severe global recession that lasted from the fall of 2008 to mid-2009 caused the first decline in global propylene demand in over 25 years. The downturn was particularly pronounced in North America and Europe, while developing regions with less exposure to the global financial market meltdown fared comparatively better. The ensuing recovery has been overshadowed by increasingly acute oversupply conditions that have primarily affected the polypropylene industry, the major consumer of propylene. Since 2009, global propylene consumption has grown by about 5% annually, on average, while capacity increased at a slightly slower pace.

Global consumption of propylene for chemical applications is projected to increase at an average rate of 4.6% annually over the next five years. While the highest growth rate is expected to be in Canada, the actual increase in propylene consumption was comparatively small and reflects the restart of polypropylene production. Outside of North America, the regions expected to exhibit the largest demand growth will likely be China in Northeast Asia, the CIS and Baltic States, and the Middle East, where most of the increase in propylene consumption was seen in the United Arab Emirates. Of the established consuming regions, Japan and Western Europe are projected to see declines as their downstream consumption decreases further and/or moves to other regions.

2.3 Dehydrogenation reaction [13, 14]

Dehydrogenation is a chemical reaction that involves the removal of hydrogen from an organic molecule. The reaction is reversible. It is an important reaction because it converts alkanes which are low-valued to olefins which are more valuable. Dehydrogenation reaction can be separated into two methods that are direct dehydrogenation and oxidative dehydrogenation. The oxidative dehydrogenation is an exothermic reaction that requires lower reaction temperature than direct dehydrogenation that is an endothermic reaction. However, the oxidative dehydrogenation requires oxidant such as oxygen or halogen. When the oxidant is used in the reaction, it may cause over oxidation of the organic reactant to carbon dioxide.

Propane dehydrogenation (PDH) is the reaction that produce propylene and also produce hydrogen as a by-product. The reaction can be occurred on the metal supported zeolite. In the first step, propane must be adsorb by C-H cleavage on the catalyst surface to form propylidene intermediate on the metal surface and leave H atom on the support. After that, the intermediate will rearrange to product propylene and leave H atom on the metal surface. Finally, H atom on the support and catalyst surface will couple to form H_2 as a by-product as shown in Figure 2.2.

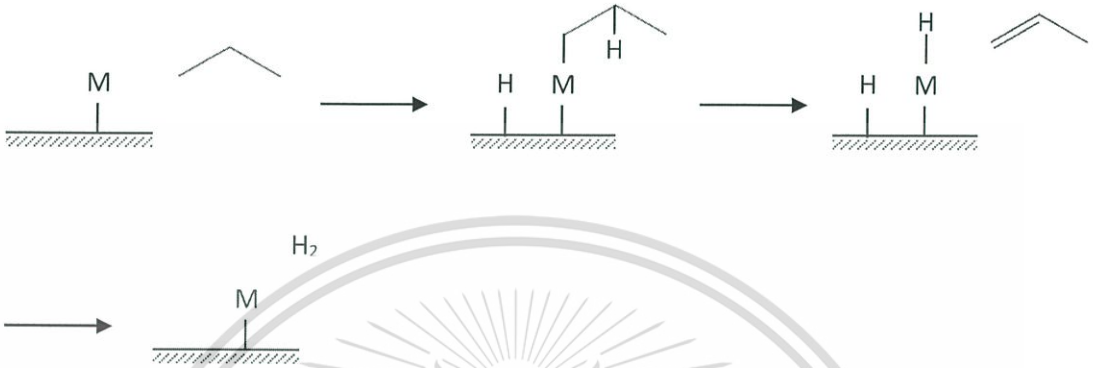

Figure 2.2 Mechanism of dehydrogenation of propane. [14]

2.4 Catalyst

2.4.1 Metal supported zeolite

2.4.1.1 Zeolite [16, 17]

Zeolites are hydrated aluminosilicate minerals made from interlinked tetrahedra of alumina (AlO_4) and silica (SiO_4). In simpler words, they are solids with a relatively open three-dimensional crystal structure built from the elements aluminum, oxygen, and silicon, with alkali or alkaline-earth metals (such as sodium, potassium, and magnesium) plus water molecules trapped in the gaps between them. Zeolites form with many different crystalline structures, which have large open pores (sometimes referred to as cavities) in a very regular arrangement and roughly the same size as small molecules.

There are about 40 naturally occurring zeolites, forming in both volcanic and sedimentary rocks; according to the US Geological Survey, the most commonly mined forms include chabazite, clinoptilolite, and mordenite. Dozens more artificial, synthetic zeolites (around 150) have been designed for specific purposes, the best known of which are zeolite A (commonly used as a laundry detergent), zeolites X and Y (two different types of faujasites, used for catalytic cracking), and the petroleum catalyst ZSM-5 (a branded name for pentasil-zeolite).

Zeolites are very stable solids that resist the kinds of environmental conditions that challenge many other materials. High temperatures don't bother them because they have relatively high melting points (over 1000 °C), and they don't burn. They also resist high pressures, don't dissolve in water or other inorganic solvents, and don't oxidize in the air. They are not believed to cause health problems through, for example, skin contact or inhalation, though in fibrous form, they may have carcinogenic (cancer-causing) effects. Since they are unreactive and based on naturally occurring minerals, they are not believed to have any harmful environmental impacts. Although zeolites might sound incredibly boring, their stable and unreactive nature is not what makes them useful.

The most interesting thing about zeolites is their open, cage-like, "framework" structure and the way it can trap other molecules inside it. This is how water molecules and alkali or alkaline-earth metal ions (positively charged atoms with too few electrons, sometimes called cations) become a part of zeolite crystals—although they do not necessarily remain there permanently. Zeolites can exchange other positively charged ions for the metal ions originally trapped inside them (technically this is known as cation exchange) and, as Cronstedt found over 250 years ago, they can gain or lose their water molecules very easily too (this is called reversible dehydration). Zeolites have regular openings in term of fixed size, which let small molecules pass straight through but trap larger ones; that is why they are sometimes referred to as molecular sieves. Unlike natural zeolites, which occur in random forms and mixed sizes, synthetic zeolites are manufactured in very precise and uniform sizes (typically from about 1 μm to 1 mm) to suit a particular application; in other words, they are made a certain size to trap molecules of a certain (smaller) size inside them.

Although all zeolites are aluminosilicate, some contain more alumina, while others contain more silica. Alumina-rich zeolites are attracted to polar molecules such as water, while silica-rich zeolites work better with nonpolar molecules.

The cage-like structure of zeolites makes them useful in all sorts of ways. One of the biggest everyday uses for zeolites is in water softeners and water filters. In ion-exchange water softeners, for example, hard water (rich in calcium and magnesium ions) is piped through a column filled with sodium-containing zeolites. The zeolites trap the calcium and magnesium ions and release sodium ions in their place, so the water becomes softer but richer in sodium. Many everyday laundry and dishwasher detergents contain zeolites to remove calcium and magnesium and soften water so they work more effectively.

Two other very common, everyday uses of zeolites are in odor control and pet litter; in both, the porous crystalline structure of the zeolites helps by trapping unwanted liquids and odor molecules. This simple idea, so effective in our homes, has much more important uses outside them: zeolites have proved extremely effective at removing radioactive particles from nuclear waste and cleaning up soils contaminated with toxic heavy metals. (Following the Fukushima nuclear disaster in Japan in 2011, rice farmers spread zeolites on their fields in an attempt to trap any lingering radioactive contaminants.) The many other uses of zeolites including concrete production, soil-conditioners, and animal food [15].

Another important use of zeolites is as catalysts in drug (pharmaceutical) production and in the petrochemical industry, where they are used in catalytic crackers to break large hydrocarbon molecules into gasoline, diesel, kerosene, waxes, and all kinds of other byproducts of petroleum. Again, it is the porous structure of zeolites that proves important. The many pores in a zeolite's open structure are like millions of tiny test tubes where atoms and molecules become trapped and chemical reactions readily take place. Since the pores in a particular zeolite are of a fixed size and shape, zeolite catalysts can work selectively on certain molecules, which is why they are sometimes referred to as shape-selective catalysts (they can select the molecules they work on in other ways beside shape and size, however). Like all catalysts, zeolites are reusable over and over again.

In industrial applications, the most important zeolites are LTA, FAU, MFI, and MOR. The dimensions of the zeolite pores allow for the separation of molecules on the basis of their sizes, so-called molecular sieving effect. In catalysis, this property is often referred to shape selectivity [16]. An example is the cracking of alkanes in acid MFI-type zeolites. Here the zeolite pores allow only the linear molecules to enter the pores containing the acid sites that regulate the cracking. Branched molecules are excluded from the pores and hence do not react [17].

2.4.1.2 ZSM-5 zeolite [18]

Zeolite ZSM-5, Zeolite Socony Mobil-5, is one type of family zeolite. It has shape selective property with unique channel structures. The secondary building unit of framework of ZSM-5 including mor 8T, case 12T, mel 14T, and mfi 14T as shown in Figure 2.3. These secondary building units can be connected to form sheet and the linking of the sheet lead to a three dimensional framework structure by the chains extend along the z-axis. The sheets parallel to [010] and [100] are shown in Figure 2.4 and 2.5.

mor 8T case 12T mfi 14T mel 14T

Figure 2.3 The secondary building unit of framework of ZSM-5. [18]

Figure 2.4 shows that the x-axis is horizontal and the z-axis vertical and the 10-membered ring apertures shown are the entrances to the straight channels which run parallel to [010] plane. While, Figure 2.5 shows that the y-axis is horizontal and the z-axis vertical and the circular 10-membered ring apertures shown are the entrances to channels which run parallel to [100] plane.

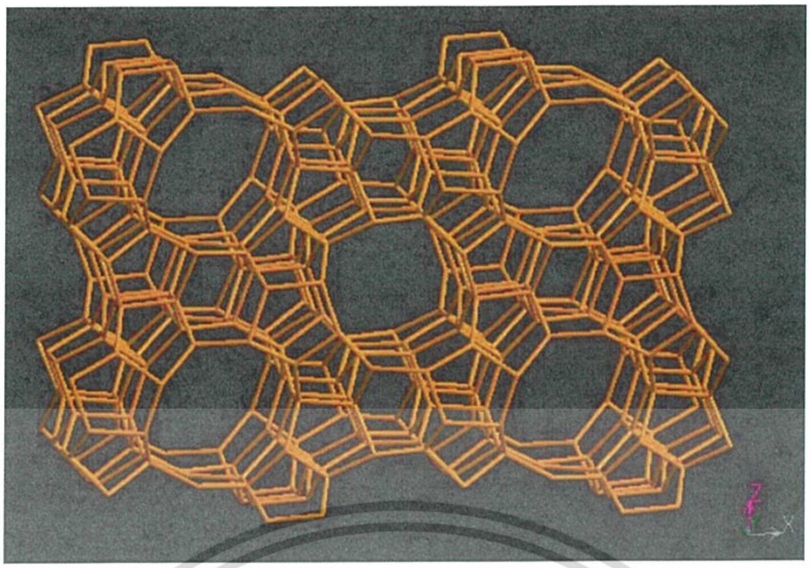

Figure 2.4 Skeletal diagram of the [010]-plane of the ZSM-5 unit cell. [18]

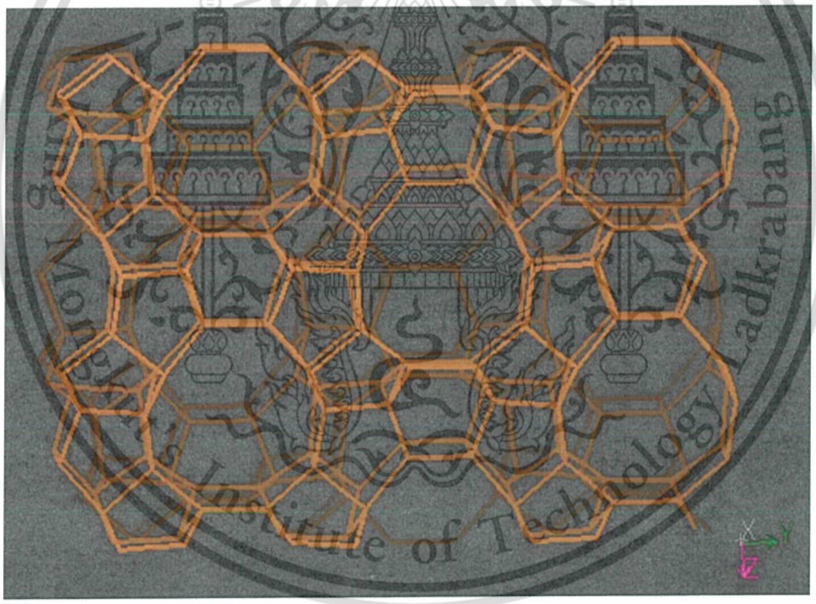

Figure 2.5 Skeletal diagram of the [100]-plane of the ZSM-5 unit cell. [18]

ZSM-5 chemical formula is $Na^{+}_{n}(H_2O)_{16}|$ $[Al_nSi_{96-n}O_{192}]$-MFI, n < 27. It is widely used in many catalytic reaction of industrial interest such as xylene isomerization, benzene ethylation, and ethanol, methanol-to-gasoline conversion. Their individual catalytic properties are mainly due to their regular framework with a pore size, which is intermediate to the large pore size zeolites (for instance, zeolites X and Y) and the small pore size zeolite (for instance the A zeolite). The shape selectivity of the pentasil zeolite is catalytically expressed by many features, such as;

1. The sieving effect, i.e. the capability of zeolite to admit into its pores or to reject reactive molecules having a critical diameter falling within a well-defined range.
2. The (reverse) sieving effect, i.e. the capability of the zeolite to allow product molecules having a certain critical diameter to diffuse out of its pores. Thus, in the case of a product molecule having a diameter exceeding to the pore size of the zeolite, this molecule will have to undergo cracking or rearrangement into a smaller molecule before diffusing out of the zeolite.
3. The effect on the reaction intermediates, i.e. the capability of certain active site to determine the length and structure of reaction intermediate species. ZSM-5 zeolite has pore system, which is believed to be significant for their low coke formation. While most industrial applications of zeolite catalyst make use of these in acid form. Zeolite is also excellent support for metal species. Zeolite supported metal species called a bi-functional catalyst is an acid zeolite on which a metal species phase is deposited. The function of the metal is to catalyze dehydrogenation and hydrogenation reaction while H-ZSM-5 possesses excellent dehydration and oligomerization properties which bi-functional catalyst can further undergo a variety of metal species and acidity reactions to form desirable product.

2.4.1.3 Metal supported zeolite [20-23]

Metal supported zeolite is a bi-functional catalyst that each component is capable of catalyzing a different reaction and compromising each other for the overall reaction. This type of catalyst is widely used in petroleum refining, especially in hydrocracking and hydroisomerization. Because transition states of catalytic mechanism occur both on metal and acid sites, the activity and selectivity of bi-functional catalysts can be determined by the characteristics of the metal sites and the zeolitic acid sites. In the other words, zeolite support enhances the catalytic activity and selectivity using the acids sites and the microporous properties [19].

The transition metal cations (TMC) that compensate the negative charge of the zeolite skeleton determine substantially the physical, chemical, and catalytic properties of the zeolite. While nontransition metal cations affect the zeolite properties through their electrostatic field or through their ability to act as Lewis centers, TMC may also act as redox sites in zeolites. TMC, localized in the cation position of the zeolite (as well as randomly located cations or metal or oxide clusters) can be present in various oxidation states in dependence on the manner of the cation introduction into zeolites and on the further zeolite treatment. The properties of the cations are also affected by the type of cation position as well as by the fact that, in addition to coordination of cations by the skeletal oxygen, further ligands may be bonded to them (H_2O, OH, O, etc.) [20].

TMC can, in principle, substitute for Si^{4+} or Al^{3+} in the zeolitic structures during synthesis, resulting in a zeolite lattice containing TMC. Parameters to be taken into account are (i) the size and charge of the TMC, (ii) the pH of the synthesis medium, and (iii) the ability of the TMC to adopt tetrahedral coordination with O atoms. In most cases, the amount of TMC incorporated in the lattice by hydrothermal synthesis is very limited. The two most common examples are Ti^{4+} and Fe^{3+}. Ti^{4+} exchanged in silicalite, for instance, is called TS-1 and is found to be an active catalyst in converting benzene with hydrogen peroxide into phenol [21, 22]. Fe^{3+} in the lattice is often due to the presence of an impurity in the zeolite synthesis, but it can also be added as a reagent into the synthesis mixture. One of the problems with TMC in the lattice is thermal stability. Upon high-temperature treatment, some of the TMC in the structure are extracted and found as so-called extralattice TMC, which can be monomeric or dimeric or appear as oligomers. All of them are possible catalytic sites. Aqueous ion exchange is the most commonly used method for preparing zeolites with TMC located at exchange sites. The resulting material contains aqueous TMC in the pores and cavities of the zeolite. Upon high-temperature treatment, water is removed and the TMC coordinate to the surface oxygen of the exchange sites. These sites had been compiled by Mortier a long time ago. They are crystallographically well-defined in the case of zeolites with low Si/Al ratios such as LTA, FAU, and MOR. This is much less so for zeolites with high Si/Al ratios such as MFI. Because aqueous solutions of TMC can be acidic, the exchange reaction can be accompanied by side reactions such as the exchange of protons and partial lattice destruction. To avoid these side effects, other exchange techniques have been developed, including solid-state exchange or simple buffering of the aqueous solution.

Metal supported zeolites are widely used for many reactions. Cobalt-exchanged zeolites ZSM-5 are active catalysts for alkane ammoxidation [23] and also active for NO_x reduction by methane in presence of excess O_2 [24]. The selective oxidation of NH_3 to N_2 can be occurred over Pd-ZSM-5 [23]. Moreover, Pd-ZSM-5 is an active catalyst for methane combustion [25]. In addition, cobalt, copper, rhodium, ruthenium, and platinum supported ZSM-5 are active for catalytic decomposition of N_2O to N_2 and O_2 [26].

2.4.2 Gallium supported ZSM-5 [27, 28]

Gallium is an element in group IIIA of the periodic table. It does not occur as a free element in nature but as gallium (III) compounds in trace amount of zinc ores. It is a soft, silvery white metal, similar to aluminum, at standard temperature and pressure, a brittle solid at low temperature, and a liquid at temperature greater than 29.76 °C. The application of gallium that has received the most attention is the production of semiconducting compounds. For many years this technology was dominated by the elemental semiconductors, silicon and germanium. But in 1952, German workers reported the achievement of semiconduction in compounds between elements in group III and group V. Of these, the most important are the compounds of gallium with antimony, arsenic or phosphorus. Nowadays gallium arsenide (Ga-As) is undoubtedly the most used. This compound is used in the production of several electronic parts such as diodes and transistors, made for voltage rectification, signal amplification, etc. Other gallium arsenide applications are the semiconductor "lasing" and microwave generation and also in several sensors to measure temperature, light or magnetic field.

Gallium supported ZSM-5 is one of the most active catalyst for light alkane dehydrogenation and aromatization [1, 7]. Its high alkane dehydrogenation and aromatization activity is attributed to the presence of bi-functional sites of non-framework gallium oxide species and zeolitic protons, located close to each other in the zeolite channels [29].

2.5 Literature review

Yingjie Ren *et al.* [1], studied on effect of acidity and pore geometry of zeolite on the propane dehydrogenation. They used 5 wt.% Ga_2O_3 supported on HZSM-48 (x), where x is the molar ratio of Si/Al that is 130, 160, and 220, and Ga_2O_3 supported on HZSM-5 (200) as catalysts. The reaction was operated using 200 mg of catalyst at 600 °C in fixed-bed flow reactor at atmospheric pressure and used CO_2 as a co-feed. It was found that Ga_2O_3/HZSM-48 (130) having higher acidity, as compared to Ga_2O_3/HZSM-48 (160) and Ga_2O_3/HZSM-48 (220), showed the highest activity. The increase in Si/Al ratio, decrease in acidity, led to the decrease in propane conversion. It was also found that Ga_2O_3/HZSM-5 (200) gave higher stability, as compared to Ga_2O_3/HZSM-48 (130) at 50 h on stream.

Shuai Tan *et al.* [2], tested the propane dehydrogenation using In_2O_3-Ga_2O_3 mixed oxides as catalysts. The reaction was performed using 0.3 g of catalysts at 600 °C in a U-shape fixed-bed reactor. It was found that all catalysts gave approximately 30% propane conversion and the catalyst with 2 mol% In_2O_3 98 mol% Ga_2O_3 gave the most propylene selectivity. However, the deactivation was found over these catalysts.

Yiwei Zhang *et al.* [4], used Pt supported on Sn-modified ZSM-5 as a catalyst for propane dehydrogenation. The reaction was operated using 2.0 g of catalyst at 590 °C and 0.1 MPa pressure in fixed-bed reactor and used H_2 as co-feed (H_2: C_3H_8 = 1: 4). It was found that PtNa/Sn-ZSM-5 gave relatively high propane conversion (~40%) and propylene selectivity (~95%), as compared to PtNa/HZSM-5 and PtSnNa/HZSM-5. However, slightly deactivation was found over these catalysts even H_2 was used as a co-feed.

Yiwei Zhang *et al.* [5], studied the propane dehydrogenation using Zn-modified supported platinum as catalyst. The reaction was occurred using the similar conditions as previous literature [4]. It was found that an increase in Zn content (0.5-1.5 wt.%) on ZSM-5 led to higher propane conversion and selectivity. However, 1.5 wt.% Zn gave lower propane conversion, as compared to 0.5 and 1.0 wt.%.

Miao Chen *et al.* [6], studied propane dehydrogenation under flow of CO_2 over supported indium oxides. The catalysts contained Al, Zn, Zr, Ti, Fe, Mg, Si, and Ce, with 20 molar percentage of In (for example In-Al-20). CO_2 was used as deactivation inhibitor that reacted with the deposited carbon on the catalyst surface to form CO (Boudouard reaction [30]). The reaction was operated using 200 mg of catalyst at 873 K under ambient pressure. The activity of catalysts were found in the order of In-Al-20 > In-Zn-20 > In-Zr-20 > In-Ti-20 > In-Fe-20 > In-Mg-20 > In-Si-20 > In-Ce-20. It was found that In-Al-20 gave a higher propane conversion (30%), as compared to In-Al-10 and In-Al-40 with 70% propylene selectivity. In addition, the deactivation was not found over these catalyst.

Fan Zhang *et al.* [31], also tested propane dehydrogenation with co-feeding CO_2 over 3 wt.% chromium oxide supported on ZSM-5 with sub-microsize. The reaction was performed using 0.2 g catalyst at 550 °C in fixed-bed reactor at atmospheric pressure. The results showed that ~30% propane conversion was obtained with 90% propylene selectivity. After the reaction, they treated catalyst with H_2/Ar and repeated the reaction. It was found that the propane conversion was decreased. It was proposed that after H_2 treatment, the active specie was Cr^{3+} where its activity is less than Cr^{6+}. In addition, regeneration of the catalyst under air flow at 550 °C provided propane conversion and propylene selectivity, similar to that over the fresh catalyst. It was suggested that the full recovery of the activity after air treatment was due to the removal of deposited carbon on the catalyst surface.

Vasant R. Choudhary *et al.* [29], studied on the effect of acidity on propane aromatization over Ga/H-ZSM-5 with 0-3 wt.% Ga loading and 35-132 Si/Al ratio. The reaction was operated at 550 °C in fixed-bed continuous flow reactor at atmospheric pressure. The results showed that an increase in Ga loading led to higher propane conversion and aromatics selectivity. However, an increase in Si/Al ratio led to lower propane conversion and aromatics selectivity.

Artit Ausavasukhi and Tawan Sooknoi [7] studied the ethane dehydrogenation over 3 wt.% [Ga]HZSM-5 using pulse reactor. The reaction was operated at 550-750 °C at atmospheric pressure under He and H_2 as carrier gas. The results showed that the ethane conversion was increased with temperature with 100% ethylene selectivity except for the reaction at 700 and 750 °C under H_2 carrier gas that methane was found as a cracking product. It was interestingly that the different carrier gas gave a significant difference in ethane conversion. It was suggested that after calcination, $[GaO]^+$ is the active species provided ~25% ethane conversion under He carrier gas. After the reduction, slightly higher activity was obtained (~30% ethane conversion), presumably due to the formation of more active Ga species (Ga^+). Under H_2 carrier gas, the catalyst show higher activity (~55% ethane conversion), presumably due to the formation of $[GaH_2]^+$ that is the most active species. However, $[GaH_2]^+$ can decompose in the absence of H_2.

CHAPTER 3

EXPERIMENTAL DETAILS

3.1 Chemicals and substrates

Chemical reagents	Grade of purity	Manufacturers
1. Gallium nitrate hydrate ($Ga(NO_3)_3.xH_2O$)	99.99%	ITALMAR
2. Propane gas	99.95%	
3. NH_4-ZSM-5 (Si/Al = 28)		ZEOLYST INTERNATIONAL
4. NH_4-ZSM-5 (Si/Al = 40)		
5. NH_4-ZSM-5 (Si/Al = 140)		ZEOLYST INTERNATIONAL
6. NH_4-ZSM-5 (Si/Al = 250)		ZEOLYST INTERNATIONAL
7. NH_4-ZSM-5 (Si/Al = 500)		ZEOLYST INTERNATIONAL
8. Deionized water		
9. Air zero gas	99.99%	PRAXAIR
10. Hydrogen gas	99.99%	PRAXAIR
11. Nitrogen gas	99.99%	PRAXAIR

3.2 Apparatus and instruments

1. Catalytic activity testing rig
2. Mass flow controller (AALBORG)
3. Tube furnace with a programmable temperature controller (CARBOLITE)
4. Quartz tube (8.0 mm O.D.)
5. Heating tape with a programmable temperature controller
6. Clamp
7. Gas chromatograph (Agilent 6890 Series)
8. Laboratory glassware
9. Laboratory plasticware
10. Trap condenser
11. Sieve (U.S.A standard sieve, AASHO N-92)
12. Gas adsorption analysis (Autosorb-1C, Quantachrome)

13. Temperature programmed reduction (TPR, Model TCD2-NIFED)

14. Temperature programmed desorption (TPD, Model TCD2-NIFED)

15. Inductively couple plasma mass spectrometer (ICP Quadrupole Mass Spectrometer, Thermo Scientific iCAP Qc ICP-MS)

3.3 Preparation of catalysts

3.3.1 Gallium loaded HZSM-5 (Ga-HZSM-5 (x))

The gallium loaded HZSM-5 catalysts with different Si/Al ratio (28, 40, 140, 250, 500) were prepared by wet-impregnation method using gallium nitrate ($Ga(NO_3)_3$) precursor. NH_4-ZSM-5 (28) was dried in an oven at 80 °C overnight and weighed (4.85 g). Gallium nitrate hydrate precursor was weighted (0.89 g) and was then dissolved using 200 drops of concentrate nitric acid and leaved it until fully dissolve. Then, 40 mL of DI water was used for dilute the dissolved precursor. The precursor solution was sprayed on the dried ZSM-5 support. After that, the prepared catalyst was dried in an oven at 80 °C overnight. The dried catalyst was calcined in a horizontal tube furnace under 60 mL/min flow of air zero at 550 °C with heating rate of 2 °C/min for 5 hours. Gallium supported on HZSM-5 with different Si/Al ratio were prepared using similar procedure.

3.4 Characterization of catalysts

3.4.1 Surface area analysis

Surface area of catalysts was determined using gas adsorption technique. The sample was weighed (40-50 mg) and loaded into a cleaned and dried sample cell. After that, the sample was degassed at 300 °C for 8 hours. The sample cell was then removed from the out-gassing station after filling up with nitrogen and was attached to the analysis station. The adsorption isotherm was measured in a pressure range of 0.05-0.30 P/P_0 at -196 °C.

3.4.2 Temperature programmed reduction

In order to investigate the reducibility of catalysts, the temperature programmed reduction (H_2-TPR) was operated using thermal conductivity detector (TCD). A 100 mg of sample was put into a quartz tube reactor that is located inside a temperature-regulated furnace. Before the H_2-TPR operation, each sample were activated under a flow of air zero with a flow rate of 30 mL/min at 450 °C with heating rate of 2 °C/min for 1 h and then cooled down to below 100 °C. A heating rate of 10 °C/min and 30 mL/min of 10% H_2 in Ar was applied for the H_2-TPR analysis. Water produced from the reduction process was trapped in a U-shape stainless trap at -196 °C (liquid nitrogen) before entering the TCD.

3.4.3 Temperature programmed desorption

3.4.3.1 Ammonia temperature programmed desorption (NH_3-TPD)

Acidity of catalysts was investigated by the temperature programmed desorption of ammonia (NH_3) using the TCD. The catalyst was pretreated with similar procedure as that for H_2-TPR except cooling down to room temperature. The NH_3 was adsorbed with a flow rate of 30 mL/min for 1 h using 1% NH_3 in He and continue with flushing of the excess physisorbed NH_3 using He with a flow rate of 30 mL/min for 1 h. The heating rate of 10 °C/min was applied for the NH_3 desorption procedure under He flow.

3.4.3.2 Isopropylamine temperature programmed desorption (IPA-TPD)

Brønsted acidity of catalysts was measured by the temperature programmed desorption of isopropylamine (IPA) using flame-ionization detector (FID). The catalyst was pretreated similar procedure as that for the NH_3-TPD. A 0.1 μL of the IPA was repeatedly injected to the reactor at 40 °C under a flow of He (30 mL/min) for the IPA adsorption (total 12 μL). Then, the temperature was increased to 100 °C (10 °C/min) in order to flush the excess physisorbed IPA for 1 h. After that, a heating rate of 10 °C/min was applied for desorption of propylene, a product from the reaction of the IPA with the Brønsted acid sites.

3.4.4 Inductively couple plasma mass spectrometry

In order to identify gallium content (%loading) of the catalysts, the inductively couple plasma mass spectrometry (ICP-MS) was operated using ICP Quadrupole Mass Spectrometer, Thermo Scientific iCAP Qc ICP-MS. The standard gallium solution was prepared with various concentration (0.01-0.1 ppm) using gallium nitrate solution. The sample solution was prepared by digesting the catalyst in the aqua regia solution (3:1 HCl: HNO_3 v/v) and then diluted with DI water. The intensity of the standard gallium solution was plotted as a calibration curve. The intensity of the sample solution was used for calculating the % Ga loading.

3.4.5 X-Ray powder diffraction

The structure of catalyst was determined by X-ray diffractometer (XRD). The sample was prepared by packing the catalyst into the sample holder. CuKα X-ray beam was used for analysis at 40 kV and 30 mA. The sample was scanned over the angle ranged from 2θ: 5° to 70° with 2 deg./min. and 0.02 2θ/step increments. X-ray diffraction pattern of the sample was compared with the X-ray diffraction pattern of standard catalyst for structure determination.

3.4.6 X-Ray absorption near edge spectroscopy

The oxidation state and species of catalysts were evaluated using Synchrotron beam. A 25 mg of calcined sample was weighted and pressed with a 5 mm diameter mold followed by placing into the sample holder. The *in-situ* experimental was operated by temperature-programming from 50-300 °C (2 °C/min) under a flow of air (30 mL/min), 300-650 °C for 1 h (5 °C/min) under a flow of 50% v/v hydrogen (30 mL/min), and held at 650 °C for 1 h under a flow of nitrogen (30 mL/min). The XANES spectrum was collected for every 10 °C interval during the ramping and every 5 min interval during the holding at 650 °C.

3.5 Catalytic activity testing

Gas phase catalytic dehydrogenation of propane was investigated using fixed-bed continuous flow reactor made with quartz tube (8.0 mm O.D.) at atmospheric pressure. The schematic diagram of the catalytic testing rig is shown in Figure 3.1. The catalyst was packed in the middle of reactor while top and bottom of the reactor was filled with quartz wool and quartz beads. The reactor was installed inside the temperature-controlled furnace. The gas flow rate was controlled by AALBORG mass flow controller and measured using bubble flow meter. Before testing, the catalyst was activated under 30 mL/min flow of air zero at 450 °C with a heating rate of 2

°C/min for 1 h. Then, N_2 was flushed to eliminate the remaining air in the line. After that, the catalyst was reduced under 50 mL/min flow of H_2 600 °C with a heating rate of 10 °C/min for 3 h. The reaction was tested at 400-550 °C.

Propane was flowed through the catalyst bed with a flow rate of 10 mL/min without carrier gas. The catalytic testing was continued at least 3 h on stream. The products mixture was flowed out of the reactor and passed through a gas sampling loop of the GC. In order to prevent products condensation, the line after the reactor was heated using temperature-controlled heating tape at 150 °C. The summary of the reactor set up and reaction conditions are shown in Table 3.1.

3.6 Products analysis

The products was analyzed using online-gas chromatograph with flame ionization detector (GC-FID). The gas sample was collected in gas sampling loop, then injected into the GC column (HP-PLOT, 30 m length, 0.53 mm internal diameter, 15.0 μm film thickness). The following column flow rate and temperature program was used for the products analysis: the initial flow rate was held at 2.8 mL/min for 4 min, then ramping to 3.8 mL/min at the rate of 1 mL/min and hold for 25 min. The initial temperature was set at 50 °C for 5 min, followed by ramping to 150 °C at a heating rate of 20 °C/min and hold for 10 min. Then the oven was ramp to 180 °C at a heating rate of 10 °C/min and hold for 7 min. N_2 was used as carrier gas. Each components was identified by comparing to the standard gas. The area of each components was measured, and then the propane conversion and products yield was calculated.

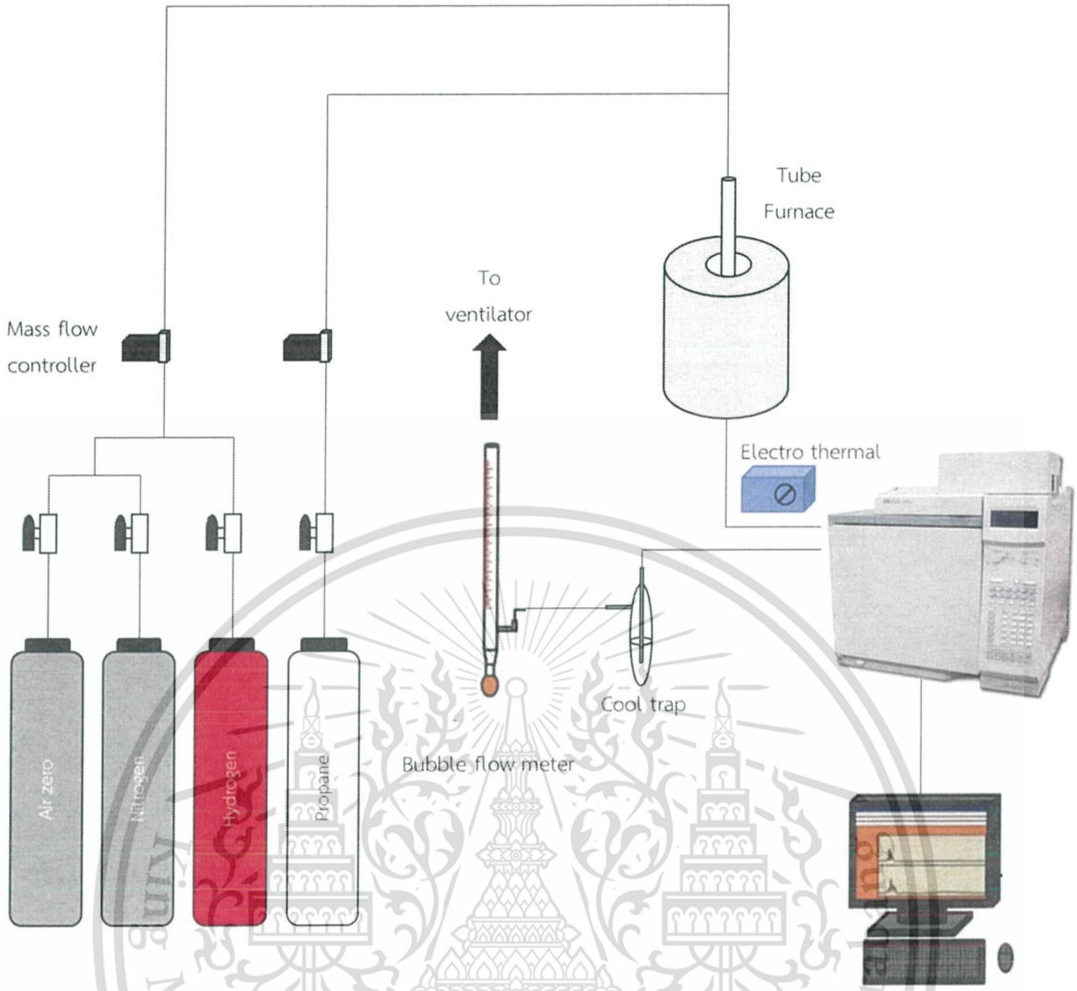

Figure 3.1 Schematic of catalytic testing rig

Table 3.1 Summary of reactor set up and reaction conditions

Parameters	Value
Reactor outside diameter (mm)	8.0
Bed length (mm)	10-50
Catalyst weight (g)	0.2-0.5
Catalyst pellet size (μm)	600-850
Catalyst activation: - Temperature (°C) - Heating rate (°C/min) - Gas	 450 °C for 1 h 2 Air zero (30 mL/min)
Catalyst reduction: - Temperature (°C)	 600 °C for 3 h

- Heating rate (°C/min) - Gas	10 H_2 (50 mL/min)
Reaction temperature (°C)	400-550
Reaction pressure (atm)	Atmospheric pressure

CHAPTER 4

RESULTS AND DISCUSSION

4.1 Characterization

4.1.1 Catalysts structure

Crystallinity of HZSM-5 (28) and Ga-HZSM-5 (28) were identified using XRD technique. The results are shown in Figure 4.1 below.

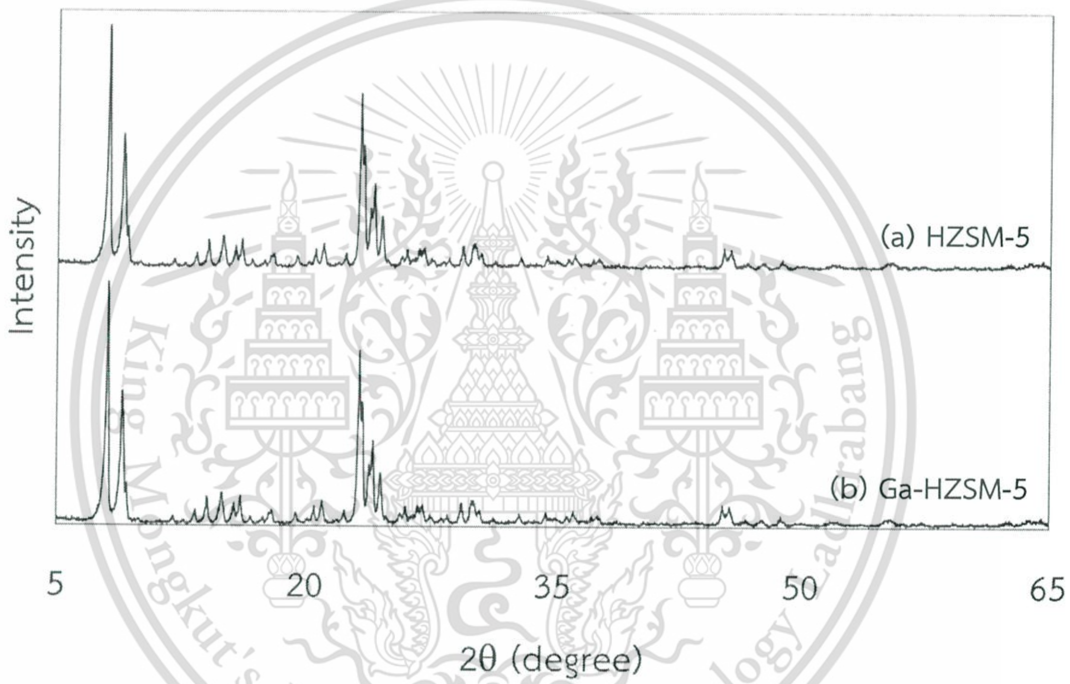

Figure 4.1 XRD patterns of (a) HZSM-5 (28) and (b) Ga-HZSM-5 (28).

It can be seen that HZSM-5 (28) and Ga-HZSM-5 (28) show similar XRD patterns, in which major peaks were found at 2θ = 8.12, 9.02, 23.24, and 24.06 degrees. No change in crystallinity was observed after gallium was incorporated, indicating that the loaded gallium is located as non-framework species on either cavities or external surface of HZSM-5. Nevertheless, there is no gallium oxide phase observed from the XRD pattern (Figure 4.1b) presumably due to the fact that the gallium species is highly dispersed on the zeolite.

4.1.2 Acidity and gallium loading

The characteristics of the catalysts including the Brønsted acidity, and percentage of gallium loading are shown in Table 4.1.

Table 4.1 Percentage of gallium loading, gallium content, and Brønsted acidity of catalysts and supports.

Catalysts	Total Ga content[a]		Excess Ga[b] (mmol/g)	Brønsted acidity of catalysts[c] (mmol H^+/g)	Brønsted acidity of HZSM-5 supports[c] (mmol H^+/g)
	(wt.%)	(mmol/g)			
Ga-HZSM-5 (28)	2.30	0.33	0.00	0.21	0.56
Ga-HZSM-5 (40)	2.34	0.34	0.00	0.00	0.38
Ga-HZSM-5 (140)	2.32	0.33	0.19	0.00	0.14
Ga-HZSM-5 (250)	2.33	0.33	0.26	0.00	0.07
Ga-HZSM-5 (500)	2.33	0.33	0.29	0.00	0.04

a: from ICP-MS

b: by subtraction of total Ga content (mmol/g) with Brønsted acidity of HZSM-5

c: from IPA-TPD

As seen in the Table 4.1, the gallium content of all catalysts are in the same range. The acidity of HZSM-5 supports were decreased with an increase in Si/Al ratio. For a certain Si/Al ratio, the acidity of catalysts was decreased when the gallium was loaded. Kikuchi *et al.* [32] reported that the loaded gallium would be in a form of Ga_2O_3 that could react with Brønsted acid site of the zeolite at high temperature, forming "exchangeable gallium oxide ($[GaO]^+$) species" as shown below.

$$Ga_2O_3 + 2H^+ Z^- \longrightarrow 2[GaO]^+ Z^- + H_2O$$

Alternatively, there are some studies [33, 34] reported that the loaded gallium can be in the form of $Ga(OH)_2^+$ species that could exchange with the proton in the zeolite. This species can also be dehydrated to form $[GaO]^+$ species after the calcination as shown below.

$$[Ga(OH)_2]^+ Z^- \longrightarrow [GaO]^+ Z^- + H_2O$$

Hence, the observed decrease in the Brønsted acidity of the catalysts after the gallium was loaded would be resulted from the fact that the proton is substituted with the exchangeable gallium oxide ($[GaO]^+$). Since the number of proton is higher or similar to the gallium content in the catalysts with Si/Al ratio 28 and 40, it was suggested that all gallium over Ga-HZSM-5 (28) and Ga-HZSM-5 (40) are in the form of $[GaO]^+$ species.

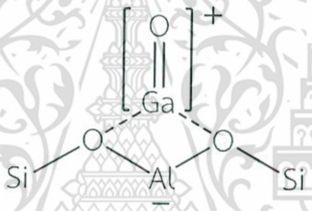

Interestingly, the Brønsted acid site is remained only in Ga-HZSM-5 (28) because the amount of gallium loaded is lower than the Brønsted acidity of the parent HZSM-5 (28). While the gallium loading in Ga-HZSM-5 (40) is similar to the Brønsted acidity. Therefore, small amount of Brønsted acid site was retained over this catalyst. In the same view, the Brønsted acidity of the catalysts containing Si/Al ratio more than 140 were not observed. This is because the gallium content is higher than the number of Brønsted acid site in the parent HZSM-5. It was suggested that the excess gallium would be presented as aggregate oxides dispersed in the cavities or external surface of the parent zeolite, so called "extra-framework gallium oxide species". Accordingly, when the gallium was incorporated to the parent HZSM-5, the BET surface area and micropore volume of catalysts are slightly decreased as shown in Table 4.2.

Table 4.2 The BET surface area and micropore volume of the catalysts.

Catalysts	Surface area (m^2/g)		Micropore volume (μL/g)	
	Without Ga	With Ga loading	Without Ga	With Ga loading
Ga-HZSM-5 (28)	414	351	192	163
Ga-HZSM-5 (40)	420	398	199	185
Ga-HZSM-5 (140)	419	378	207	158
Ga-HZSM-5 (250)	397	359	165	153
Ga-HZSM-5 (500)	402	379	169	161

It can be seen that surface area and micropore volume of all Ga-HZSM-5 catalysts are reduced after gallium was loaded. For the catalysts with Si/Al ratio of 28, a significant decrease in surface area and micropore volume is observed. It was suggested that the highly dispersed gallium oxide is located as the exchangeable site ($[GaO]^+$) in zeolite cavities leading to a lower adsorption capacities. While extra-framework gallium oxides present in catalysts with higher Si/Al ratio trend to disperse on external surface of the zeolite. Hence, the reduction in surface area and micropore volume of these catalysts is less pronounced. However, all catalysts can be referred as high surface area materials.

4.1.3 Catalysts reducibility

The reducibility of the Ga-HZSM-5 catalysts were investigated using H_2-TPR as shown in Figure 4.2.

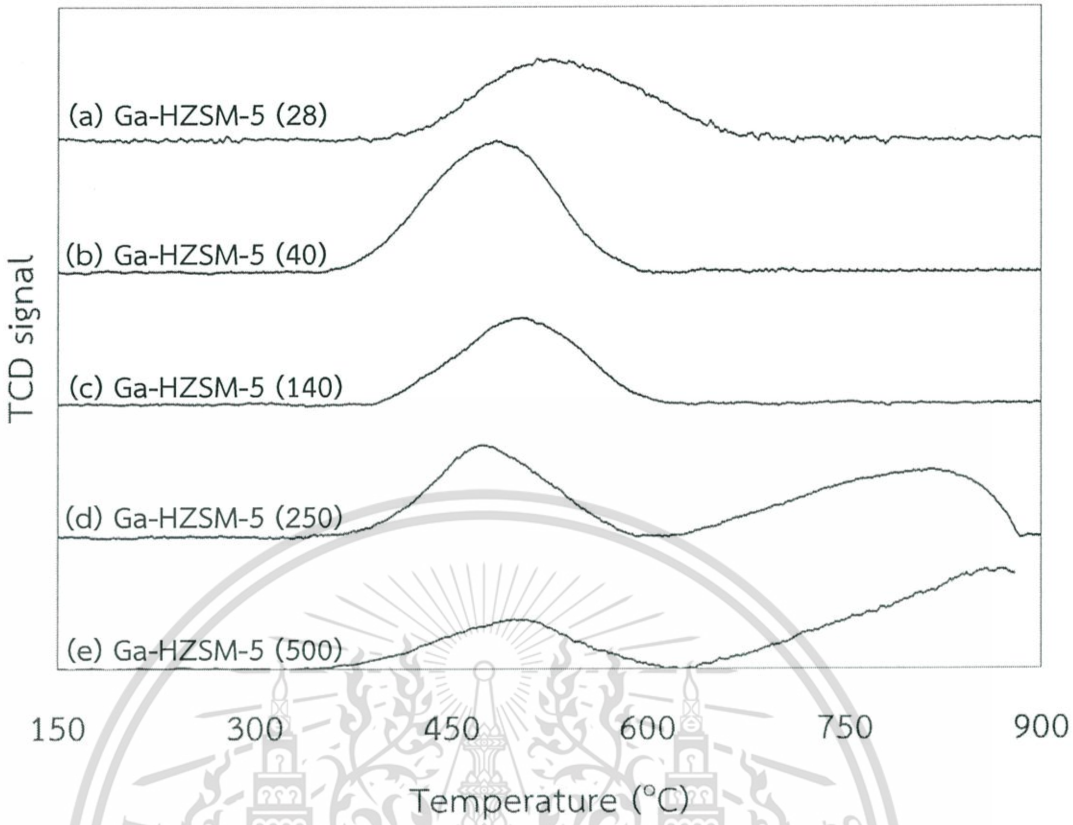

Figure 4.2 H_2-TPR profiles of (a) Ga-HZSM-5 (28), (b) Ga-HZSM-5 (40), (c) Ga-HZSM-5 (140), (d) Ga-HZSM-5 (250) and (e) Ga-HZSM-5 (500) under a flow of 10% H_2/Ar (30 mL/min) at 150-900 °C with a heating rate of 10 °C/min.

It can be seen that, the catalysts containing gallium as exchangeable species (Ga-HZSM-5 (28) and Ga-HZSM-5 (40)), show only one reduction peak in the range of 400-600 °C. This is assigned for the reduction of Ga^{3+} to Ga^{+} [7, 35]. It can be noticed that, a slight higher temperature was found for the reduction of Ga-HZSM-5 (28), as compared to Ga-HZSM-5 (40). It was suggested that in Ga-HZSM-5 (28), the $[GaO]^{+}$ species is polarized by the proximate Brønsted acid site remained in the catalysts. This results in the low electron density on the gallium species which decrease an ability for the H-H dissociation. Hence, the higher temperature is observed for the reduction of Ga-HZSM-5 (28), as compared to Ga-HZSM-5 (40).

In addition to the H_2-TPR, the presence of Ga^{3+} in the sample upon calcination is supported by in-situ XANES as shown in Figure 4.3.

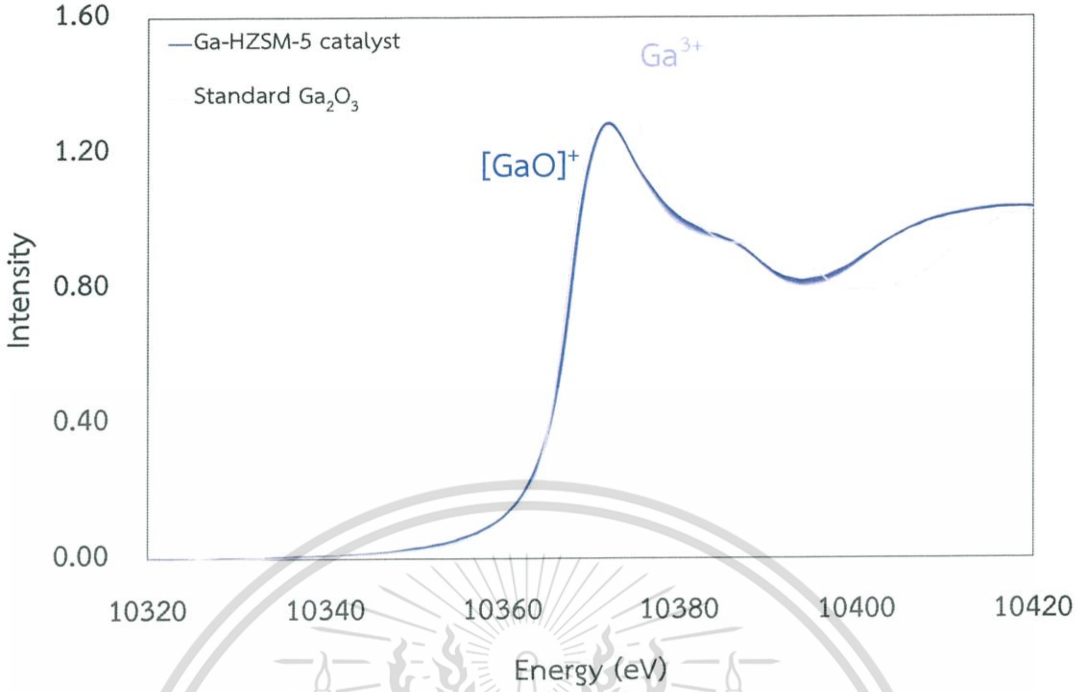

Figure 4.3 In-situ XANES spectra of Ga-HZSM-5 (28) under a flow of air (30 mL/min) at 25-300 °C with a heating rate of 2 °C/min, compared with standard Ga_2O_3.

It can be seen that the edge energy of exchangeable gallium species and standard Ga_2O_3 appear precisely at 10367.7 eV that is attributed to Ga^{3+}. In addition, the white line intensity at 10372 eV, the characteristic of gallium coordination with oxygen, of sample is lower than that of Ga_2O_3 standard suggesting that the coordination number of Ga^{3+} species in the sample is predominantly tetrahedral, as compared to the standard Ga_2O_3 that contain both tetrahedral and octahedral. This is consistent with the $[GaO]^+$ species reported in literature [36] as discussed previously in section 4.1.2.

The reduction of $[GaO]^+$ species is further investigated by in-situ XANES at 300-650 °C as shown in Figure 4.4.

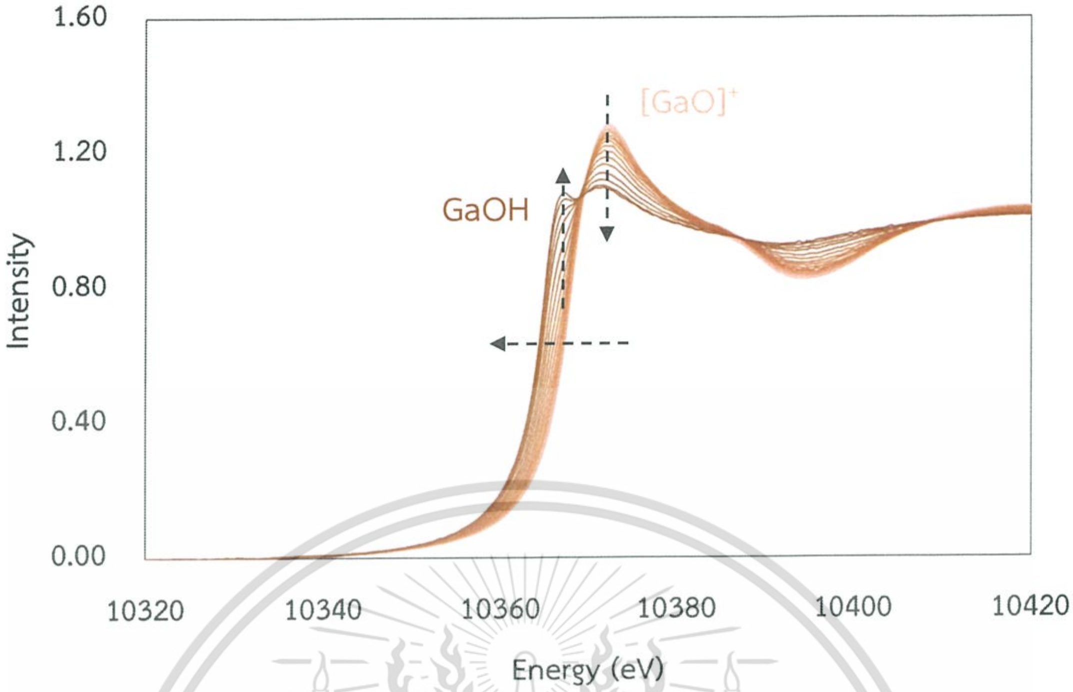

Figure 4.4 In-situ XANES spectra of Ga-HZSM-5 (28) under a flow of 50% H_2/N_2 (30 mL/min) at 300-650 °C with a heating rate of 5 °C/min.

It can be seen that the edge energy of the exchangeable gallium ($[GaO]^+$) was shifted from 10367.7 eV to 10364.7 eV with an increase in reduction temperature from 300-650 °C. In line with the H_2-TPR, this implied that the oxidation state of gallium was reduced from 3+ ($[GaO]^+$) to 1+ (Ga^+). It is suggested that the $[GaO]^+$ is subjected to reduce to form "gallium hydroxide (GaOH) species" and Brønsted acid site as shown below.

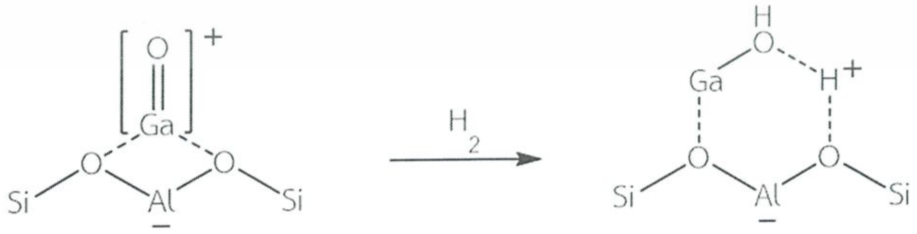

In addition, the white line at 10372 eV was also decreased together with a generation of new white line at 10366 eV. It was suggested that the coordination number of gallium with oxygen of $[GaO]^+$ species associated at the exchangeable site

(4 coordination) is decreased and the white line at 10366 eV is proposed to be a characteristic of gallium coordination with oxygen in GaOH species associated with an oxygen bridge (2 coordination). In line with this view, Kazansky *et al.* [37] reported that OH stretching of GaOH at 3665 cm^{-1} in DRIFT spectra is presented after the catalysy is reduced at 500 °C, confirming the presence of GaOH. According to the reduction of $[GaO]^+$ to the GaOH, the Brønsted acid site would be generated. This leads to the increase in the strong acid site of the catalyst after the reduction as evidenced in Table 4.3.

Table 4.3 NH_3-TPD results of non-reduced and reduced Ga-HZSM-5 (28).

Catalysts	Weak acidity (mmol/g)	Strong acidity (mmol/g)
Non-reduced Ga-HZSM-5 (28)	0.80	0.53
Reduced Ga-HZSM-5 (28)	0.86	0.82

After reduction at 650 °C and hold under N_2 for 1 h the edge energy is remained at 10364.7 eV. However, the white line at 10366 eV (GaOH species) was gradually disappeared while that at 10372 eV was proportionally increased with the longer holding time, as shown in Figure 4.5.

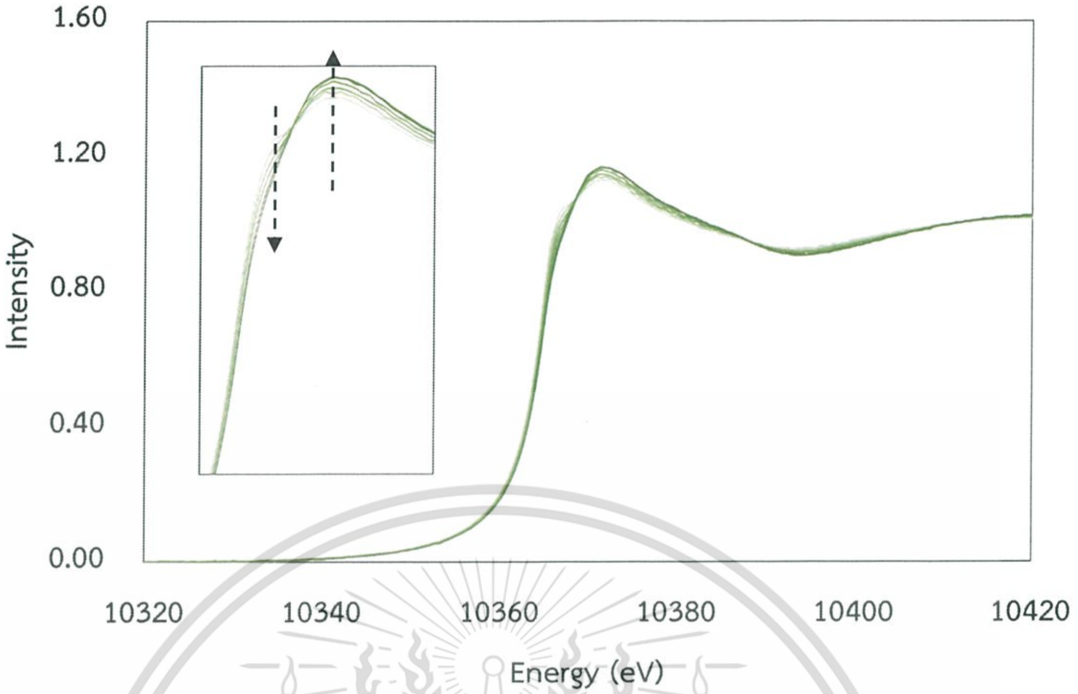

Figure 4.5 In-situ XANES spectra of Ga-HZSM-5 (28) under a flow of N_2 (30 mL/min) at 650 °C. Spectrum is collected at every 5 min interval over 1 h on stream.

This implies that the oxidation state of gallium remains the same (Ga^+). While the coordination number of gallium with oxygen is increased, as seen from the increase in white line intensity at 10372 eV. It was suggested that GaOH react with Brønsted acid site and dehydrate to Ga^+ site as shown below.

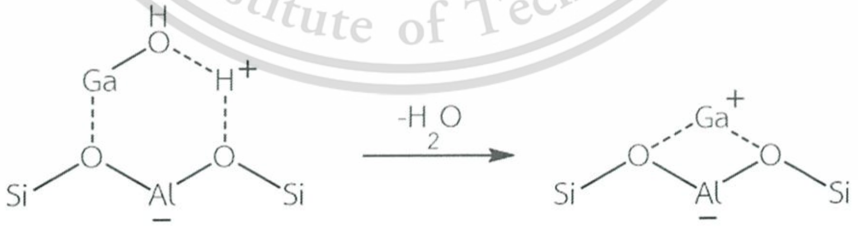

The decomposition of GaOH species is further validated by two cycles of H_2-TPR as shown in Figure 4.6.

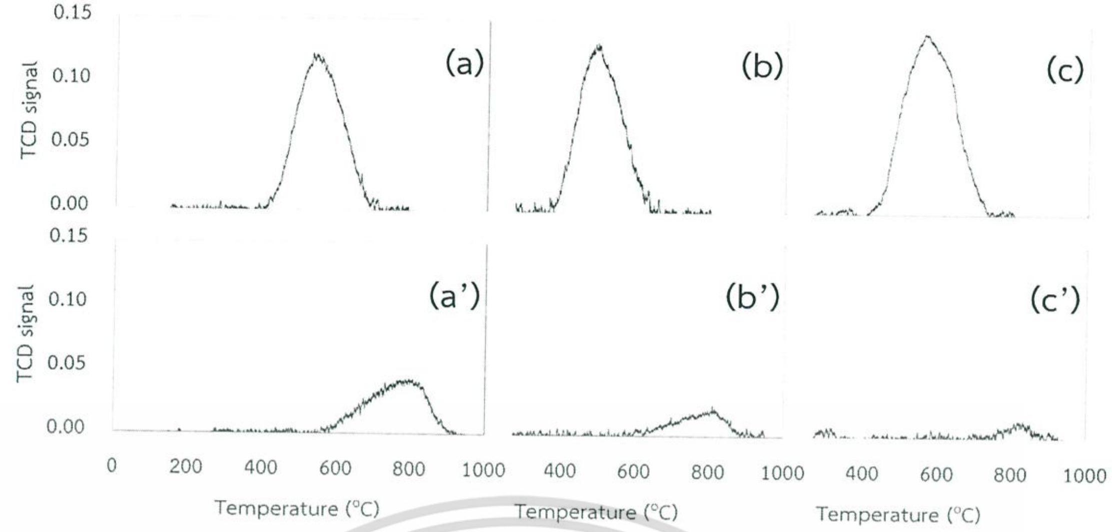

Figure 4.6 Two cycles of H_2-TPR of Ga-HZSM-5 (28); a, b, and c are the first cycle of H_2-TPR. a', b', and c' are the second cycle of H_2-TPR after holding at 800 °C under a flow of He for 3, 1, and 0 h, respectively.

As discussed previously, $[GaO]^+$ species (I) can be reduced to GaOH and Brønsted acid site (II) in a range of 400-600 °C as shown in Figure 4.6(a). After the sample was completely reduced, then held under inert gas at 800 °C for 3 h, and cooled down, the secondary H_2-TPR cycle was performed without exposing the sample to the atmospheric oxygen. Surprisingly, the H_2-consumption was found in the second cycle of H_2-TPR of the completely reduced $[GaO]^+$ (Figure 4.6(a')), indicating that the fully reduced gallium species can consume H_2. This is because the GaOH react with the Brønsted acid site to Ga^+ species (III) during holding under inert at 800 °C for 3 h and such Ga^+ formed can consume H_2 for the formation of "dihydrido gallium ($[GaH_2]^+$) species" (IV) [7, 37], as shown below. Hence, reduction temperature of the second cycle (for $[GaH_2]^+$ formation) is higher than the first cycle (reduction of GaO^+ to GaOH and Brønsted acid).

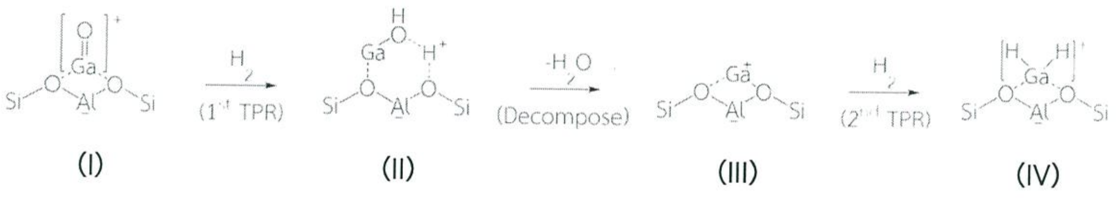

Accordingly, H_2-consumption of the second cycle would depend on number of Ga^+ available after GaOH dehydration. As GaOH is decomposed during the holding under inert gas at high temperature, the generation of Ga^+ would depend on the holding time as seen in Figure 4.6(b') and (c'). It can be seen that the shorter the holding time, the lower the H_2-consumption were observed. This indicates that the lower number of Ga^+ species can be generated. If the sample was promptly cooled down from 800 ^oC, the GaOH and the Brønsted acid site would be largely retained in the catalyst. Only small amount of Ga^+ would be presented and hence low H_2-consumption are observed in the secondary H_2-TPR of Figure 4.6(c').

It can be concluded at this stage that after the calcination, the gallium is in the form of exchangeable $[GaO]^+$ species. When this species is completely reduced, the GaOH species and the Brønsted acid site are primarily generated. However, GaOH can be dehydrated to Ga^+ by reaction with the Brønsted acid site at high temperature, as seen by the decrease in white line intensity of XANES. Under a flow of H_2, the $[GaH_2]^+$ species can be formed from the H_2 dissociation over Ga^+ after the decomposition of GaOH, as seen from the secondary H_2-TPR. The XANES spectra of sample that contain different gallium species ($[GaO]^+$, GaOH, and Ga^+) are compared in Figure 4.7.

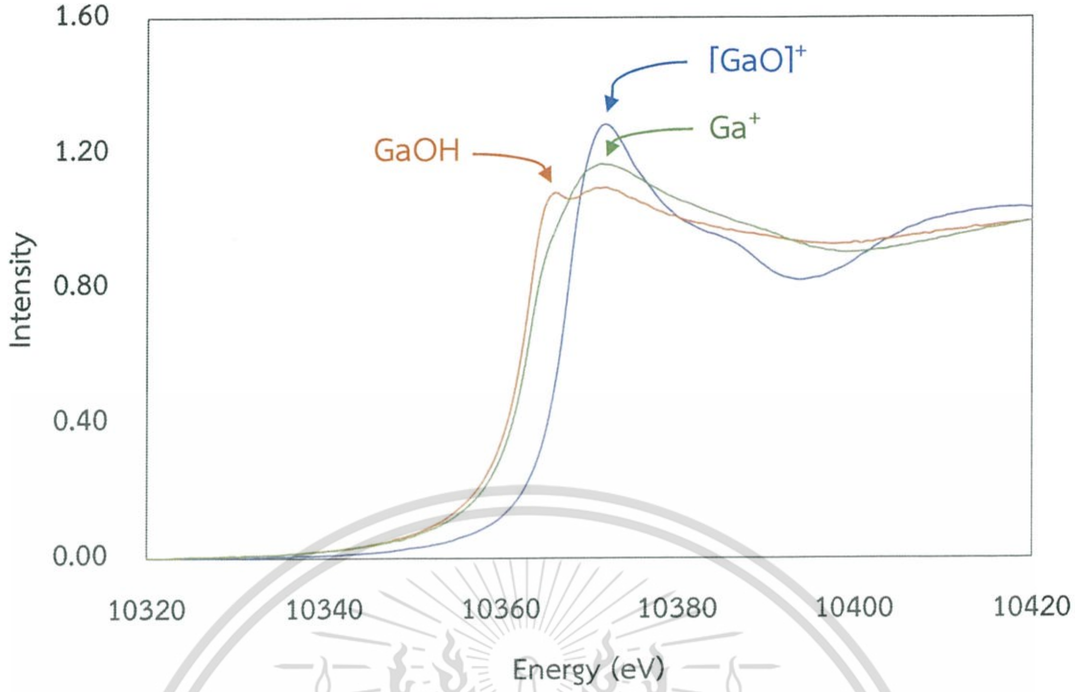

Figure 4.7 Comparison of XANES spectra of Ga-HZSM-5 (28) species: (blue) $[GaO]^+$, (orange) GaOH, and (green) Ga^+.

In addition to exchangeable $[GaO]^+$ species, the H_2-TPR also reviews the reduction of the extra-framework gallium,. As Si/Al ratio of the catalyst is increased, the reduction peak at 400-600 °C is decreased (Figure 4.2) due to the lower amount of exchangeable gallium species ($[GaO]^+$) in the catalysts. However, the new reduction peak above 600 °C appears. Such higher reduction temperature is designated for the reduction of extra-framework gallium oxide that could be Ga_xO_y aggregates [38] highly dispersed in the zeolite cavities. This is because the gallium content remain the same for all catalysts. The increase in the Si/Al ratio would lead to the increase in number of extra-framework gallium oxide species, as discussed previously by IPA-TPD in section 4.1.2. Therefore, the increase in intensity of this peak is observed over catalysts with higher Si/Al ratio (Figure 4.2). It is noted that the small amount of extra-framework gallium oxide is presented over the Ga-HZSM-5 (140). Hence, the reduction of extra-framework gallium oxide was not observed.

The reduction of catalysts that contain extra-framework gallium oxide at 650 °C was also investigated by XANES as shown in Figure 4.8.

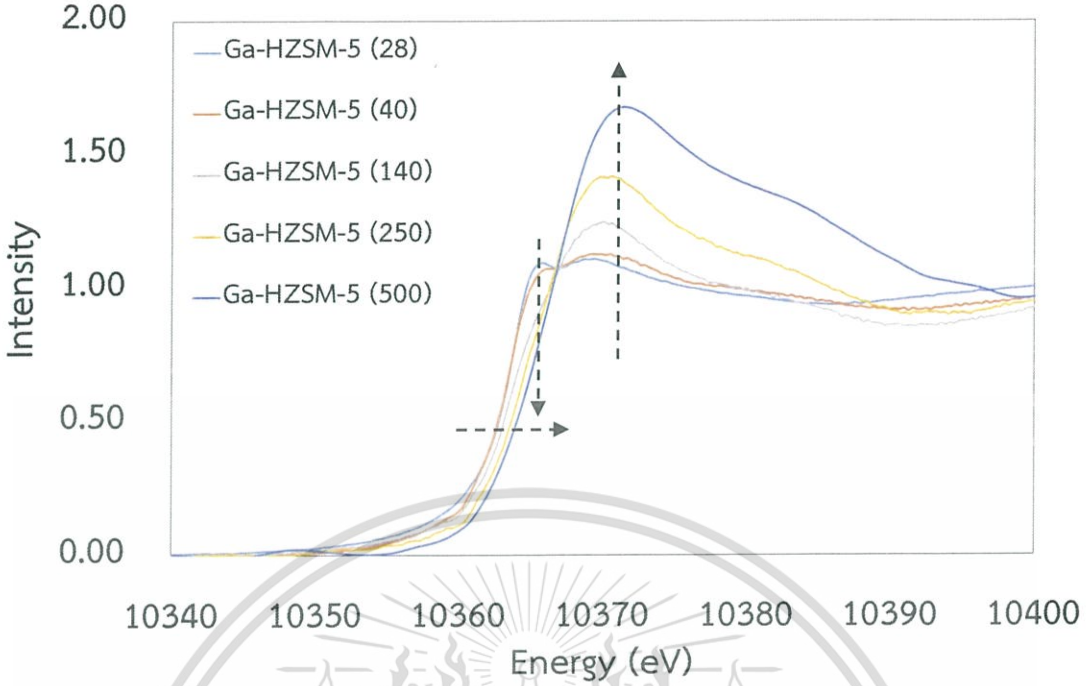

Figure 4.8 XANES spectra of Ga-HZSM-5 Si/Al ratio = 28, 40, 140, 250, and 500 after reduction at 650 °C

It can be seen that despite reduction at 650 °C, the edge energy is increased with Si/Al ratio (10364.4 to 10367.7 eV). This indicates that the Ga^{3+} is remained especially in the catalysts with high Si/Al ratio (more than 140). It is because the extra-framework gallium oxide cannot be completely reduced at 650 °C. The extra-framework gallium species over neutral charge surface has been previously proposed by Faro [39] as 4-coordinated binuclear gallium species that is presented when the gallium loading is increased. In line with this view, Cybulskis [40] reported that the gallium active site for propane dehydrogenation contain 4 coordinations with oxygen atom. This leads to the suggestion that the species of extra-framework would be presented as ($[Ga_2O_2]^{2+}$) species bonded with internal silanol as shown below [41].

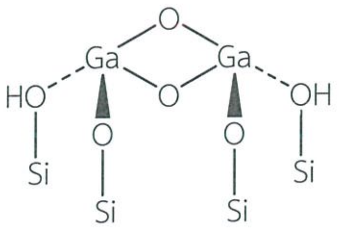

Since the extra-framework are increasingly presented in catalysts with Si/Al ratio, the reducibility of the catalysts are decreased when the Si/Al ratio is increased. In addition, the white line intensity at 10366 eV (GaOH species) is disappeared for the catalysts contain high Si/Al ratio (more than 140). This is because the small amount of GaOH is presented, as discussed previously by H_2-TPR in Section 4.1.3. While the increase in white line intensity at 10372 eV (Ga-O bond in $[Ga_2O_2]^{2+}$) is observed for the catalysts with higher Si/Al ratio (140, 250, and 500). This is due to the higher amount of extra-framework $[Ga_2O_2]^{2+}$ presents in the catalysts as shown in H_2-TPR (Figure 4.2).

4.2 Catalytic propane dehydrogenation

4.2.1 Effect of reaction temperature

The effect of reaction temperature is studied at 400, 450, 500, and 550 °C and the result is shown in Figure 4.9.

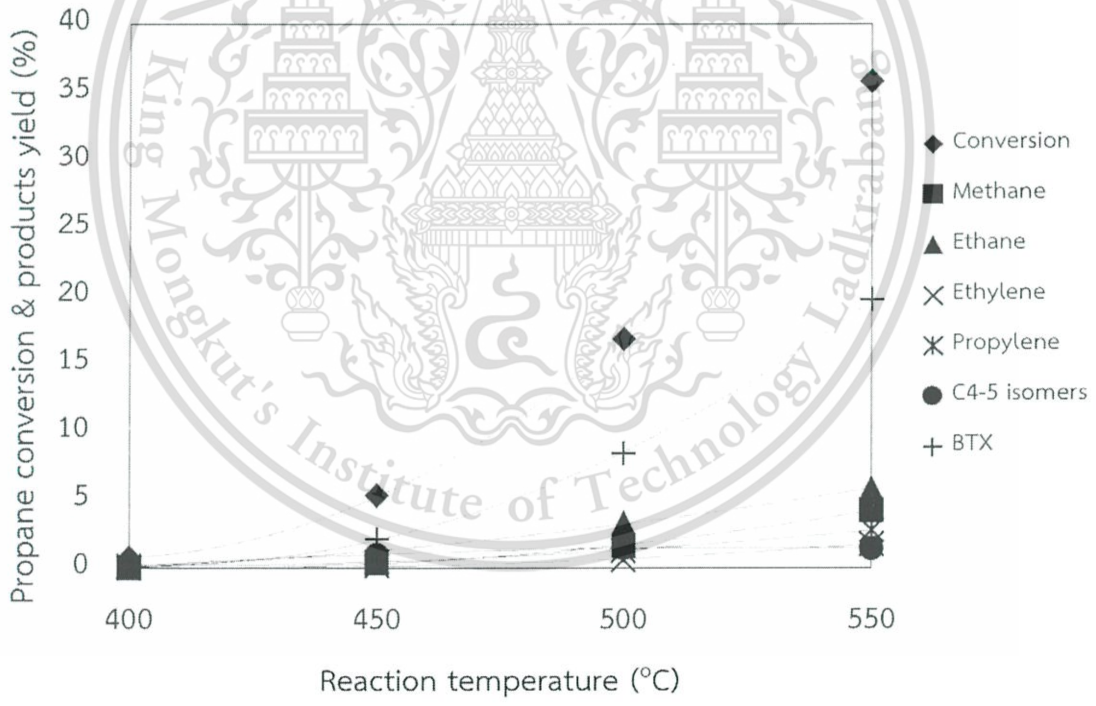

Figure 4.9 Effect of reaction temperature on propane dehydrogenation over Ga-HZSM-5 (28) catalyst. (Reaction conditions: temperature = 400-550 °C, catalyst weight = 0.2 g, W/F = 5.43 g.h.mol^{-1}, pure propane feed rate = 15 mL/min. Catalyst was activated under a flow of air (30 mL/min) at 450 °C for 1 h with a heating rate of 2 °C/min and reduced under a flow of H_2 (50 mL/min) at 600 °C for 3 h with a heating rate of 10 °C/min.)

It can be seen that propane conversion is increased (0.75-35.80%) with the reaction temperature (400-550 °C). However, the major products obtained are single ring aromatics including benzene, toluene, and xylene (BTX). Only small amount of propylene can be obtained at this reaction condition. It is suggested that the BTX are secondary products from the hydrocarbon pools. The pools are known to be produced from the conversion of propylene initially generated via propane dehydrogenation [38]. In addition, the hydrocarbon pool within the zeolite cavities containing gallium can act as hydrogen acceptor and promote dehydrogenation, particularly at high temperature. Accordingly, the secondary products formation is readily facilitated in the zeolite cavities at high conversion. Therefore, the initial activity for the propane dehydrogenation over gallium loaded HZSM-5 cannot be observed under the reaction condition with high propane concentration in the feed.

In order to avoid the formation of hydrocarbon pool and the secondary products, the propane feed was hence diluted with N_2. The result from the low concentration of propane was compared as shown in Table 4.4.

Table 4.4 The effect of feed dilution at 550 °C.

Conditions	Propane conversion (%)	Yield (%)						Selectivity (%)	
		Methane	Ethane	Ethylene	Propylene	$C_{4\text{-}5}$ isomers	BTX	Propylene	BTX
Pure feed	35.8	4.2	5.8	1.8	2.8	1.5	19.7	7.8	55.0
Diluted feed (20 %v/v)	11.1	0.3	0.4	1.6	6.4	1.0	1.4	57.7	12.6

With the same W/F, higher propylene yield and selectivity can be obtained from this condition. Nevertheless, the propane conversion was significantly dropped after the dilution of feed with N_2. This is because, as the feed concentration is decreased, the adsorption of the propane on the catalyst surface is also reduced. In addition, the produced propylene can be readily desorbed from the active site. Hence, the generation of hydrocarbon pool and BTX products are suppressed. With these conditions (diluted propane at reaction temperature 550 °C), the initial activity for propane dehydrogenation can be further investigated.

4.2.2 Effect of gallium species

As previously discussed, the $[GaO]^+$ species is presented in Ga-HZSM-5 (28) after calcination, while Ga^+ is obtained after reduction. The activity of $[GaO]^+$ and Ga^+ were tested for propane dehydrogenation, as compared with the parent HZSM-5 (Table 4.5).

Table 4.5 The effect of non-reduced and reduced gallium species. (Reaction conditions: temperature = 550 °C, catalyst weight = 0.2 g, W/F = 5.43 $g.h.mol^{-1}$, feed rate = 15 mL/min, carrier gas = 60 mL/min. Catalyst was activated under a flow of air (30 mL/min) at 450 °C for 1 h with a heating rate of 2 °C/min and reduced under a flow of H_2 (50 mL/min) at 600 °C for 3 h with a heating rate of 10 °C/min.)

Catalysts	Propane conversion (%)	Yield (%)						Selectivity (%)	
		Methane	Ethane	Ethylene	Propylene	C_{4-5} isomers	BTX	Propylene	BTX
HZSM-5 (28)	6.4	1.7	0.1	3.1	1.5	0.0	0.0	23.4	0.0
Non-reduced Ga-HZSM-5 (28)	30.5	1.2	1.6	3.1	6.5	1.2	17.0	21.3	55.7
Reduced Ga-HZSM-5 (28)	11.1	0.3	0.4	1.6	6.4	1.0	1.4	57.7	12.6

From Table 4.5, it was found that the catalysts containing gallium promote higher propane conversion, as compared to the parent HZSM-5 (28). It is well known that the C-H activation of light alkane can be facilitated over the gallium incorporated HZSM-5 [7, 29, 34]. The non-reduced catalyst provides a higher activity, but particularly for the BTX yield. While the reduced catalyst (Ga^+) shows a high selectivity to propylene, but lower activity. This may be attributed from both (i) higher crystallinity and (ii) nature of active species. As seen from the XRD pattern (Figure 4.10), the XRD of the spent catalysts show that the crystallinity of the non-reduced catalyst is higher than that of the reduced one. This is presumably due to the low stability of Ga-HZSM-5 (28) when reduced at high temperature (600 °C).

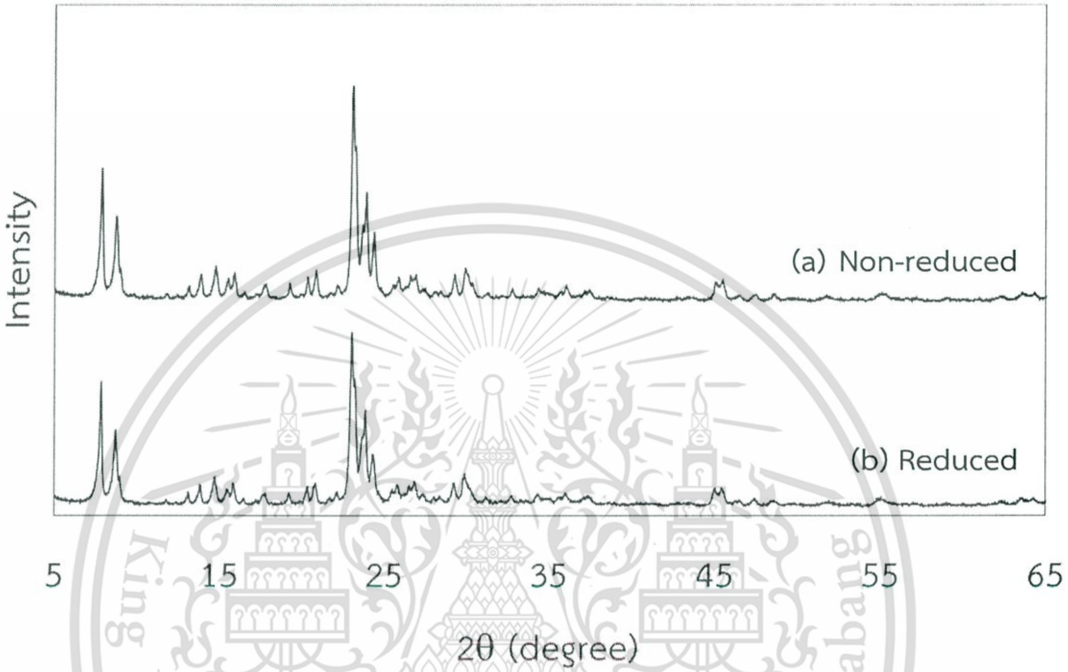

Figure 4.10 Comparison of the crystallinity of spent Ga-HZSM-5 catalysts (a) non-reduced and (b) reduced.

In addition, the $[GaO]^+$ species present in the non-reduced catalyst would be more active for propane aromatization, as compared to the Ga^+ in the reduced catalyst. This is because the $[GaO]^+$ is strong Lewis acid that can readily abstract hydride from propane leading to the generation of propyl cation within the zeolite cavities. The propyl cation can be deprotonated to propylene that further undergo the oligomerization, cyclization, and aromatization via hydrocarbon pool mechanism, leading to the higher production of BTX, as evidenced in Figure 4.11(a).

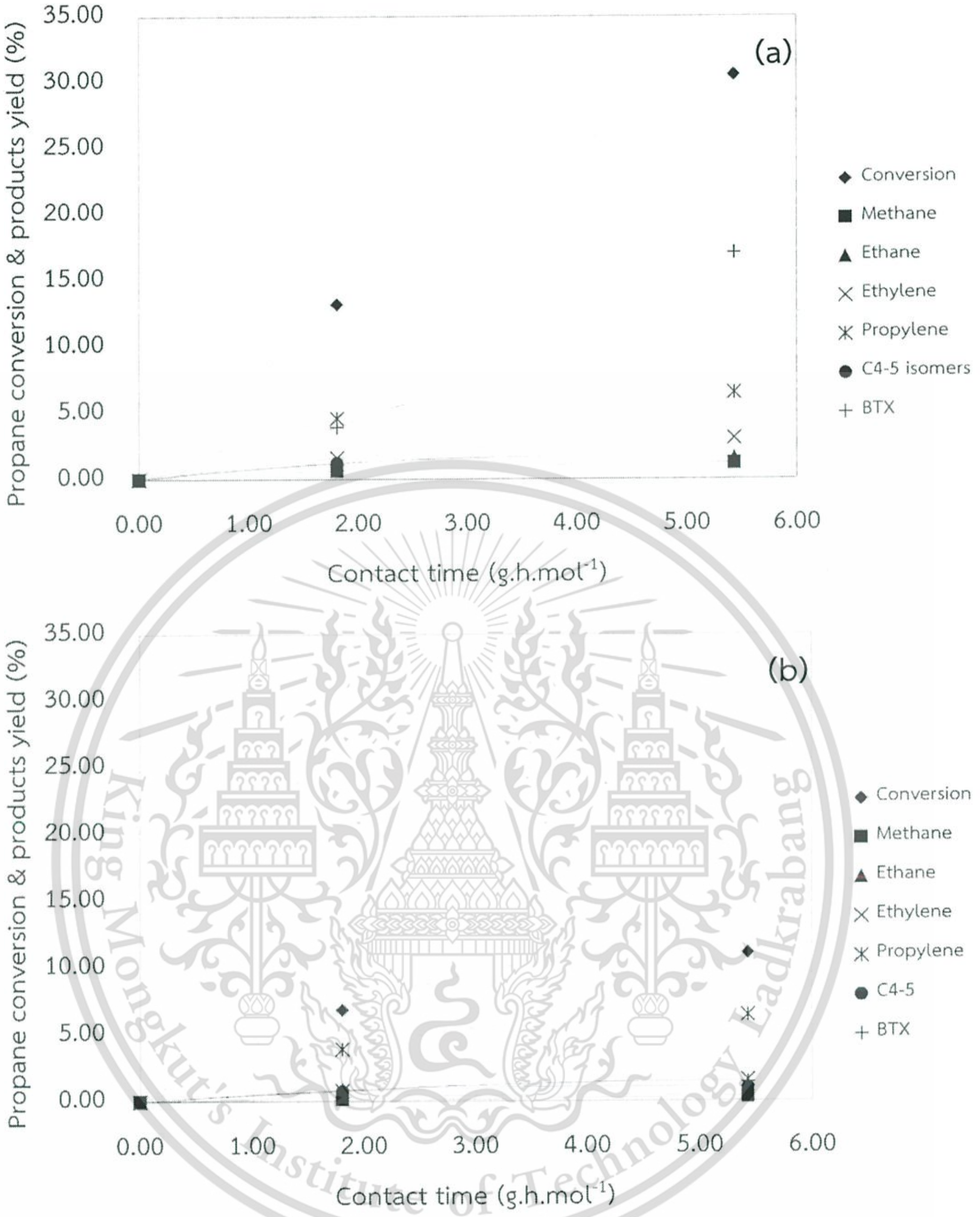

Figure 4.11 Propane conversion and products yield during different contact times using (a) non-reduced Ga-HZSM-5 (28) and (b) reduced Ga-HZSM-5 (28). (Reaction conditions: temperature = 550 °C, 20% v/v propane feed rate = 75 mL/min. Catalyst was activated under a flow of air (30 mL/min) at 450 °C for 1 h with a heating rate of 2 °C/min and reduced under a flow of H_2 (50 mL/min) at 600 °C for 3 h with a heating rate of 10 °C/min.)

It can be seen that the propane conversion is increased with contact time. Over the non-reduced catalyst, BTX are initially obtained as primary products at the contact time of 1.81 g.h.mol^{-1}. In contrast, the reduced catalyst contain Ga^{+} that possesses weaker Lewis acidity provided lower activity, as compared to [GaO]$^{+}$. Due to the lower acid strength, Ga^{+} is less active for the hydrocarbon pool generation. Nevertheless, this species seem to be active for propane dehydrogenation. Hence, propylene is only obtained as initial product from the reduced catalyst as shown in Figure 4.11(b). However, the small amount of secondary product can still be observed due to the remaining Brønsted acid site over this catalyst, as evidenced by IPA-TPD in Section 4.1.2.

It is worth noting that the observed different products selectivity is not due to the different activity. This is validated by the reaction over the non-reduced and the reduced catalysts with a similar level of propane conversion as shown in Table 4.6.

Table 4.6 Products distribution at the same level of propane conversion over the non-reduced and the reduced catalysts.

Catalysts	Propane conversion (%)	Yield (%)						Selectivity (%)	
		Methane	Ethane	Ethylene	Propylene	C_{4-5} isomers	BTX	Propylene	BTX
Non-reduced Ga-HZSM-5 (28)*	11.1	0.5	1.0	1.4	4.0	1.1	3.1	36.0	27.9
Reduced Ga-HZSM-5 (28)	11.1	0.3	0.4	1.6	6.4	1.0	1.4	57.7	12.6

* Interpolated from contact time profile (Figure 4.11(a))

Even at low propane conversion, a higher propylene selectivity was obtained from the reduced catalyst (Ga^{+} species). Accordingly, it can be concluded at this stage that the C-H activation of propane over the reduced catalyst would proceed via heterolytic C-H cleavage over Ga^{+} site [36], generating gallium propylidene intermediate (III) and Brønsted acid at the vicinity position. Such intermediate (III) is unstable and undergo oxidative addition with Brønsted acid to form hydrido gallium propylidene intermediate (Ga(H)(C_3H_7)) (IV). The dehydrogenation is suggested to proceed via decomposition of propylidene to propylene and dihydrido gallium species ($[GaH_2]^+$) (V). The $[GaH_2]^+$ is unstable and can be decomposed to Ga^+ via reductive elimination, as discussed previously in section 4.1.3. The overall mechanism is proposed as shown in Scheme 4.1.

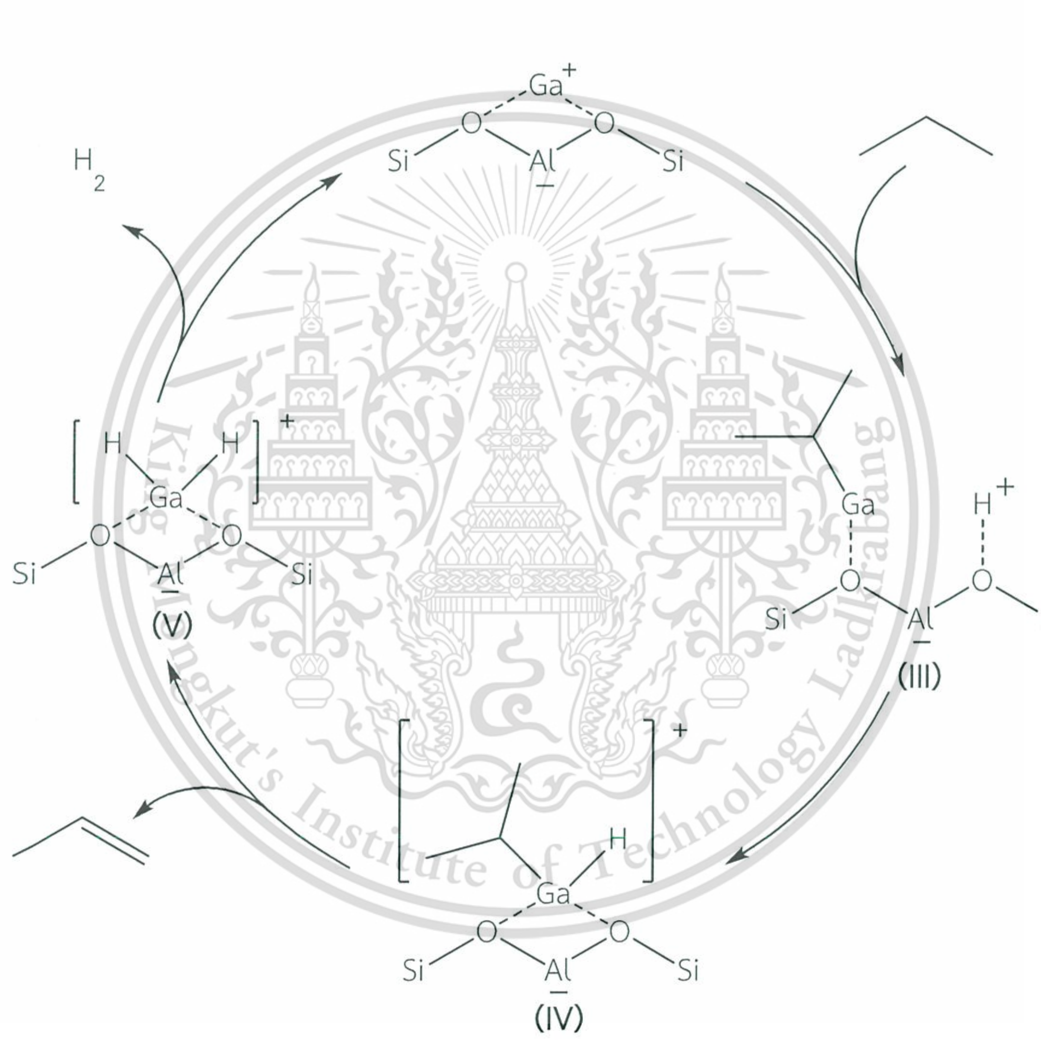

Scheme 4.1 Catalytic cycle of Ga^+ species [36].

In contrast, over the non-reduced catalyst, propane can be activated to propylene via polarization and dissociation of C-H bond through the Lewis acid center of $[GaO]^+$ species [42]. In mechanistic point of view, the gallium would bond with the propyl group while the remaining hydrogen would bond with the oxygen, generating a hydroxo gallium propylidene intermediate (Ga(OH)(C_3H_7)) (I). Then, decomposition of the propylidene would offer propylene as product and hydrido hydroxo gallium species (Ga(H)(OH)) (II). Such species (II) could possibly decompose to H_2 and the active $[GaO]^+$ species. The overall catalytic cycle is proposed as shown in Scheme 4.2.

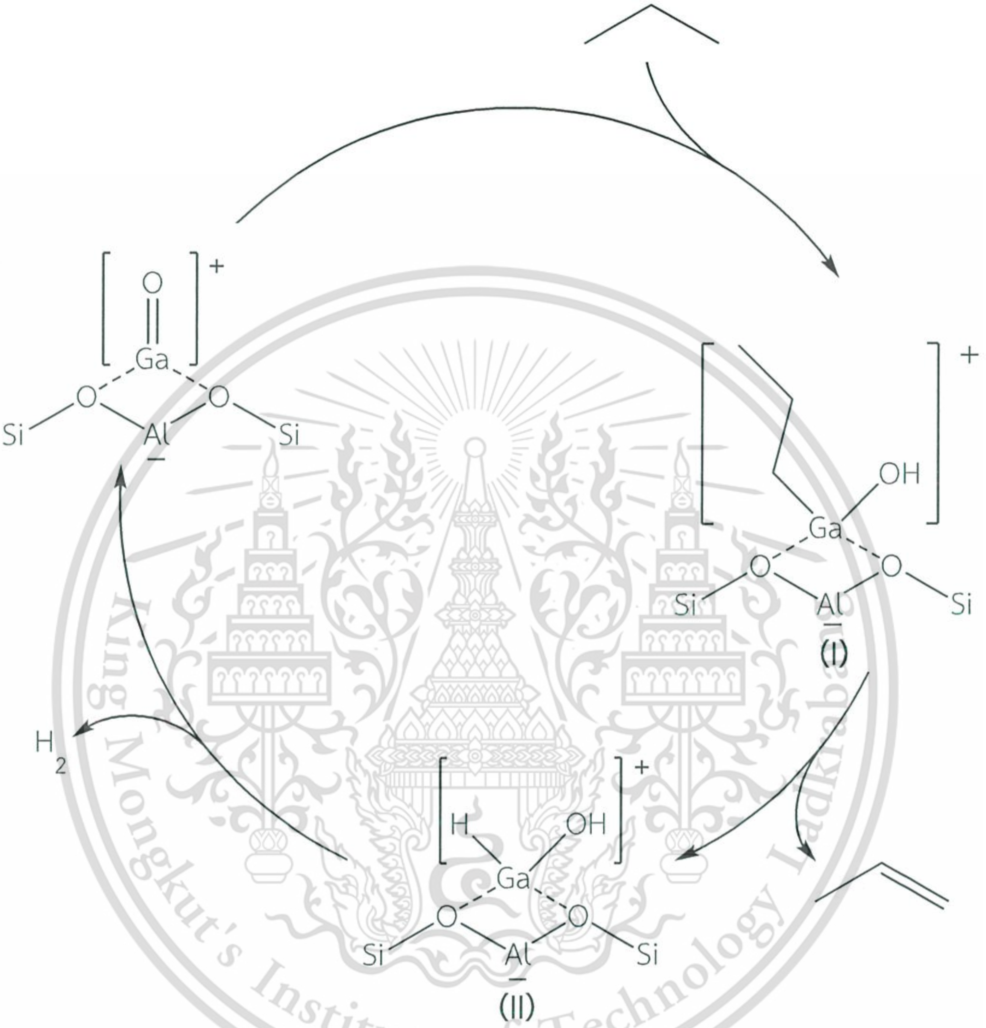

Scheme 4.2 Reaction mechanism of non-reduced Ga-HZSM-5 (28) [42].

As the $[GaO]^+$ contains higher Lewis acidity, as compared to the Ga^+, the oligomerization, cyclization, and aromatization of the produced propylene can be proceeded, leading to the low propylene selectivity in this case.

Although the non-reduced catalyst provides high propane conversion, a severe deactivation was observed as shown in Figure 4.12.

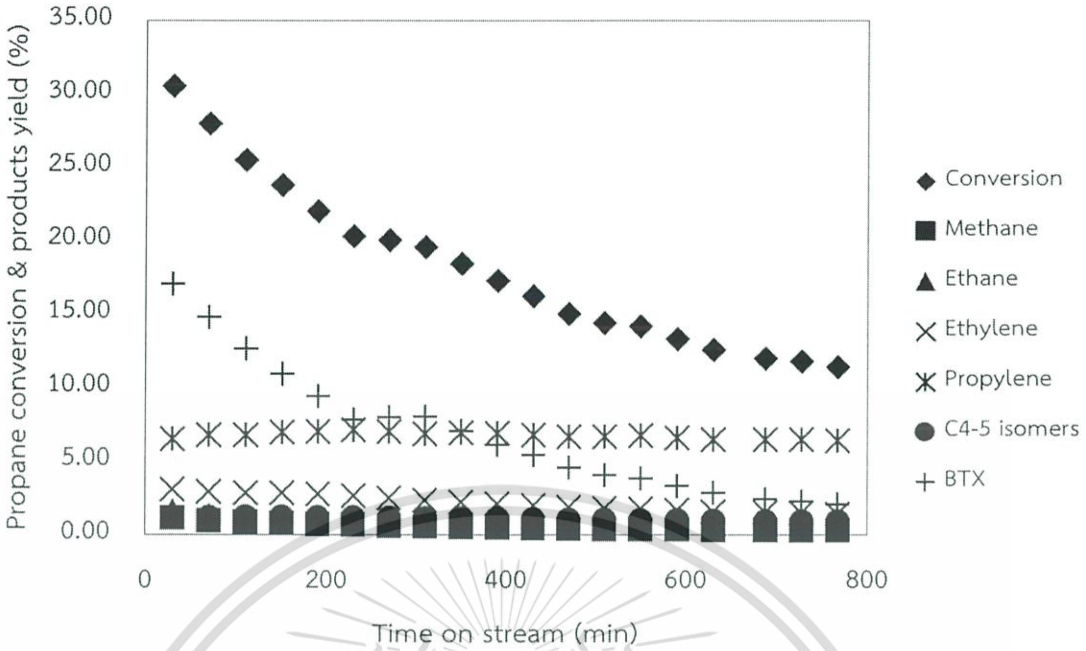

Figure 4.12 Time on stream profile of non-reduced Ga-HZSM-5 (28). (Reaction conditions: temperature = 400-550 °C, catalyst weight = 0.2 g, W/F = 5.43 g.h.mol^{-1}, 20% v/v propane feed rate = 75 mL/min. Catalyst was activated under a flow of air (30 mL/min) at 450 °C for 1 h with a heating rate of 2 °C/min.)

It can be seen that the BTX products are also decreased with the propane conversion while the propylene is continuously produced. One may expect that the propylene produced can be activated by $[GaO]^+$ leading to the generation of the hydrocarbon pool blocking the zeolite pore. If this is only the case, the propylene yield should also be reduced. The continual production of propylene leads to the suggestion that the active site is still available but not the same. It was proposed that the dehydrogenation of intermediate (II) to recover the $[GaO]^+$ (Scheme 4.2) would be in fact less facilitated [43]. Hence, the activity is decreased with time and the hydrocarbon pool formation is inhibited, resulting in the lower production of BTX. Alternatively, the intermediate (II) could be decomposed to Ga^+ via reductive elimination, as discussed previously in XANES and H_2-TPR. In other words, the catalyst is gradually reduced during the reaction. Accordingly, the Ga^+ formed can continuously activate propane to produce propylene, as proposed in Scheme 4.1. Therefore, the overall activity of the non-reduced catalyst should be concluded as shown in Scheme 4.3 while in the Scheme 4.2 is not facilitated.

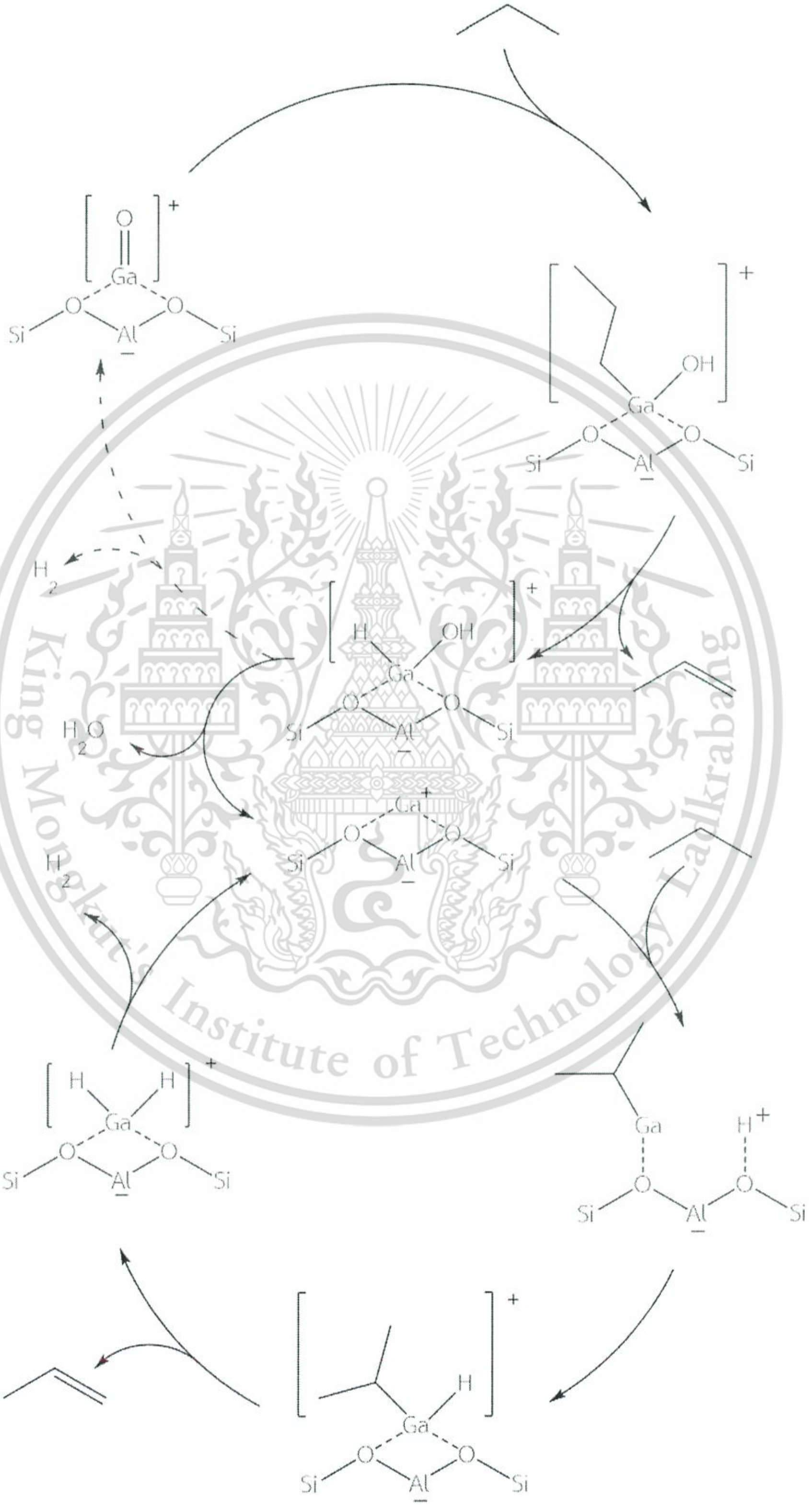

Scheme 4.3 Reaction mechanism over non-reduced Ga-HZSM-5 (28).

Accordingly, a continuous production of propylene can be observed in spite of severe deactivation for the BTX production. In a support manner, higher stability is observed for the reduced catalyst (Ga^+) in which propylene is steadily produced as major product together with light olefin as shown in Figure 4.13.

Figure 4.13 Time on stream profile of reduced Ga-HZSM-5 (28). (Reaction conditions: temperature = 550 °C, catalyst weight = 0.2 g, W/F = 5.43 $g.h.mol^{-1}$, 20% v/v propane feed rate = 75 mL/min. Catalyst was activated under a flow of air (30 mL/min) at 450 °C for 1 h with a heating rate of 2 °C/min and reduced under a flow of H_2 (50 mL/min) at 600 °C for 3 h with a heating rate of 10 °C/min.)

It is noted that the higher initial activity observed over the reduced catalyst is due to the presence of the GaOH species and the Brønsted acid site primarily formed after reduction, as discussed in XANES and H_2-TPR. The observed higher reactivity and also the BTX products are due to the higher acidity of GaOH/H^+ pairs, as compared to Ga^+. Nevertheless, the GaOH can be thermally decomposed via dehydration, as described previously in H_2-TPR and in-situ XANES. Hence, a decline in activity and the BTX yield would be observed as the GaOH converts to the Ga^+.

As seen in the Scheme 4.1, the regeneration of active Ga^+ species depends on the decomposition of the $[GaH_2]^+$ (V). If the reaction is carried out at higher concentration of H_2 in the feed stream, the decomposition of the $[GaH_2]^+$ would be inhibited leading to the lower propane conversion as shown in Figure 4.14.

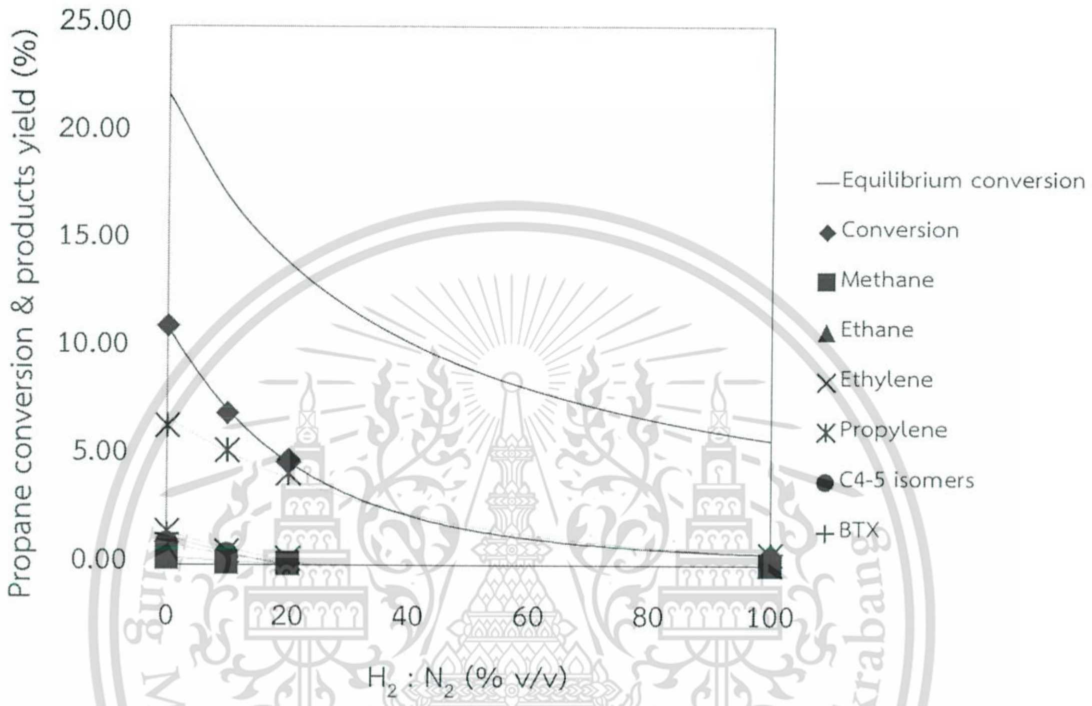

Figure 4.14 Effect of H_2 carrier gas on propane dehydrogenation. (Reaction conditions: temperature = 550 °C, catalyst weight = 0.2 g, W/F = 5.43 $g.h.mol^{-1}$, 20% propane in H_2 : N_2 (0, 10, 20, and 100% v/v) (75 mL/min). Catalyst was activated under a flow of air (30 mL/min) at 450 °C for 1 h with a heating rate of 2 °C/min and reduced under a flow of H_2 (50 mL/min) at 600 °C for 3 h with a heating rate of 10 °C/min.)

It can be seen that the propane conversion is markedly reduced with an increase in H_2 concentration. One may expect that the decline in propane conversion might be due to the hydrogenation of the propylene product back to propane. If this is only the case, the decline in propane conversion should be in line with the equilibrium propane conversion (see calculation in Appendix C2, p.77). However, the decrease in propane conversion is more significant than the equilibrium one. This leads to the suggestion that, in addition to the reversible hydrogenation of propylene, the

Ga^+ species could not be fully regenerated under a presence of H_2 [7, 37]. It can be concluded that the higher the H_2 concentration, the decomposition of $[GaH_2]^+$ species is inhibited. Hence, the catalyst retain lower amount of Ga^+ species.

4.2.3 Effect of Si/Al ratio

As the fraction of the exchangeable gallium ($[GaO]^+$ or Ga^+) and the extra-framework gallium ($[Ga_2O_2]^{2+}$) species at the same gallium loading would depend on Si/Al ratio of the parents HZSM-5, the propane dehydrogenation using catalysts with various Si/Al ratio were tested to verify role of gallium species in the different locations (as exchangeable cation and extra-framework species) as shown in Table 4.7.

Table 4.7 The effect of Si/Al ratio of non-reduced Ga-HZSM-5

Catalysts	$[GaO]^+$ content* (mmol/g)	Propane conversion (%)	Yield (%)						Selectivity (%)	
			Methane	Ethane	Ethylene	Propylene	C_{4-5} isomers	BTX	Propylene	BTX
Ga-HZSM-5 (28)	0.29	30.5	1.2	1.6	3.1	6.5	1.2	17.0	21.3	55.7
Ga-HZSM-5 (40)	0.28	21.2	1.0	0.8	3.1	7.0	1.2	8.2	33.0	38.7
Ga-HZSM-5 (140)	0.17	4.9	0.1	0.1	0.3	4.1	0.1	0.2	83.7	4.1
Ga-HZSM-5 (250)	0.15	3.6	0.1	0.0	0.2	3.3	0.0	0.1	91.7	2.8
Ga-HZSM-5 (500)	0.11	3.3	0.1	0.0	0.1	3.0	0.0	0.0	90.9	0.0

* obtained from H_2-consumption in H_2-TPR profile

It can be seen that the propane conversion is significantly decreased with an increase in Si/Al ratio. Accordingly, the propane conversion would depend largely on the $[GaO]^+$ content as shown in Figure 4.15.

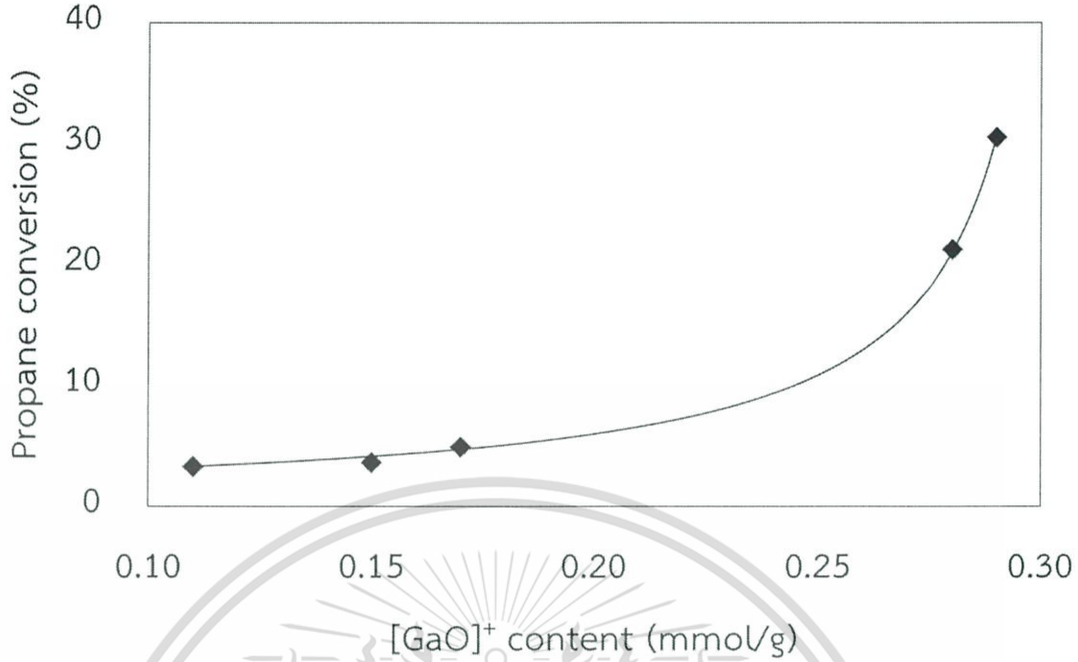

Figure 4.15 Relation between $[GaO]^+$ content (mmol/g) vs. propane conversion (%)

It is clear that the propane conversion is exponentially increased with $[GaO]^+$ content, particularly at over 0.20 mmol/g. This is due to the fact that the catalysts containing more fraction of $[GaO]^+$ species would readily promote hydride abstraction, as discussed previously in Section 4.2.2. However, the propane conversion over Ga-HZSM-5 (28) is markedly higher than Ga-HZSM-5 (40) despite the catalysts contain similar amount of $[GaO]^+$ species. This is because the remained Brønsted acid site in the Ga-HZSM-5 (28) has an interaction with gallium species leading to a greater electron deficiency of the $[GaO]^+$ active site. Such gallium site is also proximate to the Brønsted acid site, which facilitates the generation of hydrocarbon pool resulting in the production BTX as major products (Table 4.7). Accordingly, both electron deficiency and site proximity of the Brønsted acid site and gallium species synergistically promote higher propane conversion over Ga-HZSM-5 (28).

Although the catalysts with high Si/Al ratio contain more fraction of extra-framework $[Ga_2O_2]^{2+}$ species, the observed propane conversion is not readily determined by this species. In other words, the non-reduced extra-framework $[Ga_2O_2]^{2+}$ is less active for propane dehydrogenation, as compared to the $[GaO]^+$. Nevertheless, after the catalysts were reduced, the propane conversion is increased with the extra-framework gallium content as shown in Table 4.8.

Table 4.8 The effect of extra-framework gallium species of reduced Ga-HZSM-5.

Catalysts	$[Ga_2O_2]^{2+}$ content* (mmol/g)	Propane conversion (%)	Yield (%)						Selectivity (%)	
			Methane	Ethane	Ethylene	Propylene	C_{4-5} isomers	BTX	Propylene	BTX
Ga-HZSM-5 (140)	0.17	2.2	0.0	0.0	0.1	2.1	0.0	0.0	95.5	0.0
Ga-HZSM-5 (250)	0.19	2.5	0.0	0.0	0.1	2.4	0.0	0.0	96.0	0.0
Ga-HZSM-5 (500)	0.22	3.1	0.0	0.0	0.1	3.0	0.0	0.0	96.8	0.0

* obtained from H_2-consumption in H_2-TPR

In these cases, the catalysts contain only trace amount of exchangeable species (Ga^+). Hence, the observed activity for the propane conversion would virtually be a result from the extra-framework gallium species ($[Ga_2O_2]^{2+}$). It seems that the activity depends linearly on gallium content with noticeably high propylene selectivity, as shown in Figure 4.16.

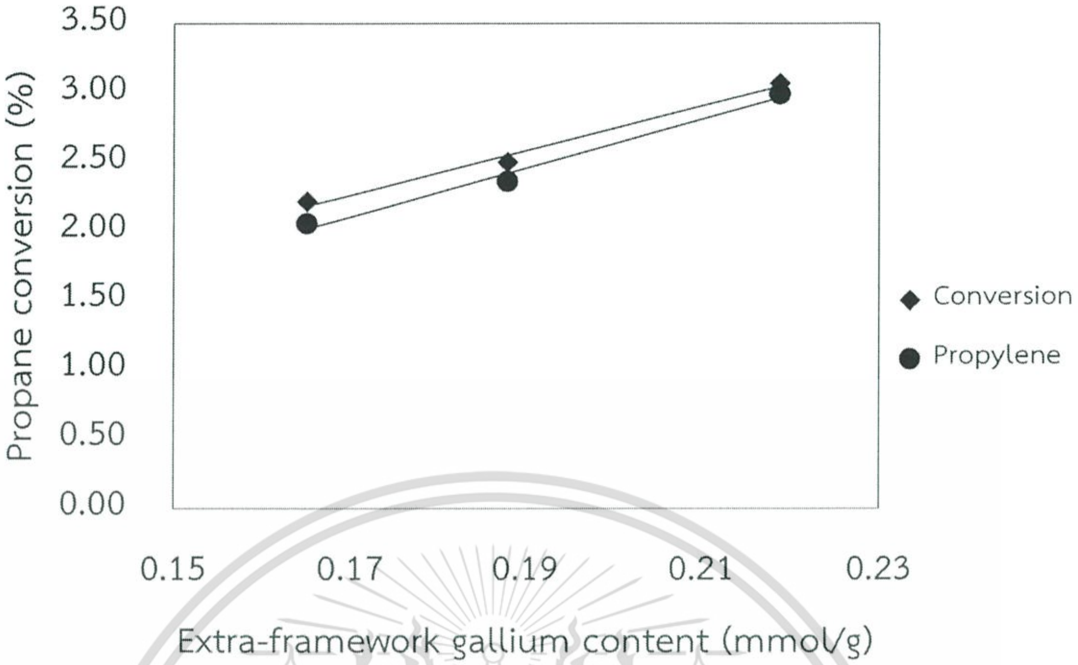

Figure 4.16 Relation between reduced extra-framework gallium content (mmol/g) vs. propane conversion (%)

According to the H_2-TPR (Figure 4.2), the extra-framework gallium species can be reduced at quite high temperature (more than 800 °C). In addition, the XANES spectra of the catalysts with various Si/Al ratio after reduction show that the catalysts with high Si/Al ratio (more than 140) cannot be completely reduced, since the oxidation state of the extra-framework gallium species retain 3+ (Figure 4.8). In the mechanistic point of view, propane dehydrogenation over the $[Ga_2O_2]^{2+}$ extra-framework species would be carried out via heterolytic cleavage of propane forming gallium propylidene and gallium hydroxide species (VI) [41]. Then, the propyl group would be dehydrogenated to propylene and hydride bonding with gallium to form hydrido gallium species (VII). The $[Ga_2O_2]^{2+}$ active site could be recovered via dehydrogenation of the intermediate (VII). The overall catalytic cycle of the extra-framework gallium species ($[Ga_2O_2]^{2+}$) is proposed as shown in Scheme 4.4 below.

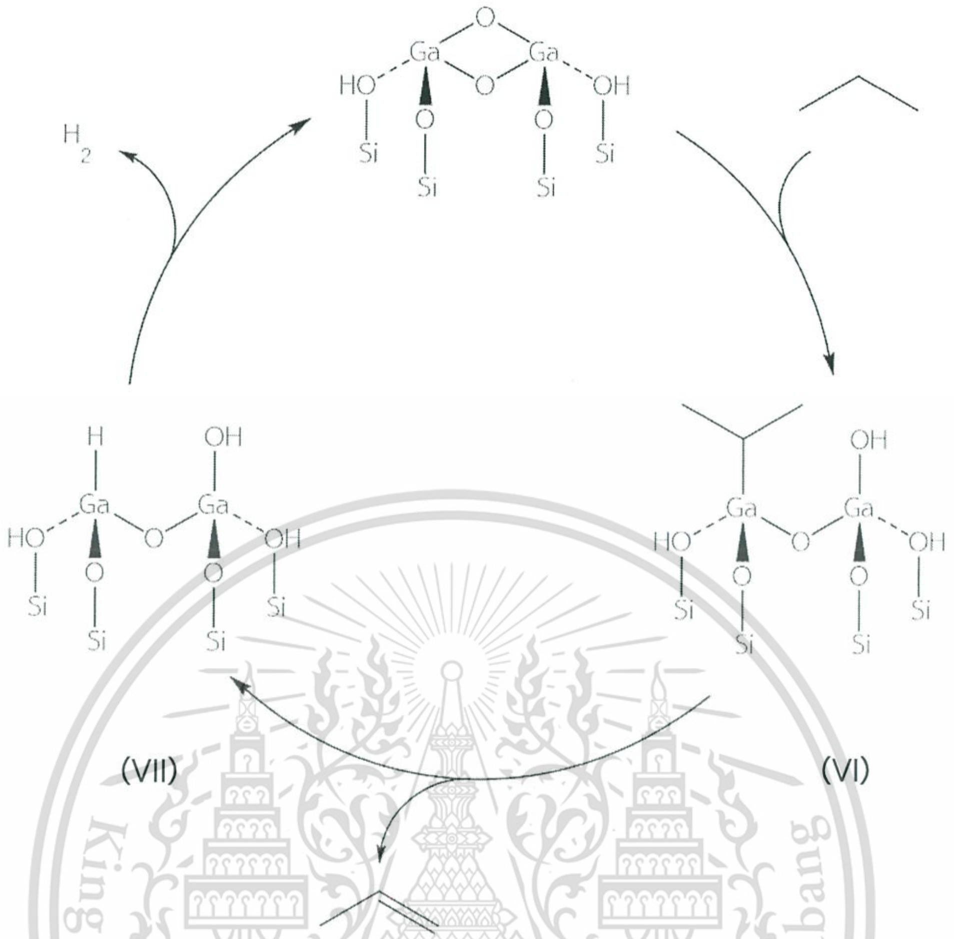

Scheme 4.4 Reaction mechanism over extra-framework gallium species ($[Ga_2O_2]^{2+}$) [41]

From Table 4.8, it can be noticed that after the catalysts were reduced, all of them provide lower propane dehydrogenation activity, as compared to the non-reduced one. Nevertheless, the formation of hydrocarbon pool does not occur over these catalysts, as observed by the lack of BTX yield, leading to a high selectivity of propylene. This presumably due to the low acidic properties of the $[Ga_2O_2]^{2+}$ species.

CHAPTER 5

CONCLUSIONS AND SUGGESTIONS

5.1 Conslusions

In this thesis, the propane dehydrogenation over gallium loaded HZSM-5 catalysts with various Si/Al ratio (28, 40, 140, 250, and 500) was investigated. All catalysts are referred as high surface area materials (351-398 m^2/g) with gallium loading approximately 0.3 mmol/g (~2.3 wt.%), as evidenced by ICP-MS. The XRD pattern of the gallium loaded catalysts show neither change in crystallinity nor impure phase, as compared to the HZSM-5 support. With a certain Si/Al ratio, the Brønsted acidity of the catalysts is decreased after the gallium is incorporated because the gallium loaded reacts with the Brønsted acid site to form an exchangeable gallium species ($[GaO]^+$). As the number of Brønsted acid site is similar or higher than the gallium loading, all gallium are in the form of $[GaO]^+$ species. On the other hands, the excess gallium loaded, with respected to the number of Brønsted acid site, would aggregate to form an extra-framework gallium species ($[Ga_2O_2]^{2+}$) bonded with internal silanol in the cavities of the parent zeolite. The H_2-TPR results confirm the presence of the $[GaO]^+$ and the ($[Ga_2O_2]^{2+}$) species, as observed by the difference in reduction temperature (400-600 °C for the $[GaO]^+$ reduction and above 600 °C for the $[Ga_2O_2]^{2+}$ reduction). However, the temperature for the reduction of $[GaO]^+$ species in the catalyst with Si/Al = 28 is higher than that in the catalyst with Si/Al ratio = 40. This is due to the polarization of the remaining Brønsted acid site in Ga-HZSM-5 (28), as evidenced by IPA-TPD. After the reduction of $[GaO]^+$, a gallium hydroxide species (GaOH) and Brønsted acid site are generated, as seen by the increase in strong acidity in NH_3-TPD. This species (GaOH) can be dehydrated by the reaction with the proximate Brønsted acid site at high temperature bearing Ga^+ species over the catalyst, as premised by XANES spectra of the Ga-HZSM-5 (28). In addition, under a flow of H_2, the $[GaH_2]^+$ species can be formed from the H_2-dissociation over Ga^+, as seen by the H_2-consumption in the second cycle of TPR. Over the catalysts with high Si/Al ratio, the presence of the extra-framework $[Ga_2O_2]^{2+}$ species bonded with internal silanol is supported by XANES. This species cannot be completely reduced up to 650 °C.

The propane dehydrogenation activity is increased with the reaction temperature. However, the major products are BTX which are the secondary products formed via hydrocarbon pool mechanism under a high concentration of propane in the feed. When the feed is diluted with nitrogen, the propane conversion is significantly dropped due to the limited adsorption of the propane on the catalyst surface. Nevertheless, propylene yield and selectivity obtained are increased when the feed is diluted.

Comparing the parent HZSM-5, the gallium incorporated HZSM-5 facilitates the C-H activation of propane leading to the higher propane conversion. In addition, the $[GaO]^+$ species provides a higher activity, as compared to the Ga^+ species. This is because the higher Lewis acidity of the $[GaO]^+$ would readily promote C-H activation. The propane is activated by polarization and dissociation of C-H bond generating hydroxo gallium propylidene intermediate ($Ga(OH)(C_3H_7)$) that is decomposed to propylene. While the active $[GaO]^+$ species was reduced to Ga^+. Accordingly, the $[GaO]^+$ species showed high initial propane conversion but a rapid deactivation due to the reduction of the $[GaO]^+$ to the Ga^+ species during the reaction. As the $[GaO]^+$ possesses strong Lewis acidity, the propylene produced can further undergo oligonerization, cyclization, and aromatization, leading to the observed high BTX yield initially. In contrast, the lower acid strength of the Ga^+ species leads to the lower acitivity for hydrocarbon pool and the BTX formation. Nevertheless, the Ga^+ species is still active for propane dehydrogenation, as observed by high selectivity of propylene. Unlike the $[GaO]^+$, the C-H activation of propane over the Ga^+ is proceeded via heterolytic cleavage of the C-H bond to form hydrido gallium propylidene intermediate ($Ga(H)(C_3H_7)$). The propyl group can be dehydrogenated to propylene and the active Ga^+ species can be recovered by reductive elimination of the $[GaH_2]^+$ intermediate. The decomposition of the $[GaH_2]^+$ was inhibited under a presence of hydrogen in the feed stream leading to the suppression of propane conversion. Over the catalysts with high Si/Al ratio, the extra-framework $[Ga_2O_2]^{2+}$ can also promote the propane dehydrogenation via heterolytic cleavage generating gallium propylidene on the surface silanol which can be dehydrogenated to propylene. The active extra-framework $[Ga_2O_2]^{2+}$ is recovered via dehydrogenation of the gallium hydroxide and the hydrido gallium intermediate.

With a presence of proximate Brønsted acid site over the catalyst, the gallium is polarized leading to increase electron deficiency. Therefore, the propane conversion is noticeably high in this cases. However, a strong acidity facilitated the hydrocarbon pool formation providing high BTX yield resulting in the low propylene selectivity. The overall results indicated that the gallium incorporated HZSM-5 catalysts are effective for propane dehydrogenation. These catalysts can be applied for both dehydrogenation and aromatization of propane depending on the Si/Al ratio and the pre-treatment conditions.

5.2 Suggestions

1. The effect of gallium loading over high Si/Al ratio of HZSM-5 on propane dehydrogenation should be investigated due to the difference in gallium dispersion.
2. To improve the thermodynamics of the dehydrogenation reaction, highly selective oxidation of the H_2 produced might be a possible way.

References

---

[1] Y. Ren, W. Wang, Y. Yue and Z. Gao. (2012). **Ga_2O_3/HZSM-48 for dehydrogenation of propane: effect of acidity and pore geometry of support.** Journal of Industrial and Engineering Chemistry. 18. 731-736.

[2] S. Tan, L. B. Gil, N. Subramanian, D. S. Sholl, S. Nair, C. W. Jones, J. S. Moore, Y. Liu, S. Dixit and J. G. Pendergast. (2015). **Catalytic propane dehydrogenation over In_2O_3-Ga_2O_3 mixed oxides.** Applied Catalysis A: General. 498. 167-175.

[3] "https://en.wikipedia.org/wiki/Propane," [Online].

[4] Y. Zhang, Y. Zhou, L. Huang, M. Xue and S. Zhang. (2011). **Sn-modified ZSM-5 as support for platinum catalyst in propane dehydrogenation.** Industrial and Engineering Chemistry Research. 50. 7896-7902.

[5] Y. Zhang, Y. Zhou, L. Huang, S. Zhou, X. Sheng, Q. Wang and C. Zhang. (2015). **Structure and catalytic properties of the Zn-modified ZSM-5 supported platinum catalyst for propane dehydrogenation.** Chemical Engineering Journal. 270. 352-361.

[6] M. Chen, J. Xu, Y. M. Liu, Y. Cao, H. Y. He and J. H. Zhuang. (2010). **Supported indium oxide as novel efficient catalysts for dehydrogenation of propane with carbon dioxide.** Applied Catalysis A: General. 377. 35-41.

[7] A. Ausavasukhi and T. Sooknoi. (2014). **Tunable activity of [Ga]HZSM-5 with H_2 treatment: ethane dehydrogenation.** Catalysis Communications. 45. 63-68.

[8] "http://www.propane.ca/en/about-propane/applications," [Online].

[9] "https://www.ihs.com/products/propylene-chemical-economics-handbook.html," [Online].

[10] "http://www.bpf.co.uk/plastipedia/polymers/pp.aspx#properties," [Online].

[11] "http://www.dow.com/propyleneoxide/app/," [Online].

[12] "https://www.ihs.com/products/acrylonitrile-chemical-economics-handbook.html," [Online].

[13] "https://en.wikipedia.org/wiki/Dehydrogenation," [Online].

[14] B. M. Weckhuysen and R. A. Schoonheydt. (1999). **Alkane dehydrogenation over supported chromium oxide catalysts.** Catalysis Today. 51. 223-232.

[15] "http://www.explainthatstuff.com/zeolites.html," [Online].

[16] P. A. Jacobs, E. M. Flanigen, J. C. Jansen and H. v. Bekkum. (2001) **Introduction to zeolite science and practice 2nd edition.** The Netherlands: Elsevier : Amsterdam.

[17] P. A. Jacobs, E. M. Flanigen, J. C. Jansen and H. v. Bekkum. (2001). **Introduction to zeolite science and practice 2nd edition.** The Netherlands: Elsevier : Amsterdam.

[18] P. Ploynisa, K. Supanat and S. Settawat. (2014). **Conversion of ethanol to gasoline over metal transition loaded H-ZSM-5 zeolite catalysts.** Bangkok: King Mongkut's Institute of Tenchnology Ladkrabang.

[19] L. Sirinuch. (2008). **Synthesis of zeolite beta as a support of metal supported catalysts for toluene hydrogenation and application of in situ XAS on catalysis characterization.** Nakhonratchasima: Suranaree University of Technology.

[20] P. J. Smeets, J. S. Woertink, B. F. Sels, E. I. Solomon and R. A. Schoonheydt. (2010). **Transition-metal ions in zeolites: coordination and activation of oxygen.** Inorganic Chemistry. 49. 3573-3583.

[21] P. J. Grobet, W. J. Mortier, E. F. Vansant and G. Schulz-Ekloff. (1988). **Innovation in zeolite materials science 1st edition.** The Netherlands: Elsevier : Amsterdam.

[22] C. Novara, A. Alfayate, G. Berlier, S. Maurelli and M. Chiesa. (2013). **The interaction of H_2O_2 with TiAlPO-5 molecular sieves: probing the catalytic potential of framework substituted Ti ions.** Physical Chemistry Chemical Physics. 15. 11099-11105.

[23] J. N. Armor. (1998). **Metal-exchanged zeolites as catalysts.** Microporous and Mesoporous Materials. 22. 451-456.

[24] Y. Li and J. N. Armor. (1992). **Catalytic reduction of nitrogen oxides with methane in the presence of excess oxygen.** Applied Catalysis B: Environmental. 1. L31-L40.

[25] Y. Li and J. N. Armor. (1994). **Catalytic combustion of methane over palladium exchanged zeolites.** Applied Catalysis B. 3. 275-282.

[26] Y. Li and J. N. Armor. (1992). **Catalytic decomposition of nitrous oxide on metal exchanged zeolites.** Applied Catalysis B: Environmental. 1. L21-L29.

[27] "https://en.wikipedia.org/wiki/Gallium," [Online].

[28] "http://nautilus.fis.uc.pt/st2.5/scenes-e/elem/e03130.html," [Online].

[29] V. R. Choudhary, K. Mantri and C. Sivadinarayana. (2000). **Influence of zeolite factors affecting zeolitic acidity on the propane aromatization activity and selectivity of Ga/H-ZSM-5.** Micropourous and Mesoporous Meterials. 37. 1-8.

[30] "https://en.wikipedia.org/wiki/Boudouard_reaction," [Online].

[31] F. Zhang, R. Wu, Y. Yue, W. Yang, S. Gu, C. Miao, W. Hua and Z. Gao. (2011). **Chromium oxide supported on ZSM-5 as a novel efficient catalyst for dehydrogenation of propane with CO_2.** Microporous and Mesopourous Materials. 145. 194-199.

[32] E. Kikuchi, M. Ogura, I. Terasaki and Y. Goto. (1996). **Selective Reduction of Nitric Oxide with Methane on Gallium and Indium Containing H-ZSM-5 Catalysts: Formation of Active Sites by Solid-State Ion Exchange.** Journal of Catalysis. 161. 465-470.

[33] K. M. Dooley, C. Chang and G. L. Price. (1992). **Effects of pretreatments on state of gallium and aromatization activity of gallium/ZSM-5 catalysts.** Applied Catalysis A: General. 84. 17-30.

[34] V. O. Rodrigues, J.-G. Eon and A. C. Faro. (2010). **Correlations between Dispersion, Acidity, Reducibility, and Propane Aromatization Activity of Gallium Species Supported on HZSM5 Zeolites.** Journal of Physical Chemistry. 114. 4557-4567.

[35] Y. Fang, X. Su, X. Bai, W. Wu, G. Wang, L. Xiao and A. Yu. (2017). **Aromatization over nanosized Ga-containing ZSM-5 zeolites prepared by different methods: Effect of acidity of active Ga species on the catalytic performance.** Journal of Energy Chemistry. 26. 768-775.

[36] E. A. Pidko, V. B. Kazansky, E. J. Hensen and R. A. Santen. (2006). **A comprehensive density functional theory study of ethane dehydrogenation over reduced extra-framework gallium species in ZSM-5 zeolite.** Journal of Catalysis. 240. 73-84.

[37] V. B. Kazansky, I. R. Subbotina, R. v. Santen and E. M. Hensen. (2004). **DRIFTS study of the chemical state of modifying gallium ions in reduced Ga/ZSM-5 prepared by impregnation I. Observation of gallium hydrides and application of CO adsorption as a molecular probe for reduced gallium ions.** Journal of Catalysis. 227. 263-269.

[38] I. Nowak, J. Quartararo, E. G. Derouane and J. C. Védrine. (2003). **Effect of H_2–O_2 pre-treatments on the state of gallium in Ga/H-ZSM-5 propane aromatisation catalysts.** Applied Catalysis A: General. 251. 107-120.

[39] A. C. Faro, V. Rodrigues and J.-G. Eon. (2011). **In Situ X-ray Absorption Study of the Genesis and Nature of the Reduced Gallium Species in Ga/HZSM5 Catalysts.** The Journal of Physical Chemistry C. 115. 4749-4756.

[40] V. J. Cybulskis, S. U. Pradhan, J. J. Lovón-Quintana, A. S. Hock, B. Hu, G. Zhang, W. N. Delgass, F. H. Ribeiro and J. T. Mille. (2017). **The Nature of the Isolated Gallium Active Center for Propane Dehydrogenation on Ga/SiO_2.** Catalysis Letters. 147. 1252-1262.

[41] E. A. Pidko, E. J. Hensen, G. M. Zhidomirov and R. A. Santen. (2008). **Non-localized charge compensation in zeolites: A periodic DFT study of cationic gallium-oxide clusters in mordenite.** Journal of Catalysis. 255. 139-143.

[42] M. V. Frash and R. A. Santen. (2000). **Activation of Small Alkanes in Ga-Exchanged Zeolites: A Quantum Chemical Study of Ethane Dehydrogenation.** Journal of Physical Chemistry A. 104. 2468-2475.

[43] A. Sierraalta, Y. Guillen, C. M. Lop´ez, R. Martinez, F. Ruette, F. Machado, M. Rosa-Brussin and H. Sosc´un. (2005). **Theoretical study of the Ga/SAPO-11 catalyst Extra-framework gallium species and n-butane transformation.** Journal of Molecular Catalysis A: Chemical. 242. 233-240.

[44] E. S. Shpiro, D. P. Shevchenko, O. P. Tkachenko and R. V. Dmitriev. (1994). **Platinum prornoting effects in Pt/Ga zeolite catalysts of lower alkane aromatization. I. Ga and Pt electronic states, dispersion and distribution in zeolite crystals in dependence of preparation techniques. Dynamic effects caused by reaction mixture.** Applied Catalysis A: General. 107. 147-164.

[45] A. Serykh and M. D. Amiridis. (2009). **In situ X-ray photoelectron spectroscopy study of gallium-modified MFI zeolite.** Surface Science. 603. 2037-2041.

APPENDICES

Appendix A

CATALYSTS CHARACTERIZATION

A1: Gas adsorption

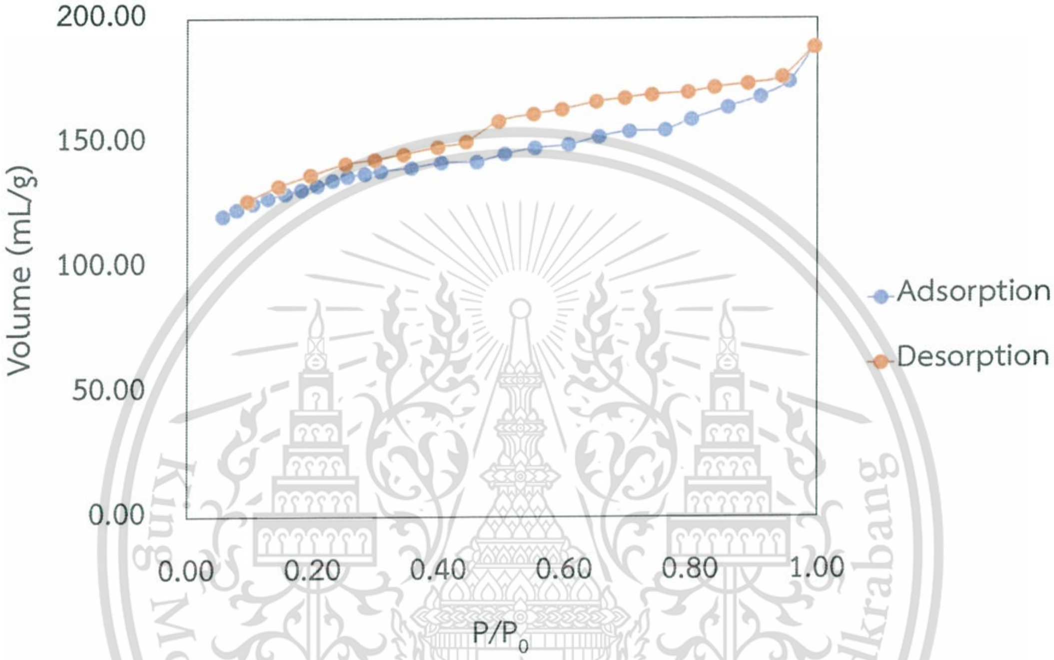

Figure A1 Adsorption isotherm of HZSM-5 (28)

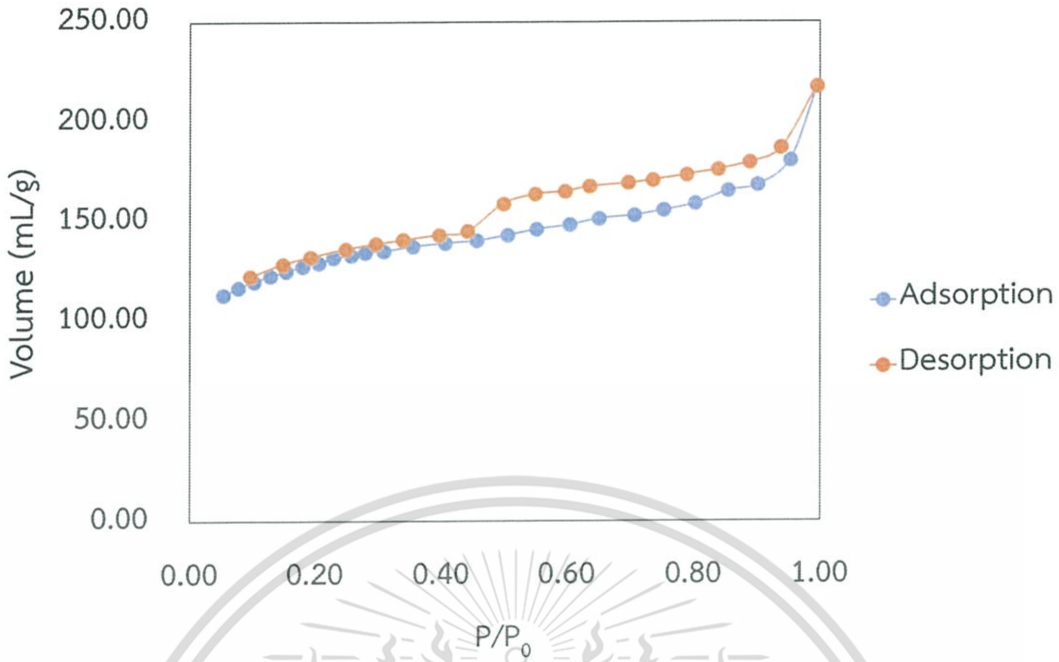

Figure A2 Adsorption isotherm of HZSM-5 (40)

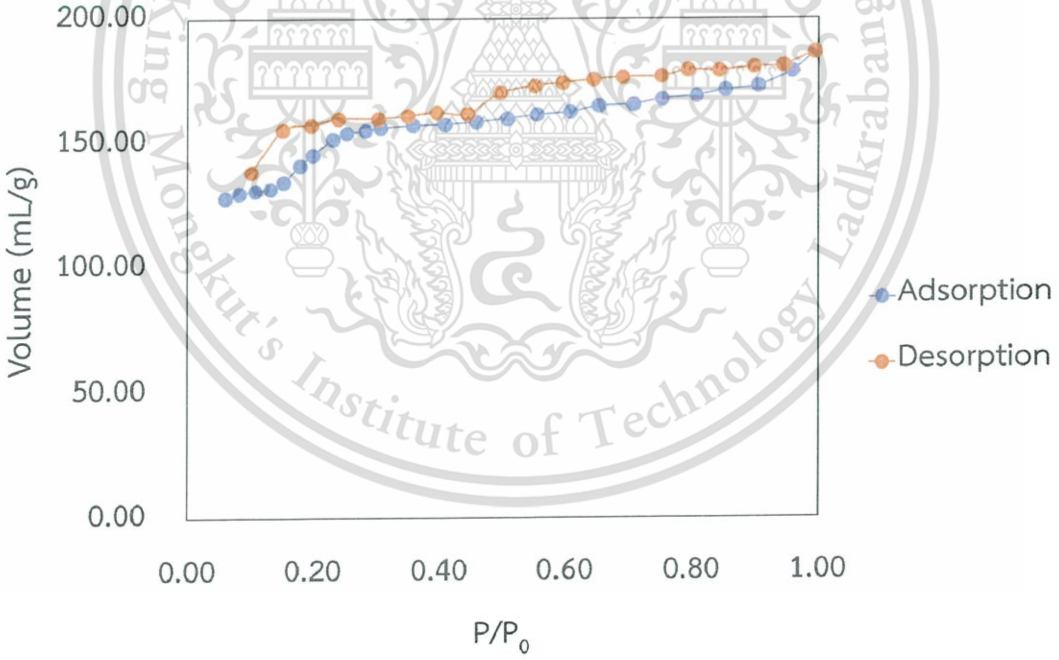

Figure A3 Adsorption isotherm of HZSM-5 (140)

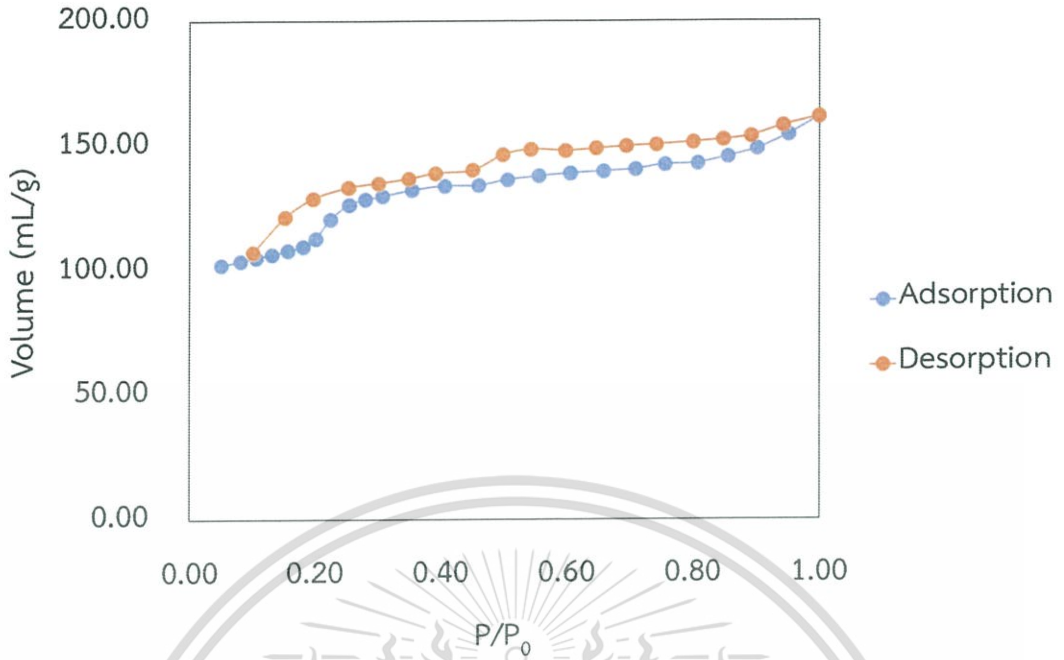

Figure A4 Adsorption isotherm of HZSM-5 (250)

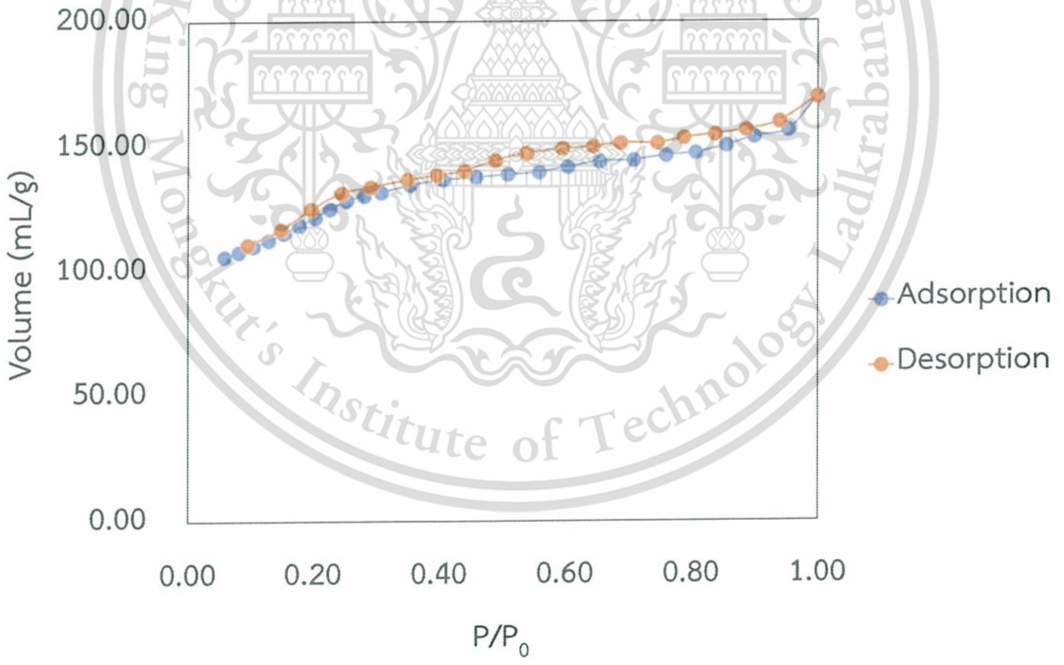

Figure A5 Adsorption isotherm of HZSM-5 (500)

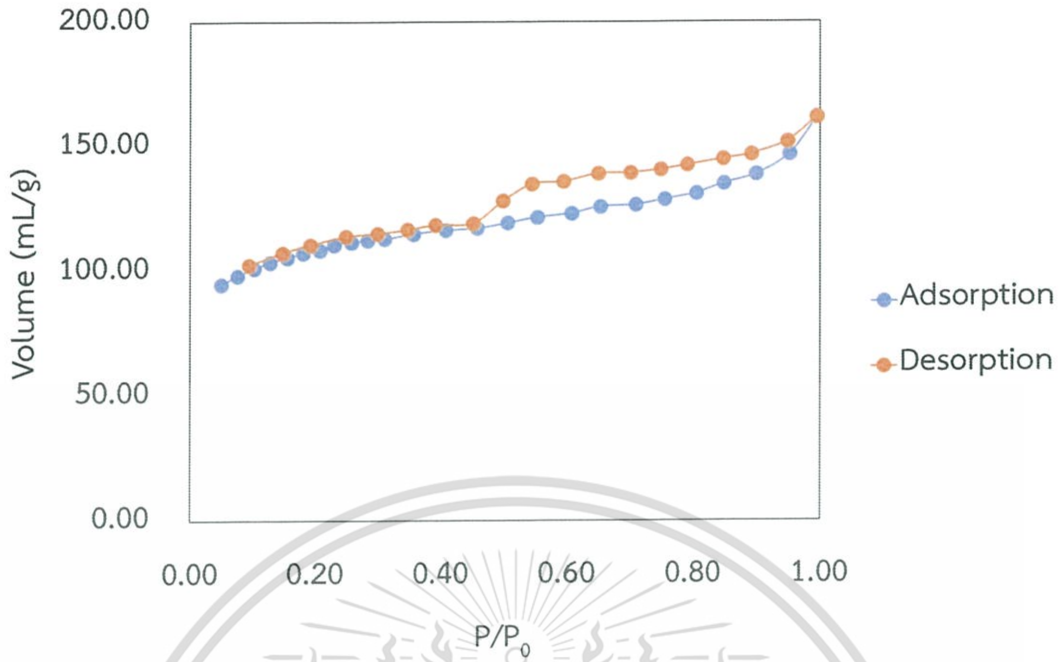

Figure A6 Adsorption isotherm of 3% Ga-HZSM-5 (28)

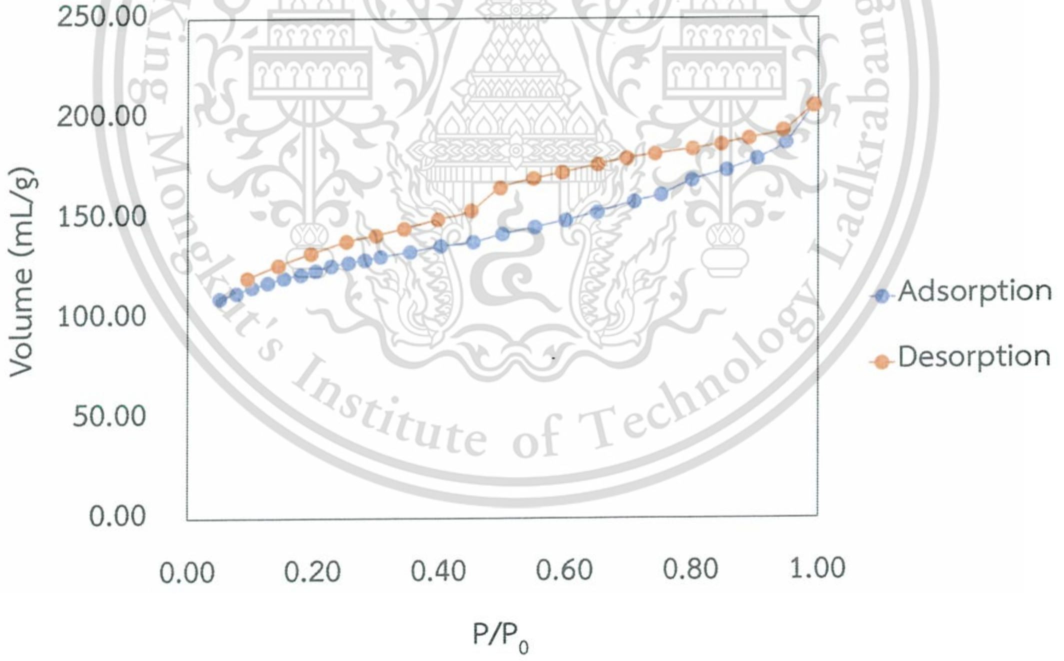

Figure A7 Adsorption isotherm of 3% Ga-HZSM-5 (40)

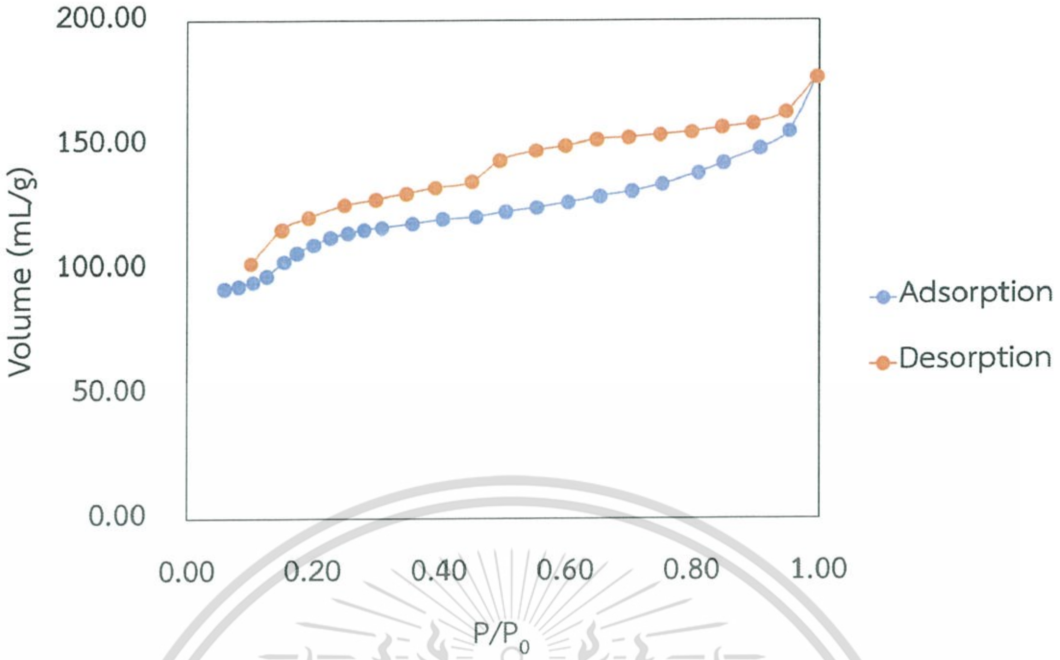

Figure A8 Adsorption isotherm of 3% Ga-HZSM-5 (140)

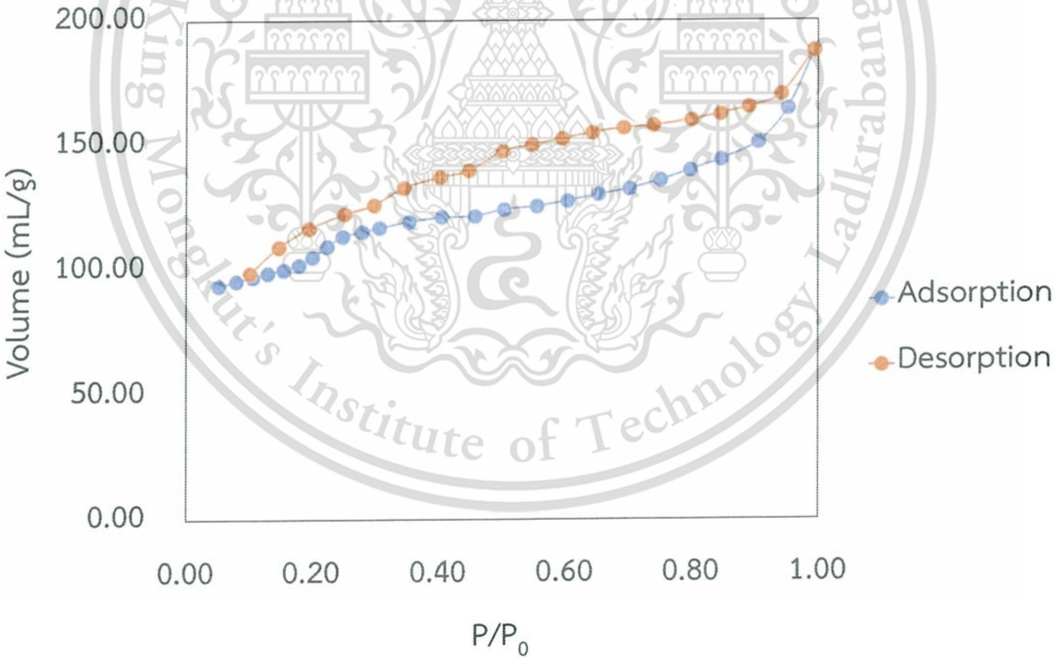

Figure A9 Adsorption isotherm of 3% Ga-HZSM-5 (250)

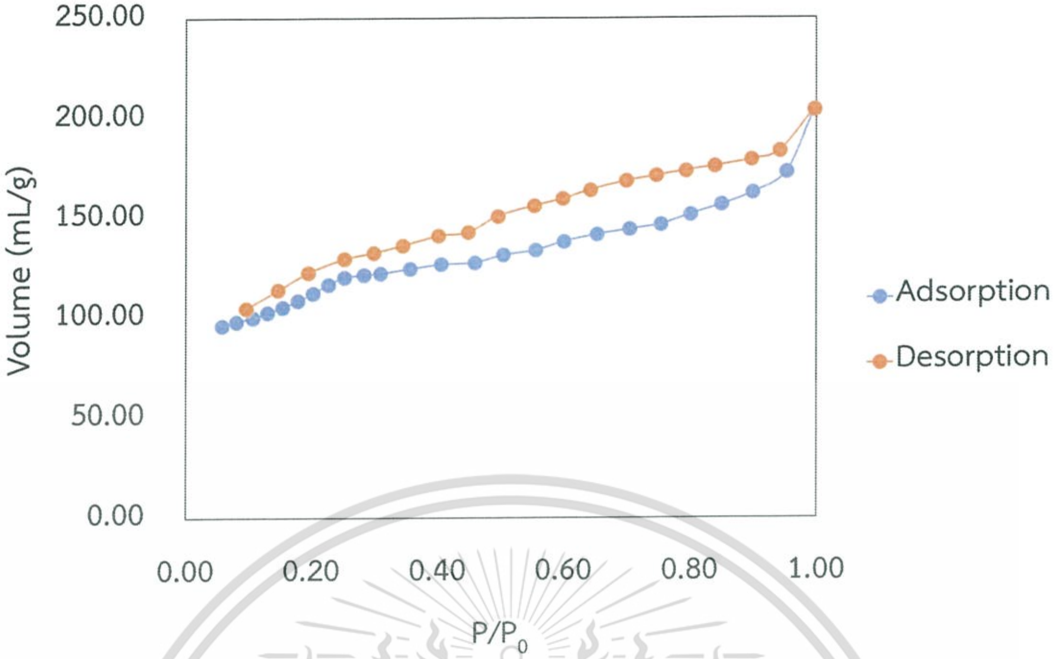

Figure A10 Adsorption isotherm of 3% Ga-HZSM-5 (500)

A2: ICP-MS

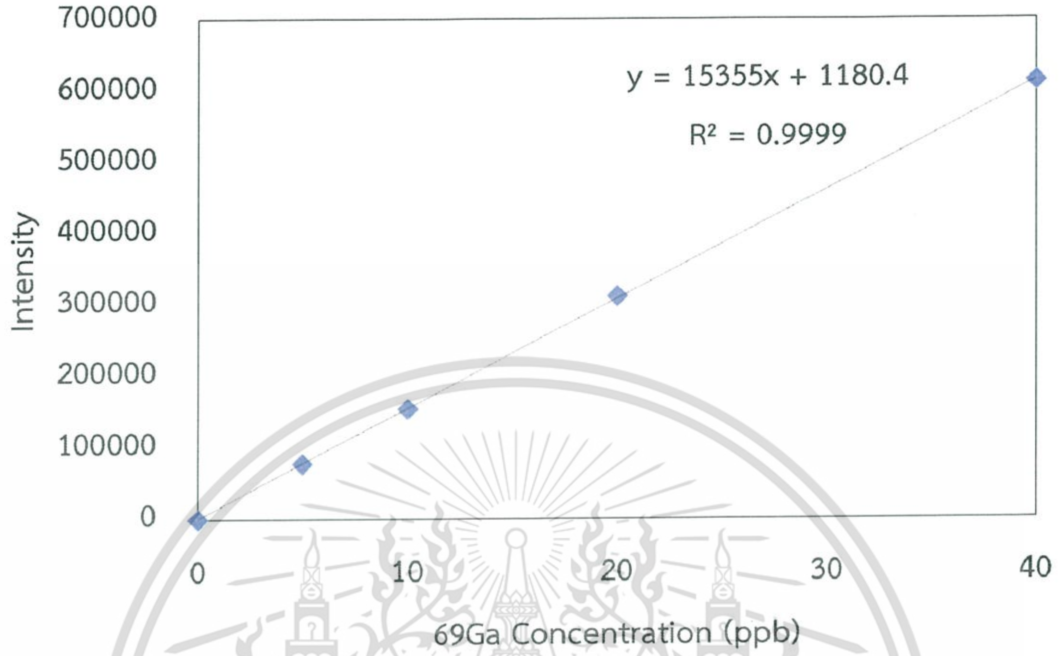

Figure A11 Calibration curve of standard gallium solution

Table A1 Intensity of gallium in catalysts

Catalysts	Intensity	Gallium concentration (ppb)	Gallium loading (wt.%)
3% Ga-HZSM-5 (28)	36499.90	2.30	2.30
3% Ga-HZSM-5 (40)	37150.30	2.34	2.34
3% Ga-HZSM-5 (140)	36792.00	2.32	2.32
3% Ga-HZSM-5 (250)	36971.55	2.33	2.33
3% Ga-HZSM-5 (500)	37010.72	2.33	2.33

Example of gallium loading calculation of 3% Ga-HZSM-5 (28).

Replace the y parameter with 36496.90, then solve for x

$$36496.90 = 15355x + 1180.4$$

$$x = 2.30 \text{ ppb}$$

Dilution factor of catalyst is 1000000, so the concentration = 2300000 ppb = 2300.00 ppm for 0.1 g of catalyst

$$2300L/0.1\ g_{cat} = 2.3\ g/L/0.1\ g_{cat} = 23\ g/L = 23\ g/1000\ g = 2.3\ wt.\%$$

A3: IPA-TPD

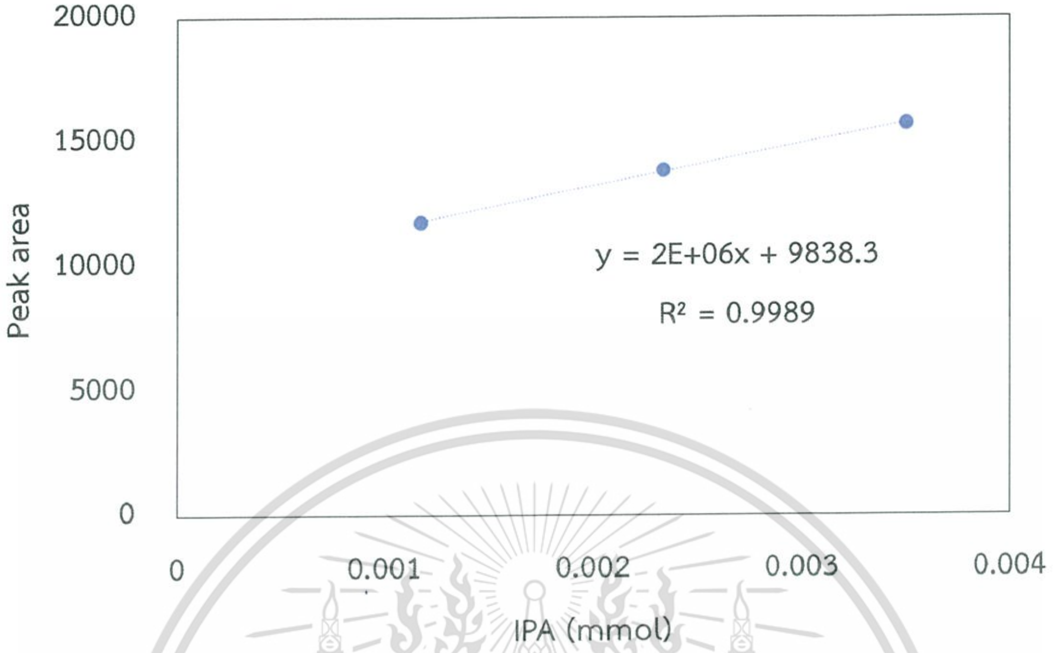

Figure A12 Calibration curve of standard isopropylamine

Table A2 Peak area of desorbed IPA of catalysts

Catalysts	Peak area	Brønsted acid site (mmol/g)
HZSM-5 (28)	121870	0.56
HZSM-5 (40)	85794	0.38
HZSM-5 (140)	37811	0.14
HZSM-5 (250)	23768	0.07
HZSM-5 (500)	17904	0.04
3% Ga-HZSM-5 (28)	52369	0.21
3% Ga-HZSM-5 (40)	0	0.00
3% Ga-HZSM-5 (140)	0	0.00
3% Ga-HZSM-5 (250)	0	0.00
3% Ga-HZSM-5 (500)	0	0.00

Example of calculation of Brønsted acid site of HZSM-5 (28)

Replace y with 121870, then solve for x ; x = 0.056 mmol for catalyst 0.1 g

0.056 mmol/0.1 g = 0.56 mmol/g

A4: NH_3-TPD

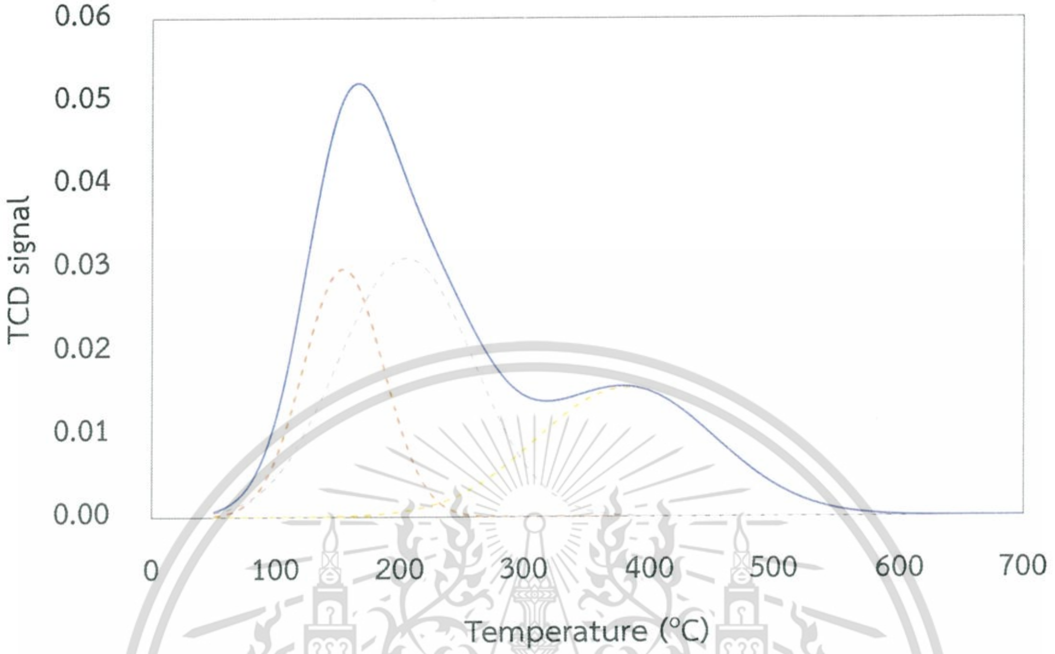

Figure A13 NH_3-TPD of non-reduced 3% Ga-HZSM-5 (28)

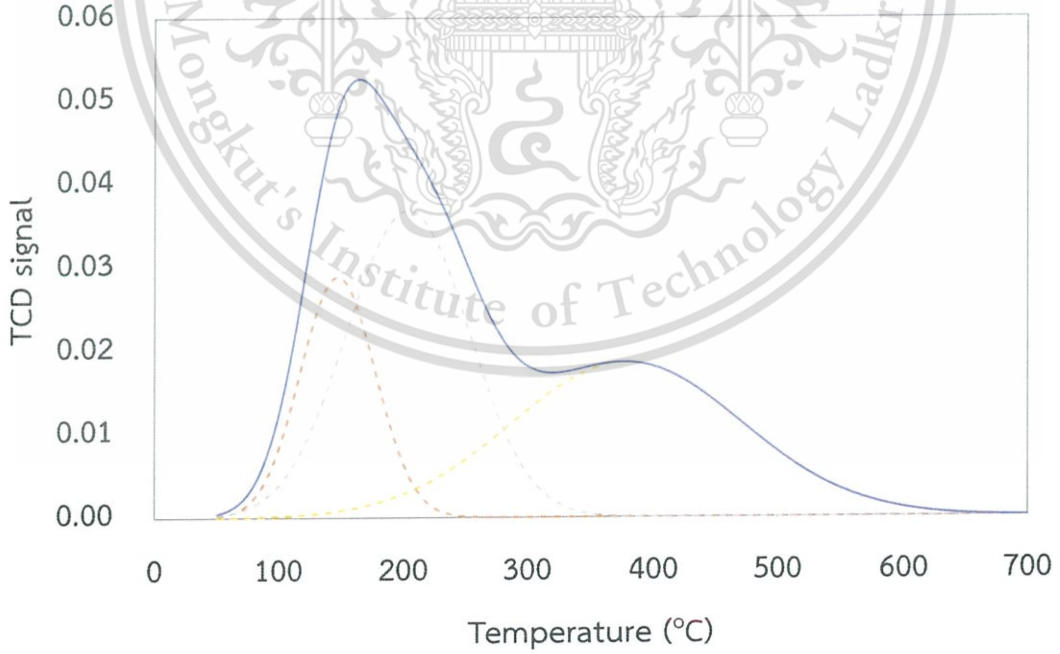

Figure A14 NH_3-TPD of reduced 3% Ga-HZSM-5 (28) (reduce at 600 °C for 3 h)

Appendix B

GAS CHROMATOGRAM

Table B1 GC conditions for quantitative analysis

Column	HP-PLOT, 30 m x 0.53 mmID x 15 μm
Temperature program	50 °C (5 min hold) ramp to 150 °C (10 min hold) at 20 °C/min and ramp to 180 °C (7 min hold) at 10 °C/min
Carrier gas	Nitrogen gas, flow rate 2.8 mL/min (4 min hold) and ramp to 3.8 mL/min (1 mL/min, 25 min hold), Linear velocity = 21.15 to 28.71 cm/sec
Injector temperature	250 °C
Detector temperature	FID at 250 °C

The products from propane conversion were identified by comparing the retention time to the standard gas as listed in Table B2.

Table B2 Chromatogram data of feed and products component

Component	Retention time
Methane	2.582
Ethane	2.800
Ethylene	3.055
Propane	3.469
Propylene	4.795
C_{4-5} isomers	5.312-7.580
BTX	>21.000

Appendix C

CALCULATIONS

C1: Catalytic parameters

Contact time (W/F)

$$\frac{W}{F} = \frac{\text{weight of catalyst (g)}}{\text{feed rate (mol/h)}}$$

Example

In the reaction using 0.0368 mol/h of propane in feed and using 0.2000 grams of catalyst, the W/F is calculated as follow:

$$W/F = (0.2000\ \text{g}) / (0.0368\ \text{mol/h})$$

$$W/F = 5.4342\ \text{g.h.mol}^{-1}$$

In similar manner; W/F of catalyst with different catalyst weight and different feed rate are calculated.

Calculation of % yield of products from gas chromatography

From the chromatogram, the peaks of each component were identified and summarized using reference standard for comparison. The example of the peak area obtained from chromatogram of a mixture reactor outlet is shown in Table C1.

Table C1 the summation of peak area of all components (information of HZSM-5 (28) at 15 min on stream)

Component	Peak area
Methane	3456.7
Ethane	255.2
Ethylene	6413.8
Propane	201522.2
Propylene	3005.0
C_{4-5} isomers	0.0
BTX	0.0
Total	214652.9

The %yield of each products was calculated by normalization method as follows:

$$\%\text{yield} = \frac{\text{area of product}}{\text{total area}} \times 100$$

For example

$$\%\text{yield of propylene} = \frac{3005.0}{214652.9} \times 100$$

$$= 1.40$$

The yield of each products from this calculation is shown in **Table C2**.

Table C2 %yield of products derived by normalization method

Product	%yield
Methane	1.61
Ethane	0.12
Ethylene	2.99
Propylene	1.40
C_{4-5} isomers	0.00
BTX	0.00
Total	6.12

Conversion

%Conversion can be calculated from the following equation:

$$\%\text{conversion} = \frac{(\text{total area - feed area})}{\text{total area}} \times 100$$

For example;

$$\%\text{conversion} = \frac{(214652.9 - 201522.2)}{214652.9} \times 100$$

$$= 6.12$$

Selectivity

%Selectivity can be obtained from the following equation:

$$\%\text{selectivity} = \frac{\%\text{yield of product}}{\%\text{conversion}} \times 100$$

For example;

$$\%\text{selectivity of propylene} = \frac{1.40}{6.12} \times 100$$

$$= 22.88$$

C2: Equilibrium propane conversion

From

$$\Delta G^0 = \Delta H^0 - T\Delta S^0$$

$\Delta H^0 = \sum h_f^0$ of products - $\sum h_f^0$ of reactants (from Table A-26, Thermodynamics: An engineering approach 8th edition)

$\Delta S^0 = \sum s^0$ of products - $\sum s^0$ of reactants (from Table A-26, Thermodynamics: An engineering approach 8th edition)

$\Delta H^0 = 124$ kJ/mol

$\Delta S^0 = 0.13$ kJ/mol/K

So $\Delta G^0 = 124 - 0.13T$

At 550 °C (823 K); $\Delta G^0 = 19.15$ kJ/mol

From

$$\Delta G = \Delta G^0 + RT\ln K_{eq}$$

At equilibrium: $\Delta G = 0$

So

$$\Delta G^0 = -RT\ln K_{eq}$$

$$19.15 = -8.3145 \times 10^{-3}\ \text{kJ.mol}^{-1}.\text{K}^{-1} \times 823\ \text{K}\ \ln K_{eq}$$

$$K_{eq} = 0.0608$$

From equilibrium propane conversion under an absence of H_2;

$$K_{eq} = X^2 / (1-X)$$

$$0.0608 = X^2 / (1-X)$$

Solve for X; X = 21.81, where X is the equilibrium propane conversion.

From equilibrium propane conversion under an excess of H_2;

$$K_{eq} = X / (1-X)$$

$$0.0608 = X / (1-X)$$

Solve for X; X = 5.74, where X is the equilibrium propane conversion.

The rate equation from these data can be derived as follows;

$$\text{rate} = kC / (1 + K_{ad}[H_2])$$

Under an absence of H_2;

$$21.81 = kC / (1 + K_{ad}(0))$$

$$kC = 21.81$$

Under an excess of H_2;

$$\text{rate} = kC / (1 + K_{ad}(1))$$

$$5.74 = 21.81 / (1 + K_{ad})$$

$$K_{ad} = 2.80$$

So the rate equation is

$$\text{rate} = 21.81 / (1 + 2.80[H_2])$$

The propane conversion with a presence of H_2 is shown in **Table C3.**

Table C3 equilibrium propane conversion with a presence of H_2

H_2 (%)	[H_2]	X
0	0.0	21.81
10	0.1	17.04
20	0.2	13.98
30	0.3	11.85
40	0.4	10.29
50	0.5	9.09
60	0.6	8.14
70	0.7	7.37
80	0.8	6.73
90	0.9	6.20
100	1.0	5.74

Appendix D

REACTION DATA

D1: Effect of temperature

Table D1 product distribution from propane conversion (contact time 5.43 g.h.mol^{-1})

Temperature (°C)	%Conversion	%Yield					
		Methane	Ethane	Ethylene	Propylene	C_{4-5} isomers	BTX
400	0.7	0.1	0.1	0.0	0.1	0.2	0.3
450	5.3	0.4	1.2	0.2	0.5	1.0	2.2
500	16.8	1.6	3.4	0.6	1.3	1.5	8.4
550	35.8	4.2	5.8	1.8	2.8	1.5	19.7

Reaction condition; Catalyst: Ga-HZSM-5 (28), Temperature: 400-550 °C, Feed rate: 15 mL/min of propane, Carrier gas; - mL/min of nitrogen, Ambient pressure.

D2: Dilution effect

Table D2 product distribution from propane conversion over 3% Ga-HZSM-5 (28) after feed dilution (contact time 5.43 g.h.mol^{-1})

Time on stream (min)	%Conversion	%Yield					
		Methane	Ethane	Ethylene	Propylene	C_{4-5} isomers	BTX
30	11.07	0.31	0.38	1.56	6.41	0.98	1.42
70	9.88	0.25	0.25	1.23	6.13	0.94	1.08
110	9.35	0.23	0.21	1.11	6.09	0.86	0.85
150	8.83	0.22	0.18	1.02	5.95	0.71	0.75
190	8.51	0.20	0.17	0.96	5.84	0.68	0.67
230	8.32	0.20	0.15	0.92	5.77	0.66	0.62
270	8.33	0.20	0.15	0.90	5.82	0.66	0.61
310	8.24	0.19	0.14	0.87	5.73	0.74	0.58
350	8.03	0.18	0.13	0.83	5.59	0.76	0.54

Reaction condition; Catalyst: Ga-HZSM-5 (28), Temperature: 550 °C, Feed rate: 15 mL/min of propane, Carrier gas; 60 mL/min of nitrogen, Ambient pressure.

D3: Effect of gallium incorporate HZSM-5

Table D3 product distribution from propane conversion (contact time 5.43 g.h.mol^{-1})

Time on stream (min)	%Conversion	%Yield					
		Methane	Ethane	Ethylene	Propylene	C_{4-5} isomers	BTX
30	6.12	1.61	0.12	2.99	1.40	0.00	0.00
70	6.40	1.69	0.13	3.13	1.46	0.00	0.00
110	6.57	1.74	0.13	3.20	1.50	0.00	0.00

Reaction condition; Catalyst: HZSM-5 (28), Temperature: 550 °C, Feed rate: 15 mL/min of propane, Carrier gas; 60 mL/min of nitrogen, Ambient pressure.

Table D4 product distribution from propane conversion (contact time 5.43 g.h.mol^{-1})

Time on stream (min)	%Conversion	%Yield					
		Methane	Ethane	Ethylene	Propylene	C_{4-5} isomers	BTX
30	30.52	1.16	1.61	3.06	6.48	1.19	17.03
70	27.97	0.98	1.32	2.94	6.76	1.19	14.79
110	25.46	0.86	1.08	2.86	6.78	1.22	12.64
150	23.76	0.81	0.96	2.85	6.98	1.23	10.94
190	21.96	0.74	0.86	2.75	7.02	1.21	9.39
230	20.27	0.68	0.79	2.66	7.11	1.20	7.83
270	20.00	0.62	0.71	2.51	7.02	1.17	7.97
310	19.51	0.55	0.63	2.33	6.86	1.13	8.00
350	18.41	0.52	0.59	2.24	6.90	1.12	7.04
390	17.23	0.48	0.54	2.12	6.87	1.10	6.12
430	16.18	0.44	0.49	1.99	6.77	1.07	5.42
470	14.98	0.41	0.45	1.87	6.67	1.04	4.54
510	14.34	0.39	0.42	1.80	6.66	1.03	4.04
550	14.11	0.38	0.40	1.77	6.74	1.01	3.81
590	13.27	0.36	0.37	1.67	6.59	0.99	3.29
630	12.54	0.34	0.35	1.58	6.47	0.97	2.84
687	11.96	0.32	0.32	1.51	6.44	0.94	2.43
727	11.76	0.31	0.31	1.49	6.47	0.93	2.24
767	11.37	0.30	0.29	1.42	6.36	0.91	2.07

Reaction condition; Catalyst: Ga-HZSM-5 (28), Temperature: 550 °C, Feed rate: 15 mL/min of propane, Carrier gas; 60 mL/min of nitrogen, Ambient pressure.

Table D5 product distribution from propane conversion (contact time 5.43 g.h.mol^{-1})

Time on stream (min)	%Conversion	%Yield					
		Methane	Ethane	Ethylene	Propylene	C_{4-5} isomers	BTX
30	11.07	0.31	0.38	1.56	6.41	0.98	1.42
70	9.88	0.25	0.25	1.23	6.13	0.94	1.08
110	9.35	0.23	0.21	1.11	6.09	0.86	0.85
150	8.83	0.22	0.18	1.02	5.95	0.71	0.75
190	8.51	0.20	0.17	0.96	5.84	0.68	0.67
230	8.32	0.20	0.15	0.92	5.77	0.66	0.62
270	8.33	0.20	0.15	0.90	5.82	0.66	0.61
310	8.24	0.19	0.14	0.87	5.73	0.74	0.58
350	8.03	0.18	0.13	0.83	5.59	0.76	0.54

Reaction condition; Catalyst: Ga-HZSM-5 (28), Reduced 600 °C, Temperature: 550 °C, Feed rate: 15 mL/min of propane, Carrier gas; 60 mL/min of nitrogen, Ambient pressure.

D4: Effect of contact time

D4.1: non-reduced catalyst

Table D6 product distribution from propane conversion (contact time 1.81 g.h.mol^{-1})

Time on stream (min)	%Conversion	%Yield					
		Methane	Ethane	Ethylene	Propylene	C_{4-5} isomers	BTX
30	13.15	0.63	1.20	1.61	4.58	1.22	3.91
70	11.90	0.52	0.96	1.53	4.67	1.17	3.06
110	10.96	0.46	0.81	1.48	4.64	1.12	2.46
150	10.32	0.41	0.71	1.41	4.60	1.08	2.10
190	9.74	0.38	0.65	1.34	4.56	1.02	1.79
230	9.29	0.34	0.59	1.26	4.50	0.99	1.61
270	8.80	0.32	0.55	1.19	4.44	0.96	1.35
310	8.42	0.29	0.51	1.13	4.37	0.93	1.20

Reaction condition; Catalyst: Ga-HZSM-5 (28), Temperature: 550 °C, Feed rate: 15 mL/min of propane, Carrier gas; 60 mL/min of nitrogen, Ambient pressure.

Table D7 product distribution from propane conversion (contact time 5.43 g.h.mol^{-1})

Time on stream (min)	%Conversion	%Yield					
		Methane	Ethane	Ethylene	Propylene	C_{4-5} isomers	BTX
30	30.52	1.16	1.61	3.06	6.48	1.19	17.03
70	27.97	0.98	1.32	2.94	6.76	1.19	14.79
110	25.46	0.86	1.08	2.86	6.78	1.22	12.64
150	23.76	0.81	0.96	2.85	6.98	1.23	10.94
190	21.96	0.74	0.86	2.75	7.02	1.21	9.39
230	20.27	0.68	0.79	2.66	7.11	1.20	7.83
270	20.00	0.62	0.71	2.51	7.02	1.17	7.97
310	19.51	0.55	0.63	2.33	6.86	1.13	8.00
350	18.41	0.52	0.59	2.24	6.90	1.12	7.04
390	17.23	0.48	0.54	2.12	6.87	1.10	6.12
430	16.18	0.44	0.49	1.99	6.77	1.07	5.42
470	14.98	0.41	0.45	1.87	6.67	1.04	4.54
510	14.34	0.39	0.42	1.80	6.66	1.03	4.04
550	14.11	0.38	0.40	1.77	6.74	1.01	3.81
590	13.27	0.36	0.37	1.67	6.59	0.99	3.29
630	12.54	0.34	0.35	1.58	6.47	0.97	2.84
687	11.96	0.32	0.32	1.51	6.44	0.94	2.43
727	11.76	0.31	0.31	1.49	6.47	0.93	2.24
767	11.37	0.30	0.29	1.42	6.36	0.91	2.07

Reaction condition; Catalyst: Ga-HZSM-5 (28), Temperature: 550 °C, Feed rate: 15 mL/min of propane, Carrier gas; 60 mL/min of nitrogen, Ambient pressure.

D4.2: reduced catalyst (600 °C)

Table D8 product distribution from propane conversion (contact time 1.81 g.h.mol^{-1})

Time on stream (min)	%Conversion	%Yield					
		Methane	Ethane	Ethylene	Propylene	C_{4-5} isomers	BTX
30	6.85	0.18	0.34	0.81	3.91	0.75	0.85
70	6.13	0.15	0.25	0.65	3.75	0.64	0.68
110	5.60	0.14	0.21	0.59	3.64	0.59	0.43
150	5.18	0.13	0.19	0.53	3.51	0.54	0.29
190	5.15	0.13	0.18	0.51	3.53	0.53	0.28
230	4.91	0.12	0.16	0.48	3.41	0.50	0.25
270	4.98	0.12	0.16	0.48	3.47	0.51	0.25
310	4.87	0.12	0.15	0.46	3.42	0.49	0.23

Reaction condition; Catalyst: Ga-HZSM-5 (28), Temperature: 550 °C, Feed rate: 15 mL/min of propane, Carrier gas; 60 mL/min of nitrogen, Ambient pressure.

Table D9 product distribution from propane conversion (contact time 5.43 g.h.mol^{-1})

Time on stream (min)	%Conversion	%Yield					
		Methane	Ethane	Ethylene	Propylene	$C_{4\text{-}5}$ isomers	BTX
30	11.07	0.31	0.38	1.56	6.41	0.98	1.42
70	9.88	0.25	0.25	1.23	6.13	0.94	1.08
110	9.35	0.23	0.21	1.11	6.09	0.86	0.85
150	8.83	0.22	0.18	1.02	5.95	0.71	0.75
190	8.51	0.20	0.17	0.96	5.84	0.68	0.67
230	8.32	0.20	0.15	0.92	5.77	0.66	0.62
270	8.33	0.20	0.15	0.90	5.82	0.66	0.61
310	8.24	0.19	0.14	0.87	5.73	0.74	0.58
350	8.03	0.18	0.13	0.83	5.59	0.76	0.54

Reaction condition; Catalyst: Ga-HZSM-5 (28), Temperature: 550 °C, Feed rate: 15 mL/min of propane, Carrier gas; 60 mL/min of nitrogen, Ambient pressure.

D5: A presence of H_2

Table D10 product distribution from propane conversion (contact time 5.43 g.h.mol^{-1})

H_2 amount (%v/v)	%Conversion	%Yield					
		Methane	Ethane	Ethylene	Propylene	C_{4-5} isomers	BTX
0	11.07	0.31	0.38	1.56	6.41	0.98	1.42
10	7.01	0.15	0.13	0.63	5.27	0.48	0.35
20	4.85	0.10	0.05	0.29	4.22	0.08	0.10
100	0.48	0.00	0.00	0.00	0.48	0.00	0.00

Reaction condition; Catalyst: Ga-HZSM-5 (28), Reduced 600 °C, Temperature: 550 °C, Feed rate: 15 mL/min of propane, Carrier gas; 60 mL/min of nitrogen, Ambient pressure.

D6: Effect of Si/Al ratio

D6.1: non-reduced catalysts

Table D11 product distribution from propane conversion (contact time 5.43 g.h.mol^{-1})

Time on stream (min)	%Conversion	%Yield					
		Methane	Ethane	Ethylene	Propylene	C_{4-5} isomers	BTX
30	30.52	1.16	1.61	3.06	6.48	1.19	17.03
70	27.97	0.98	1.32	2.94	6.76	1.19	14.79
110	25.46	0.86	1.08	2.86	6.78	1.22	12.64
150	23.76	0.81	0.96	2.85	6.98	1.23	10.94
190	21.96	0.74	0.86	2.75	7.02	1.21	9.39
230	20.27	0.68	0.79	2.66	7.11	1.20	7.83
270	20.00	0.62	0.71	2.51	7.02	1.17	7.97
310	19.51	0.55	0.63	2.33	6.86	1.13	8.00
350	18.41	0.52	0.59	2.24	6.90	1.12	7.04
390	17.23	0.48	0.54	2.12	6.87	1.10	6.12
430	16.18	0.44	0.49	1.99	6.77	1.07	5.42
470	14.98	0.41	0.45	1.87	6.67	1.04	4.54
510	14.34	0.39	0.42	1.80	6.66	1.03	4.04
550	14.11	0.38	0.40	1.77	6.74	1.01	3.81
590	13.27	0.36	0.37	1.67	6.59	0.99	3.29
630	12.54	0.34	0.35	1.58	6.47	0.97	2.84
687	11.96	0.32	0.32	1.51	6.44	0.94	2.43
727	11.76	0.31	0.31	1.49	6.47	0.93	2.24
767	11.37	0.30	0.29	1.42	6.36	0.91	2.07

Reaction condition; Catalyst: Ga-HZSM-5 (28), Temperature: 550 °C, Feed rate: 15 mL/min of propane, Carrier gas; 60 mL/min of nitrogen, Ambient pressure.

Table D12 product distribution from propane conversion (contact time 5.43 g.h.mol^{-1})

Time on stream (min)	%Conversion	Yield					
		Methane	Ethane	Ethylene	Propylene	C_{4-5} isomers	BTX
40	21.20	0.96	0.75	3.10	7.03	1.15	8.21
80	19.86	0.82	0.62	2.93	7.30	1.14	7.05
120	18.64	0.73	0.53	2.76	7.41	1.11	6.09
160	17.51	0.65	0.47	2.56	7.40	1.13	5.30
200	16.66	0.59	0.42	2.40	7.43	1.10	4.72
280	15.35	0.50	0.34	2.12	7.50	1.05	3.84
320	14.53	0.45	0.31	1.96	7.40	1.01	3.40
360	13.82	0.41	0.28	1.81	7.34	0.97	3.01
400	13.22	0.38	0.25	1.69	7.26	0.94	2.71
440	12.96	0.36	0.23	1.61	7.31	0.92	2.52
480	12.34	0.33	0.21	1.49	7.17	0.88	2.25
520	11.83	0.31	0.19	1.39	7.05	0.84	2.04
560	11.54	0.30	0.18	1.33	7.03	0.82	1.88
600	11.01	0.28	0.17	1.24	6.89	0.74	1.70
640	10.81	0.27	0.16	1.19	6.88	0.72	1.59
680	10.50	0.25	0.14	1.13	6.79	0.70	1.48
720	10.15	0.24	0.14	1.07	6.68	0.68	1.35

Reaction condition; Catalyst: Ga-HZSM-5 (40), Temperature: 550 °C, Feed rate: 15 mL/min of propane, Carrier gas; 60 mL/min of nitrogen, Ambient pressure.

Table D13 product distribution from propane conversion (contact time 5.43 g.h.mol^{-1})

Time on stream (min)	%Conversion	%Yield					
		Methane	Ethane	Ethylene	Propylene	C_{4-5} isomers	BTX
40	4.90	0.14	0.05	0.32	4.10	0.05	0.24
80	5.20	0.15	0.00	0.38	4.36	0.06	0.25
120	5.14	0.15	0.00	0.38	4.32	0.06	0.23
160	5.10	0.15	0.00	0.38	4.30	0.06	0.22
200	4.98	0.14	0.00	0.36	4.22	0.06	0.20

Reaction condition; Catalyst: Ga-HZSM-5 (140), Temperature: 550 °C, Feed rate: 15 mL/min of propane, Carrier gas; 60 mL/min of nitrogen, Ambient pressure.

Table D14 product distribution from propane conversion (contact time 5.43 g.h.mol^{-1})

Time on stream (min)	%Conversion	%Yield					
		Methane	Ethane	Ethylene	Propylene	C_{4-5} isomers	BTX
40	3.63	0.08	0.00	0.16	3.33	0.00	0.06
80	3.61	0.08	0.00	0.17	3.31	0.00	0.06
120	3.56	0.08	0.00	0.17	3.25	0.00	0.06
160	3.55	0.07	0.00	0.15	3.27	0.00	0.06
217	3.47	0.07	0.00	0.15	3.20	0.00	0.05
257	3.28	0.08	0.00	0.17	2.99	0.00	0.05

Reaction condition; Catalyst: Ga-HZSM-5 (250), Temperature: 550 °C, Feed rate: 15 mL/min of propane, Carrier gas; 60 mL/min of nitrogen, Ambient pressure.

Table D15 product distribution from propane conversion (contact time 5.43 g.h.mol^{-1})

Time on stream (min)	%Conversion	%Yield					
		Methane	Ethane	Ethylene	Propylene	C_{4-5} isomers	BTX
40	3.29	0.06	0.00	0.14	3.04	0.00	0.04
80	3.25	0.07	0.00	0.14	3.00	0.00	0.04
120	3.24	0.07	0.00	0.15	2.99	0.00	0.04
160	3.21	0.07	0.00	0.15	2.95	0.00	0.04
200	3.18	0.07	0.00	0.13	2.94	0.00	0.04
240	3.22	0.07	0.00	0.14	2.98	0.00	0.04
280	3.20	0.07	0.00	0.14	2.97	0.00	0.03

Reaction condition; Catalyst: Ga-HZSM-5 (500), Temperature: 550 °C, Feed rate: 15 mL/min of propane, Carrier gas; 60 mL/min of nitrogen, Ambient pressure.

D6.2: reduced catalysts (600-700 °C)

Table D16 product distribution from propane conversion (contact time 5.43 g.h.mol^{-1})

Time on stream (min)	%Conversion	%Yield					
		Methane	Ethane	Ethylene	Propylene	$C_{4\text{-}5}$ isomers	BTX
30	11.07	0.31	0.38	1.56	6.41	0.98	1.42
70	9.88	0.25	0.25	1.23	6.13	0.94	1.08
110	9.35	0.23	0.21	1.11	6.09	0.86	0.85
150	8.83	0.22	0.18	1.02	5.95	0.71	0.75
190	8.51	0.20	0.17	0.96	5.84	0.68	0.67
230	8.32	0.20	0.15	0.92	5.77	0.66	0.62
270	8.33	0.20	0.15	0.90	5.82	0.66	0.61
310	8.24	0.19	0.14	0.87	5.73	0.74	0.58
350	8.03	0.18	0.13	0.83	5.59	0.76	0.54

Reaction condition; Catalyst: Ga-HZSM-5 (28), Reduced 600 °C, Temperature: 550 °C, Feed rate: 15 mL/min of propane, Carrier gas; 60 mL/min of nitrogen, Ambient pressure.

Table D17 product distribution from propane conversion (contact time 5.43 g.h.mol^{-1})

Time on stream (min)	%Conversion	%Yield					
		Methane	Ethane	Ethylene	Propylene	C_{4-5} isomers	BTX
30	18.63	0.63	0.69	2.65	7.22	1.17	6.27
70	16.08	0.48	0.49	2.20	7.34	1.12	4.44
110	14.59	0.41	0.39	1.94	7.27	1.05	3.54
150	13.66	0.37	0.33	1.76	7.17	1.00	3.02
190	12.86	0.33	0.29	1.62	7.03	0.95	2.64
230	12.32	0.31	0.26	1.52	6.95	0.91	2.37
270	11.93	0.30	0.24	1.44	6.88	0.89	2.18
310	11.58	0.29	0.23	1.38	6.81	0.86	2.02
350	11.40	0.28	0.21	1.34	6.81	0.85	1.92

Reaction condition; Catalyst: Ga-HZSM-5 (40), Reduced 600 °C, Temperature: 550 °C, Feed rate: 15 mL/min of propane, Carrier gas; 60 mL/min of nitrogen, Ambient pressure.

Table D18 product distribution from propane conversion (contact time 5.43 g.h.mol^{-1})

Time on stream (min)	%Conversion	%Yield					
		Methane	Ethane	Ethylene	Propylene	C_{4-5} isomers	BTX
30	2.21	0.05	0.00	0.11	2.05	0.00	0.00
70	1.82	0.04	0.00	0.09	1.69	0.00	0.00
110	1.73	0.04	0.00	0.08	1.60	0.00	0.00
150	1.72	0.04	0.00	0.09	1.59	0.00	0.00
190	1.66	0.04	0.00	0.08	1.53	0.00	0.00
230	1.63	0.04	0.00	0.08	1.51	0.00	0.00

Reaction condition; Catalyst: Ga-HZSM-5 (140), Reduced 700 °C, Temperature: 550 °C, Feed rate: 15 mL/min of propane, Carrier gas; 60 mL/min of nitrogen, Ambient pressure.

Table D19 product distribution from propane conversion (contact time 5.43 g.h.mol^{-1})

Time on stream (min)	%Conversion	%Yield					
		Methane	Ethane	Ethylene	Propylene	C_{4-5} isomers	BTX
30	2.50	0.05	0.00	0.09	2.36	0.00	0.00
70	2.26	0.05	0.00	0.09	2.12	0.00	0.00
110	2.19	0.05	0.00	0.09	2.05	0.00	0.00
150	2.12	0.05	0.00	0.09	1.99	0.00	0.00
190	2.05	0.04	0.00	0.09	1.92	0.00	0.00
230	2.04	0.04	0.00	0.09	1.91	0.00	0.00
270	1.98	0.04	0.00	0.08	1.85	0.00	0.00

Reaction condition; Catalyst: Ga-HZSM-5 (250), Reduced 700 °C, Temperature: 550 °C, Feed rate: 15 mL/min of propane, Carrier gas; 60 mL/min of nitrogen, Ambient pressure.

Table D20 product distribution from propane conversion (contact time 5.43 g.h.mol^{-1})

Time on stream (min)	%Conversion	%Yield					
		Methane	Ethane	Ethylene	Propylene	C_{4-5} isomers	BTX
30	3.07	0.03	0.00	0.05	2.99	0.00	0.00
70	2.65	0.03	0.00	0.05	2.57	0.00	0.00
110	2.44	0.03	0.00	0.06	2.35	0.00	0.00
150	2.30	0.04	0.00	0.07	2.20	0.00	0.00
190	2.21	0.04	0.00	0.07	2.10	0.00	0.00
230	2.14	0.04	0.00	0.07	2.04	0.00	0.00
270	2.08	0.04	0.00	0.07	1.97	0.00	0.00
310	2.02	0.04	0.00	0.07	1.92	0.00	0.00

Reaction condition; Catalyst: Ga-HZSM-5 (500), Reduced 700 °C, Temperature: 550 °C, Feed rate: 15 mL/min of propane, Carrier gas; 60 mL/min of nitrogen, Ambient pressure.